Battery Aging and Characterization of Nickel Metal Hydride and Lead Acid Batteries

A Thesis

Presented in Partial Fulfillment for

A Mechanical Engineering Honors Undergraduate Research Program Requirement for

Graduation with Distinction in Mechanical Engineering

In Conjunction with a Bachelor of Science Degree in Mechanical Engineering

at The Ohio State University

By

Nick Picciano

The Ohio State University

2007

Advisor

Dr. Giorgio Rizzoni

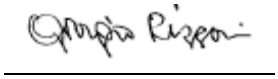

ABSTRACT

This thesis discusses the research done on battery aging characteristics for both Nickel Metal Hydride and Lead-Acid batteries. In an effort to relate real duty cycles of Hybrid Electric Vehicles and their effects on battery aging, a set of basis current profiles were created. The basis current waveforms can effectively make up any duty cycle a Hybrid Electric Vehicle encounters. These basis profiles can then be characterized for their effect on battery aging. Once their effect on aging is determined, a comprehensive aging model can be created in order to determine a battery's age and predict its future aging.

Lead-Acid batteries were studied for their two common failure modes: loss of capacity and loss of power. Developing different current profiles through which the battery will be aged is expected to provide insight into how real world activities affect the battery differently. These differences will help provide further insight into the development of a similar comprehensive aging model for Lead-Acid batteries.

The effects of State of Charge (SOC) on internal battery resistance were examined and showed that as the SOC decreases, the battery resistance increases, which can be justly related to physical interactions inside the battery. EIS model fitting showed that a third order Randle Model was needed in order to fit to an open circuit battery's frequency response spectrum. However, a Large Signal Response analysis showed that a second order model was sufficient to fit to the response. Regardless of the discrepancy, these models and parameters can be used to investigate and quantify aging. Additionally, these tests prove the battery parameters' dependence on current level, which means that the

battery is inherently a non-linear system. Engine cranking tests also showed the relationship between SOC and internal resistance, as well as the change in battery performance at different temperatures.

Finally, the relationship between a Lead-Acid battery's open circuit voltage and its SOC was investigated. The relationship proved to be nearly linear and a reasonable approximation for establishing a desired battery SOC for a given test.

ACKNOWLEDGEMENTS

Many thanks to Dr. Rizzoni for the opportunity to conduct undergraduate research at the Center for Automotive Research and for all of his wonderful help and guidance. To Dr. Guezennec for his immense support with the project and helpful answers to all my questions. To John Neal, BJ Yurkovich, and Jim Shively. Without their knowledge and technical support, the project would have never have been achieved. To all the students at CAR for broadening my life with their cultures. Special thanks to Lorenzo Serrao and Zakaria Chehab for teaching me about batteries. Thanks so much to Chris Suozzo for his modeling expertise. And last but not least I would like to thank Andrea Storti, Weiwu Li, and especially William Pinelli for providing me with an unforgettable work experience everyday. Thanks to all I have met during this experience. And thanks to all my friends I avoided who stuck around while I tried to complete this thing.

TABLE OF CONTENTS

LIST OF TABLES

LIST OF EQUATIONS

LIST OF FIGURES

1. INTRODUCTION

This section provides some background information for the research included in the thesis, as well as the motivation behind it.

1.1. *BACKGROUND*

Two of the most widely used secondary batteries are the Lead-Acid and Nickel Metal Hydride batteries. Each has many commercial uses based on their advantages and disadvantages. This thesis discusses their use in hybrid-electric vehicles and automotive electrical systems and more specifically, their degradation during use.

The Nickel Metal Hydride (NiMH) battery is used in Hybrid-Electrical Vehicles (HEV), and in order to improve the advantages of hybrid technology, an explicit aging model is needed which can describe and predict the battery's life. The research carried out in this thesis on NiMH batteries is a continuation of the thesis of work done by Zakaria Chehab [1] whose research was aimed at characterizing the aging the aging of the battery. Further research is needed to implement these characterizations for better use in a HEV. Moreover, using real HEV data to predict and test battery aging through the decomposition of the HEV's current profiles can provide a more comprehensive aging model and more insight into using NiMH batteries more efficiently. Once a basis set of current profiles can be created, any random profile demanded by an HEV can be able to be analyzed and its effects predicted.

Lead-Acid batteries are desired for their tolerance to abuse and high power capabilities. However, as newer technologies emerge, for example NiMH batteries, the disadvantages

of the Lead-Acid battery, most notably its low energy density, become more and more evident. This paper discusses the most prominent failure modes of the Lead-Acid battery in its common automotive use: Capacity Loss and Power Loss.

In this thesis, the aging of the battery is quantified through a set of aging diagnostic tests: i) a capacity test; ii) a large signal response test; iii) a cranking test; and iv) electrochemical impedance spectroscopy (EIS). The EIS test can help describe the state of health of the battery without degrading the battery, unlike standard capacity tests which age the battery due to their large depth of discharge. These battery-related terms will be clarified later in section 1.7 'Battery Characteristics.'

1.2. *MOTIVATION*

The importance of researching the characteristics of alternative fuels in an effort to advance their use is growing with the increase in price of fossil fuels. Oil prices continue to climb making it more and more likely that alternative fuels will become an integral part in global industry and economics. Electricity, produced by a variety of means and stored in batteries, is an alternative fuel that has been used for many years; new technologies are improving battery performance and the use of batteries in many applications is increasing. The Lead-Acid battery, also commonly known as a car, or 12-V starter battery, has been utilized for its high power and tolerance to abusive conditions for many years. In spite of the decreasing cost of higher-performance batteries, such as NiMH and lithium-ion and lithium-polymer batteries, Lead-Acid batteries still find almost exclusive use as automotive starter batteries and to provide an energy buffer for

12-V automotive electrical systems. Today, the cost/performance ratio is still in favor of the Lead-Acid batter for routine automotive applications. On the other hand, the emergence of HEV's, and the re-emergence of electrical vehicles (EV) as viable alternatives to conventional internal combustion engine-based propulsion systems has seen significant growth in the use of NiMH batteries, and will soon result in a similar expansion of batteries based on lithium technologies. For all of these battery chemistries, determining the exact sources of failure and performance degradation is an important step towards improving the technology, and even to find ways to restore their health for longer continued use.

1.3. *GENERAL BATTERY BACKGROUND*

There rarely ever exists one product that can operate ideally for any and all applications. The same goes for batteries. There are many different battery chemistries since each can deliver different desirable characteristics. These characteristics make it advantageous for specific applications to use certain batteries.

Most battery differences are characterized by a few qualities. These qualities help determine which application is most suitable. Batteries can be compared by their energy density. This describes the amount of energy deliverable while taking into account their mass. It can also be called their *specific energy*. Other desirable attributes include *specific power*, and the *cycle life*. These terms are defined in section 1.7 'Battery Characteristics.' Table 1summarizes the major differences of the some of the most common batteries.

Table 1: General Battery Differences [1]

Battery Type	Advantages	Disadvantages
Lead - Acid	Can be designed for high power Inexpensive Safe Reliable	Poor Cold temperature Performance Short Calendar and Cycle Life
Nickel- Cadmium	High Specific Energy Good Cycle life compared with lead acid	Does not deliver sufficient power
Nickel-Metal Hydride	Reasonable Specific Energy Reasonable Specific Power Much longer cycle life than lead acid Safe Abuse-tolerant	High Cost Heat Generation at High Temperatures Low cell efficiency Need to control Hydrogen Losses
Lithium Ion	High Specific Energy High Specific Power High Energy Efficiency Good High temperature performance Low Self-Discharge	Needs Improvement in: Calendar and Cycle life Abuse Tolerance Acceptable Cost Higher degree of Battery safety
Lithium Polymer	High Specific Energy Has potential in providing high specific power Safe Good Cycle and Calendar Life	Only viable if: The cost is lower dramatically Specific Power is increased

As can be seen in the Table 1, Lead-Acid batteries remain very beneficial for applications that need high power with safe and inexpensive technology. These attributes explain why the Lead-Acid battery dominates the conventional automobile industry. If one looks at the newer HEV technology, Nickel Metal Hydride is leading the way in current production HEV's, but many believe that NiMH batteries will be replaced by Lithium-based batteries once the technology becomes more cost effective.

It is useful to compare the performance characteristics of different energy storage systems, so as to put batteries into perspective. Figure 1 provides a graphical comparison of some energy storage devices.

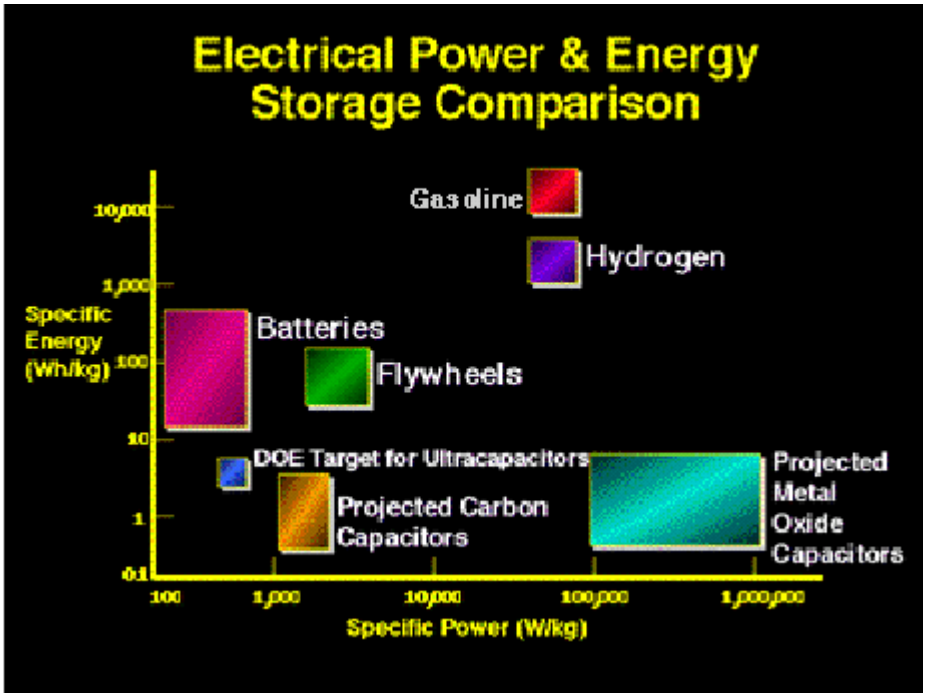

Figure 1: Energy Storage and Electrical Power Comparison [1]

Figure 1 and Table 1 help understand why certain applications would lean towards older or newer battery technologies. For instance, cell phone batteries are using Lithium Ion batteries more and more for their high energy density. They also contain no toxic materials and will generally last long enough to span the normal life of the product [2]. Another portable communication device would be the two-way radio. This device generally runs on Nickel Cadmium batteries for their ability to be forgiving if abused and durable. NiMH may soon become more used for two-way radios since they have a higher energy density and contain no toxic materials; however, testing has shown they provide shorter than expected service life for this application [2]. Lithium Ion batteries are generally used in laptops for the same reasons they are used in cellular phones. Their high energy density allows for great service for portable devices. High power requirements for laptops, however, really degrade the battery performance, so there are

still aspects that the Lithium Ion battery falls short on for portable computing. For wheeled and stationary applications, many still trust the inexpensive and durable Lead-Acid battery. Its weight is less of an issue when the application is on wheels or stationary [2].

1.4. *AUTOMOTIVE ELECTRICAL NETWORK*

1.4.1. CONVENTIONAL

In the conventional automotive electrical network, the lead-acid battery serves relatively few and simple functions. In general it is used to start the engine by providing a high current and help operate on-board electrical devices. An automotive electrical power generation and storage (EPGS) system consists of a battery, an alternator, a voltage regulator, and serves all the electrical loads in the vehicle. The alternator is an electrical generator that converts mechanical energy into electrical energy. The alternator is a synchronous electric machine that receives input mechanical energy from the engine shaft through a belt coupling. The alternator produces an AC output, and therefore requires a rectification circuit, implemented by means of a bridge solid-state rectifier. In addition, a voltage regulator controls the rectifier DC output to a desired specification, so that the battery can maintain the desirable state of charge [3].

The lead-acid battery's main function in this system, besides providing high current to start the engine, is to act as a buffer to the alternator. The battery absorbs high frequency pulses that the alternator may generate, and provides energy for the transient loads demanded when the electric loads are turned on and off while the alternator adjusts to the

new load [4]. Moreover, the battery generally provides the required energy during transient current demands from the load while driving, and provides the short burst of high current needed to start the engine and power all electric loads until the alternator takes control.

1.4.2. HYBRID ELECTRIC VEHICLES

HEV electrical networks are a bit more complicated than the 12-V electrical system described in the preceding section. HEV's combine different energy conversion (IC engine and electrical machines) and energy storage systems to achieve improved fuel economy and performance. Thus, a battery system in a HEV not only provides the power and energy that a conventional system would need, but it also is required to provide traction power through electric motors. The two basic configurations are a parallel hybrid and a series hybrid.

In a parallel hybrid, the electric motor and the combustion engine are both connected to the wheels by way of a mechanical transmission. The combustion engine provides most of the necessary driving power, while the electric motor is used whenever a higher demand is needed, like for passing, hill climbs, or acceleration, as well as to provide energy recovery through braking regeneration. This allows for the implementation of a smaller and more efficient combustion engine with the potential to greatly increase fuel economy. A generator is not needed in a parallel hybrid because the electric motor can be used to generate the battery.

In a series hybrid, the electric motor is directly connected to the wheels, while the combustion engine is connected to a generator that can generate electric power to charge the battery and run the electric motor. The combustion engine in this configuration never actually powers the vehicle. It converts chemical energy to mechanical energy, to electrical energy for direct use for traction or for charging the batteries. The traction motors can also serve as generators to recover kinetic energy during braking. The advantage of this configuration is that the combustion engine never idles and can operate in its most efficient range, with benefits in both fuel economy and reduced emissions. Additionally, a transmission is not needed since the electric motor controls the wheels. This system can require a very large (and therefore heavy) battery pack and can be less efficient than a parallel hybrid because of the bidirectional energy conversion chain [1].

Toyota has introduced a third configuration that takes advantage of the advantages of both parallel and series hybrids, and which is appropriately called the parallel-series (or power-split) hybrid. This system has its own advantages and disadvantages much like those of the other configurations. Regardless of the configuration, the HEV's have been demonstrated to successfully meet the objectives of lower emissions and higher fuel economy.

1.5. *BATTERY OPERATION*

All chemical batteries have the same basic characteristics. Inside each chemical battery there exist four main components…

- **Anode**: The anode is the negative electrode that provides the electrons.

- **Cathode**: The cathode is the positive electrode that collects the electrons.
- **Electrolyte**: The electrolyte is the conductor between the electrodes. It provides the means for electron transfer between the positive and negative electrodes.
- **Separator**: The separator is the medium that prevents transfer of electrons while the battery is at rest.

The battery's function is to store energy. This energy is in the form of a voltage potential. Charge separation between the electrodes provides a potential that can give rise to a current flow in the presence of an electrical load. During operation, chemical reactions occur inside the battery at the surface of the electrodes. These reactions are called oxidation-reduction or 'red-ox' reactions. The reactions are most simply described as a chemical reaction through a transfer of electrons, which provides the ability to create electricity. An advantage of chemical (secondary) batteries is their ability to replenish their energy. When the chemical reaction is reversed between the two electrodes, energy can be returned to the battery.

1.5.1. NiMH Chemical Reactions

The NiMH battery consists of a nickel metal cathode and a hydrogen absorbing metal alloy consisting of an earth/nickel alloy or a titanium and zirconium alloy anode. The electrolyte is made of alkaline, a dilute solution of potassium hydroxide [5]. The chemical reactions that occur within the battery are listed in Table 2.

Table 2: Ni-MH Electrode Surface Reactions

Negative Electrode:
$M + H_2O + e^- \leftrightarrow MH + OH^-$
Positive Electrode:
$Ni(OH)_2 + OH^- \leftrightarrow NiOOH + H_2O + e^-$
Full Cell Reaction:
$Ni(OH)_2 + M \leftrightarrow MH + NiOOH$

1.5.2. LEAD-ACID REACTIONS

The Lead Acid battery consists of a lead dioxide cathode and a lead anode. The electrolyte is a sulfuric acid solution. The chemical reactions that occur within this battery are summarized in Table 3 [4].

Table 3: Lead-Acid Electrode Surface Reactions

Positive Electrode:
$PbO_2 + 4H^+ + 2e^- \rightarrow Pb^{2+} + 2H_2O$ $Pb^{2+} + SO_4^{2-} \rightarrow PbSO_4$
Negative Electrode:
$Pb \rightarrow Pb^{2+} + 2e^-$ $Pb^{2+} + SO_4^{2-} \rightarrow PbSO_4$
Full Cell Reaction:
$PbO_2 + Pb + 2H_2SO_4 \leftrightarrow 2PbSO_4 + 2H_2O$

1.6. *CELL CONSTRUCTION*

While the chemical reactions of the battery remain the same, the battery cell construction can differ. Each chemical battery has the same core components: i) two electrodes; ii) a separator; iii) an electrolyte; and iv) a housing. The construction of these components is based on the chemistry of the battery and the desired application.

1.6.1. NICKEL METAL HYDRIDE CELL CONSTRUCTION

The NiMH battery has two basic construction possibilities: cylindrical or prismatic. The cylindrical construction takes the positive and negative electrodes and the separator and wraps them together. They are then enclosed by a metallic casing. The electrolyte is then injected into the battery [5]. Figure 2 provides a view of the cylindrical design.

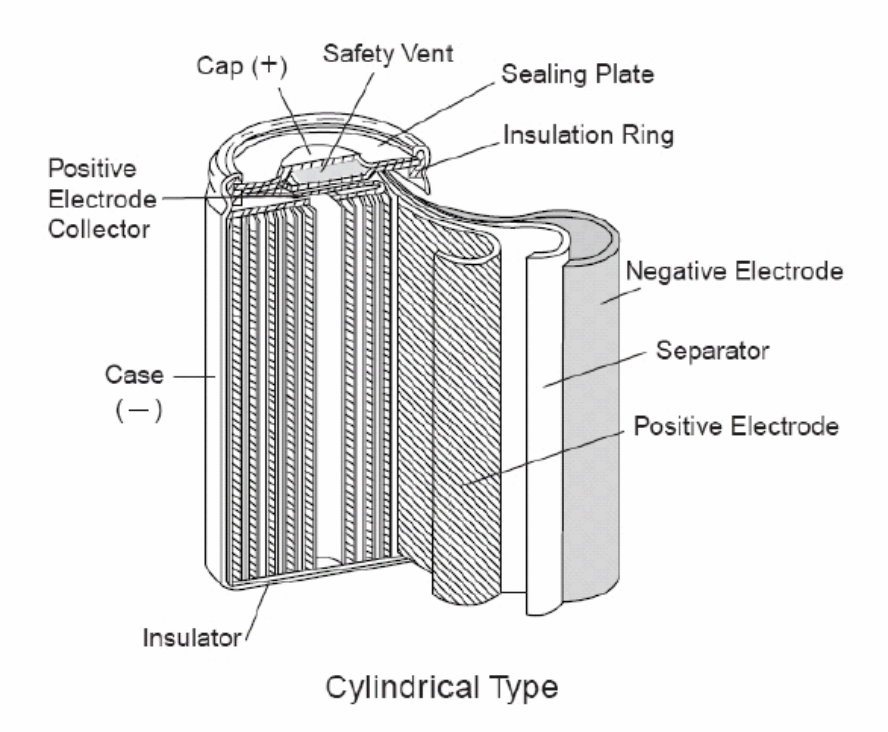

Figure 2: Cylindrical Design of NiMH Cell [5]

The prismatic design may offer better volumetric advantages for certain applications. This design is very similar to the cylindrical design except the single positive and negative electrodes are replaced with multiple electrode sets. Figure 3 provides an example of this cell design.

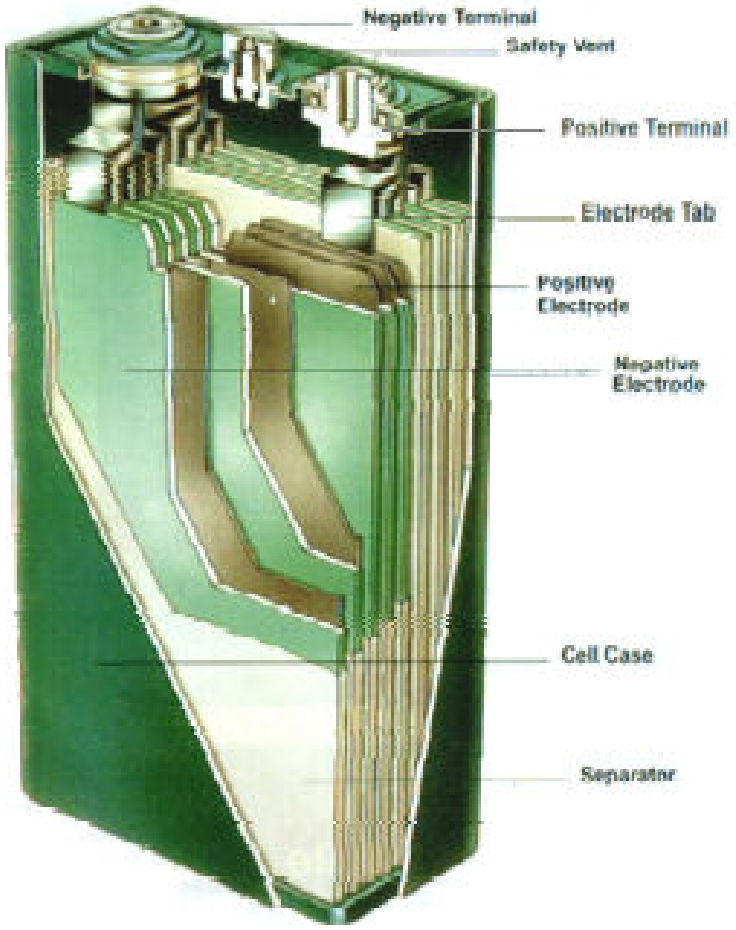

Figure 3: Prismatic Design of NiMH Cell [7]

1.6.2. Lead-Acid Cell Construction

The Lead-Acid battery has a slightly more complicated construction than the NiMH construction. Where the NiMH cell utilizes metal plates as its electrodes, the Lead-Acid battery uses a lead grid structure that contains a lead oxide paste. This is the most

common construction for the electrodes. It is often called the 'pasted flat plate' design. The lead oxide paste is applied to a lead alloy grid structure and then allowed to dry. The cell is then immersed in the sulfuric acid electrolyte and then encased in a plastic as is common for car batteries. When current passes through the plates it converts the lead oxide into lead dioxide for the positive plate, and lead oxide into lead for the negative plate [8]. Figures 4, 5 and 6 show the cell construction.

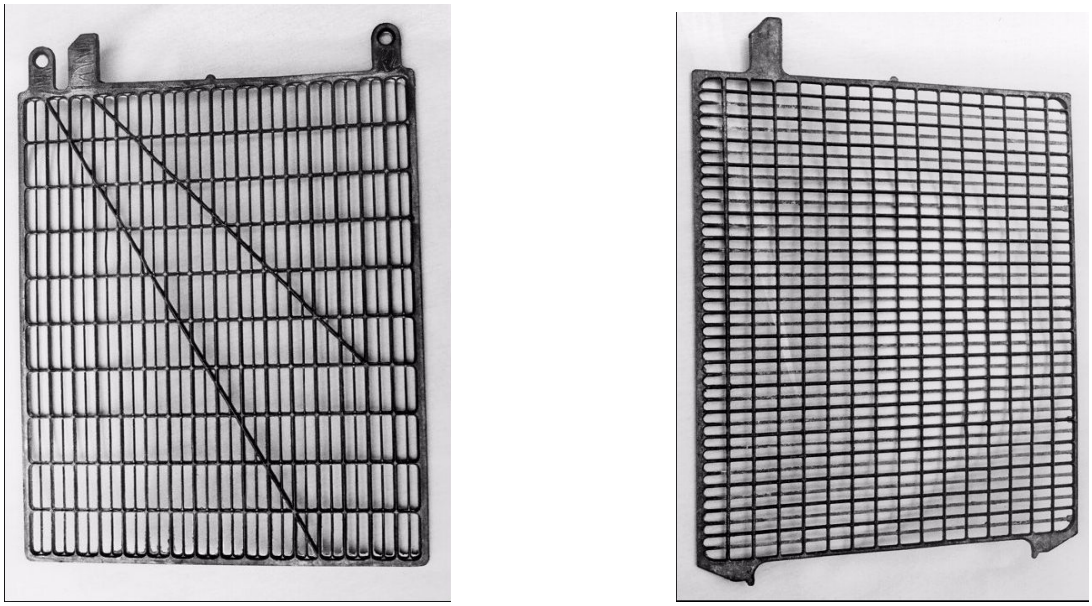

Figure 4: Positive and Negative Grids [8]

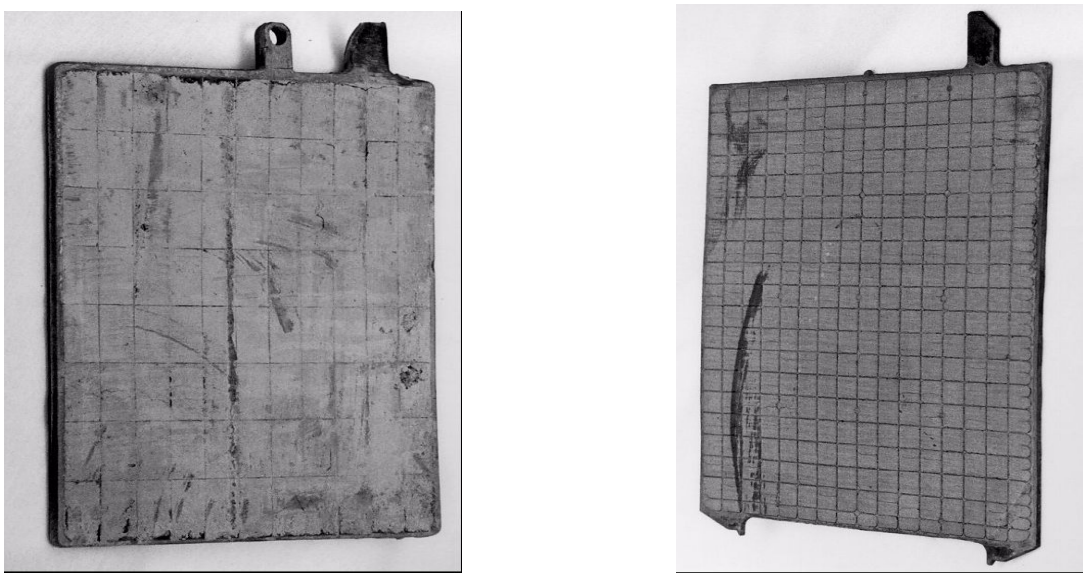

Figure 5: Positive and Negative Pasted Flat Plates [8]

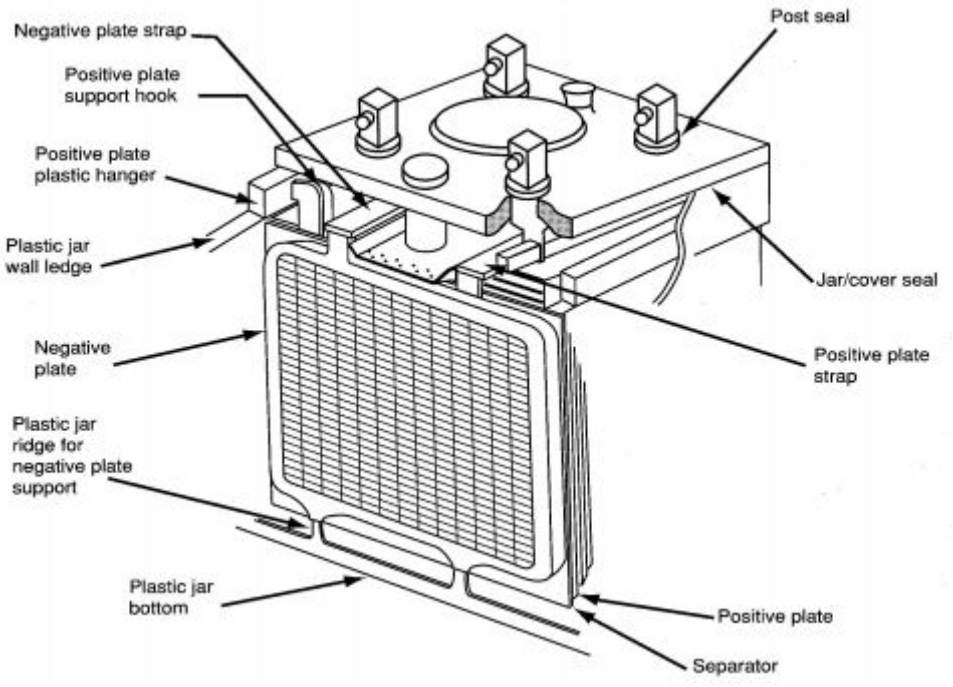

Figure 6: Plate Assembly in Cell [8]

1.7. *BATTERY CHARACTERISTICS*

Batteries are compared and described by certain characteristics. Additionally, certain terms are used to explain battery operation. These terms are defined below, and will be used throughout this thesis.

- **Capacity**: The amount of energy the battery can deliver under specific conditions. This is represented in amp-hours, which means the battery can provide energy at a rated amount of amps for a certain amount of time. A 50 Amp-hour battery can deliver 50 amps for 1 hour or 5 amps for 10 hours, etc.
- **State of Charge (SOC)**: The state of charge is a measure of the amount of energy remaining in the battery. It is often displayed as a percent of the battery's nominal capacity.
- **Depth of Discharge (DOD)**: The opposite of state of charge. The depth of discharge is the amount of energy removed from the battery. Also represented as a percent of nominal capacity.
- **State of Health (SOH)**: The state of health of a battery is a gage of the battery's condition and ability to perform as compared to a new battery. This can also be described as the battery's age.
- **Specific Energy**: The amount of energy contained in a specified amount of mass. It is expressed as a ratio of energy capability to mass, Wh/kg.
- **Specific Power**: The amount of power contained in a specified amount of mass. It is expressed as a ratio of power capability to mass, W/kg.
- **Calendar Life**: The length of time the battery is able to provide the energy for performance.

- **Cycle Life**: The number of cycles the battery is able to undergo while providing the necessary amount of energy for an application.
- **Impedance**: The impedance of a battery is a presentation of its voltage-current relationship as a function of frequency and other variables, such as temperature and SOC. Batteries have losses during operation, and these losses may be simply represented as a resistance. It is important to understand that the impedance of a battery is a nonlinear, state-dependent quantity.
- **Power**: The power of the battery is generalized through its ability to provide current. The more powerful the battery, the higher the current it is able to provide.

Every battery has different advantages and disadvantages that often can be described based on these characteristics. Chemical batteries have vastly different characteristics based on the chemicals used. The above characteristics do not describe all aspects of a battery's performance but do a decent job in explaining the major differences in many battery types.

1.8. *BATTERY AGING – GENERAL PRINCIPLES*

This thesis focuses on the aspects of battery aging. In every rechargeable battery, it is theoretically capable of infinite life if one was able to continually replace the all the energy it removed. However, as it is known all too well, batteries eventually die. There are two general aging mechanisms for batteries. They can either become unable to provide the energy that is needed to run an operation for the time needed, known as

capacity loss, or incapable of providing the power to run the operation, known as power loss. Through repeated cycles of charging and discharging, there are small and permanent damages that cause the battery to never regain its original capabilities. These effects are called battery aging. Most research has been done to relate the aging characteristics of the battery to actual failure mechanisms inside the chemistry of the battery, like grid corrosion of lead-acid batteries. A summary of these mechanisms can be found in sections 2.1.4 and 2.2.3 'Failure Modes' for NiMH and Lead-Acid respectively. Since there are many possibilities that could limit the battery's performance based on its chemistry, it is difficult to precisely determine which mode of failure is profoundly responsible for capacity loss or power loss.

More generally, a battery can be qualitatively compared to that of a water tank with three imaginary elements. The first element is the water inside the water tank, which would relate to the available charge in the battery, or SOC. The second element is the empty space that can be refilled. This relates to the DOD, but without any considerations of permanent aging. The last element is an unusable section in the form of rocks. This constitutes the accumulated aging of the battery due to the small permanent degradations of the battery. Figure 7 provides depicts this qualitative relationship.

Figure 7: Water Tank with 3 Sections [2]

If the aging mechanism that dominates the degradation of the battery is the capacity loss, then one should imagine a water tank slowly being refilled with more and more unusable rock content after every use. If the aging mechanism that dominates the degradation of the battery is power loss, then one should imagine a water tank that cannot deliver as high a flow as before. Figure 8 below illustrates power loss through the water tank analogy.

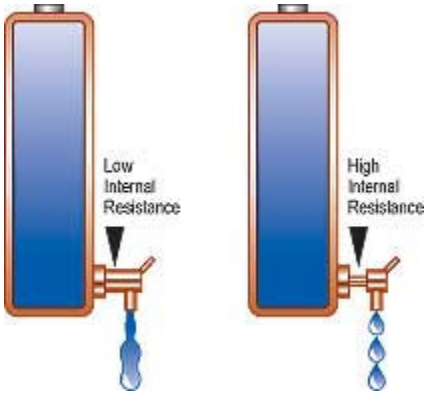

Figure 8: Water Tanks with Different Resistances for Loss of Power [2]

Capacity loss can also come in the form of an elevated self discharge. As a battery is cycled over time, the self discharge characteristics of the battery can increase. Imagine a water tank with holes in the sides which decreases the available water inside the tank.

Figure 9: Water Tank with Self Discharge for Loss of Capacity [2]

1.9. *GENERAL TEMPERATURE EFFECTS*

Temperature is closely related to battery aging and performance, and much research has been done to determine its relationship. Battery performance depends highly on operating temperature. It is very closely associated with the Arrhenius law that simply describes how endothermic chemical reactions occur at a faster rate at higher temperatures. Thus, temperature plays a large role in discharge and charge characteristics of batteries.

This set of experiments will avoid unnecessary temperature effects on aging by controlling the operating temperature in an environmental chamber. This will ensure the aging of the battery will be due to desired aging characteristics. Additionally, keeping all test batteries at the same temperature will allow for accurate comparison because all aging effects and battery performance will be temperature independent.

2. LITERATURE REVIEW

This section provides the literature review for both Nickel Metal Hydride and Lead-Acid batteries. It includes more detailed characteristics as well as battery aging information.

2.1. NICKEL METAL HYDRIDE

2.1.1. *BACKGROUND INFORMATION*

Research on a NiMH battery began in the 1970's, but a stable hydride alloy was not developed until the 1980's. The NiMH battery became commercially available in the 1990's. The motivation to develop a NiMH battery was due to the high potential for improving the current Nickel Cadmium technologies, and as a means for a newer nickel hydrogen battery. Nickel Cadmium has relatively low energy density, and it also has a phenomenon known as memory. Battery memory describes how batteries (most prominently nickel-based batteries) tend to remember the depth of its previous discharge cycles. In a sense, the battery begins to acquire a 'false bottom,' and effectively reduces its available capacity. If the battery is not periodically fully discharged, large crystals will form on the electrodes and the battery's performance will suffer. Additionally, Nickel Cadmium materials are toxic, and the battery has a high self discharge. The NiMH battery was developed to reduce these disadvantages from nickel-based batteries [2].

The NiMH battery offers a higher energy density and environmentally friendly materials. The only shortcoming of this battery compared to that of Nickel Cadmium is its higher

self discharge. While the battery still has some memory characteristics, it is less problematic than Nickel Cadmium [2].

2.1.2. *BATTERY PERFORMANCE*

As briefly mentioned before, the charge and discharge performance of the NiMH battery involves the simple transfer of hydrogen between the electrodes. The electrolyte is so conducive to this reaction that it does not even enter into the full cell reaction of the battery. Figure 10 shows a graphical description of the charge and discharge reactions.

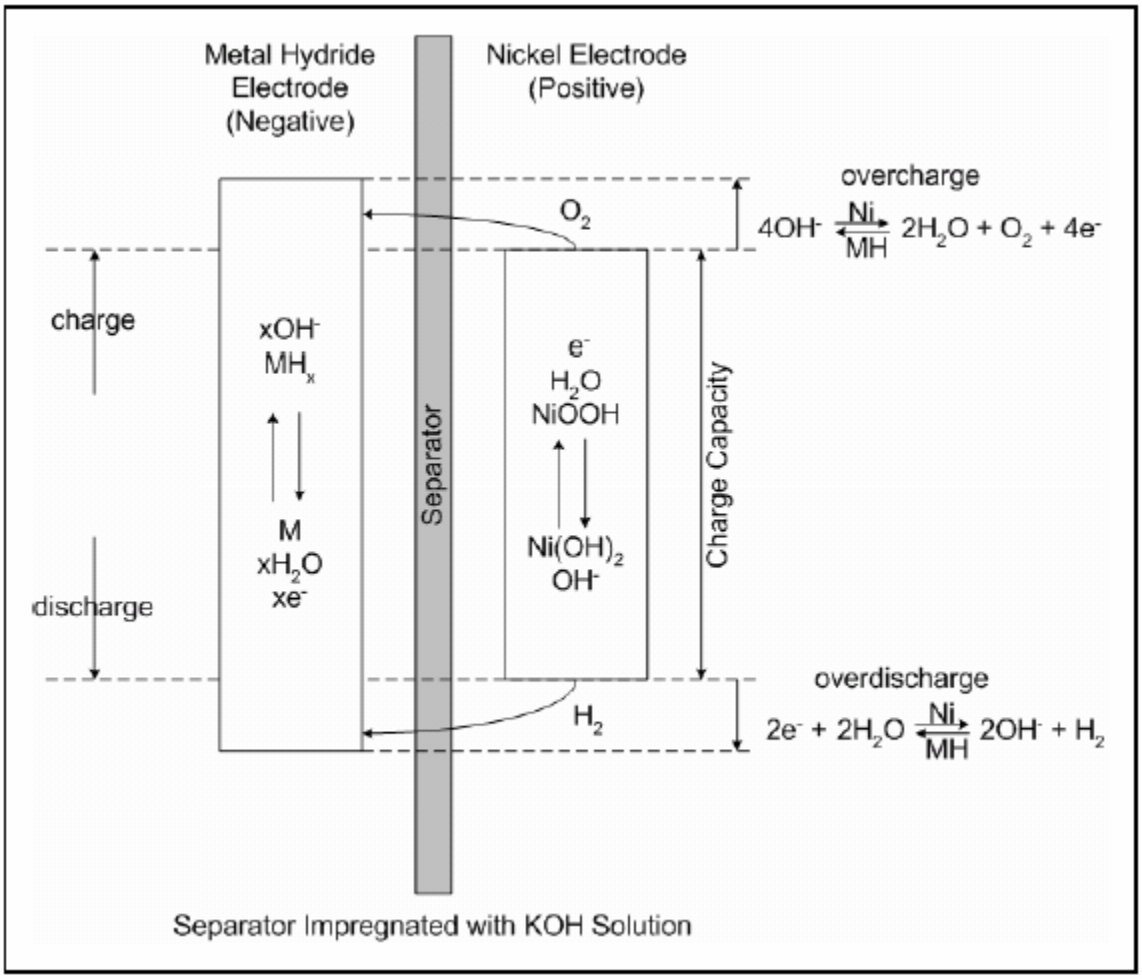

Figure 10: Charge and Discharge Reactions of NiMH [9]

2.1.2.1. DISCHARGE PERFORMANCE

One of the most advantageous characteristics of the NiMH battery is its discharge performance. As the battery discharges, the voltage level remains nearly constant for the entire discharge. As the discharge time increases and the SOC decreases, the voltage level will remain relatively flat until it comes to the 'knee' where the voltage will begin to decrease rapidly. When the voltage reaches the 'knee' there is relatively little charge left in the battery.

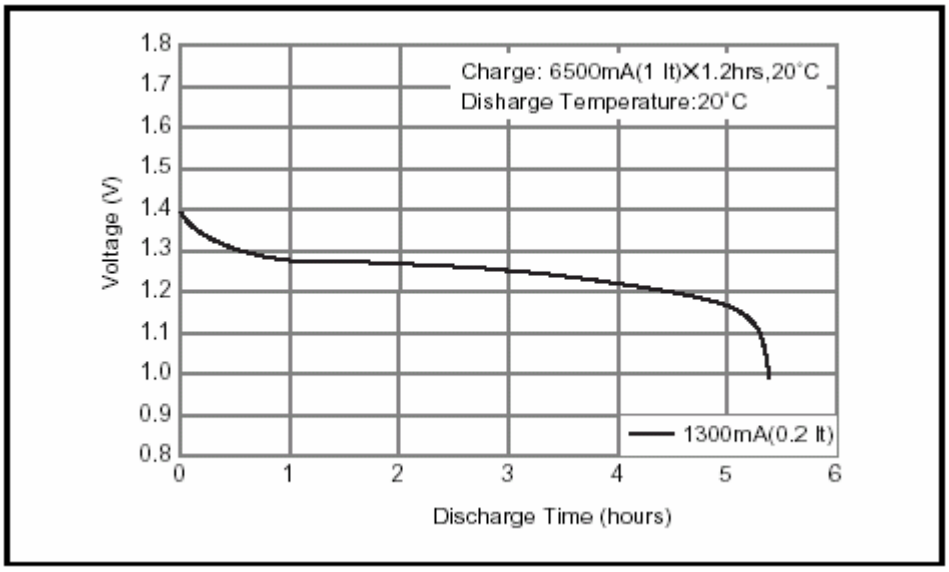

Figure 11: Discharge of NiMH [10]

This voltage curve is heavily dependent on many conditions like ambient temperature and discharge rate from any electric loads. As the temperature decreases, the voltage curve will be shifted downward, or to the left. Similarly, as the load or discharge rate increases, the voltage curve will shift downward. Since one is removing charge at a higher rate, the voltage level will drop accordingly. Additionally, the voltage curve will lose its

'flatness,' or its ability to remain constant over the prolonged discharge. Discharge characteristics are often described through the battery's rated capacity. A 1C discharge of a 6.5 Ah battery is a discharge of 6.5 amps that will provide charge for 1 hour. Likewise, a 2C discharge of the same battery will provide 30 minutes of charge at 13 amps. Figure 12 and 13 below help show these effects.

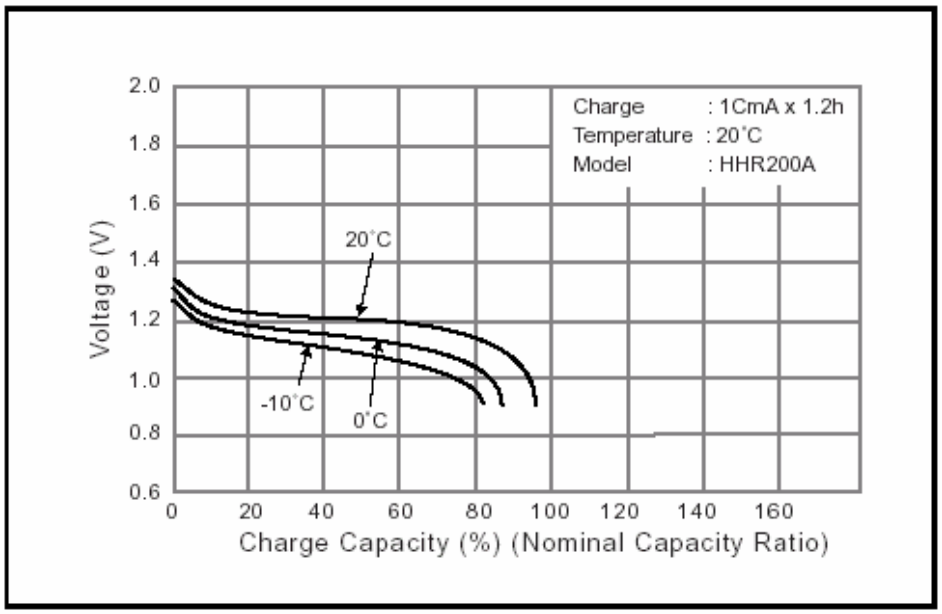

Figure 12: Temperature Effects on Discharge [10]

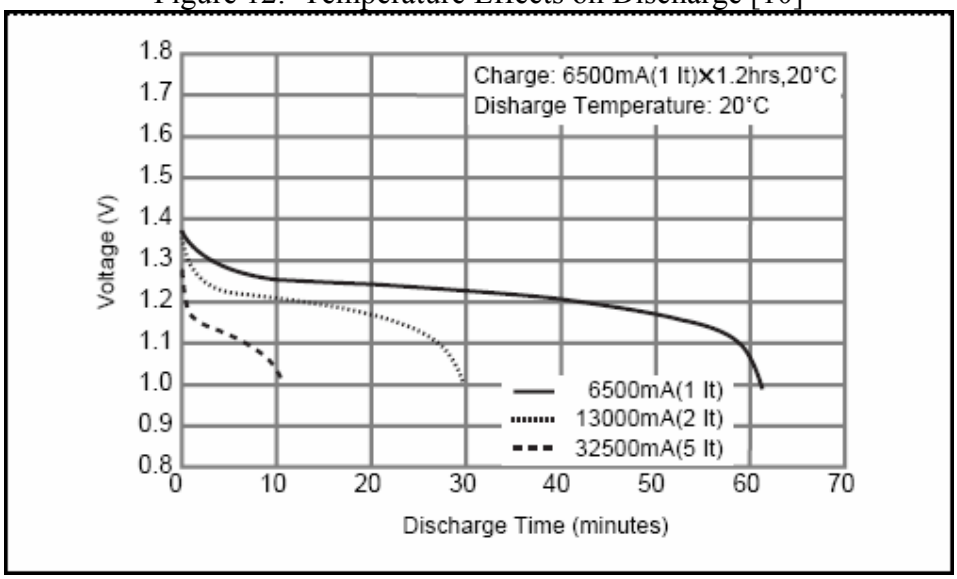

Figure 13: Discharge Rate Effects on Discharge [10]

2.1.2.2. CHARGE CHARACTERISTICS

Charging performance of NiMH is very different than their discharge performance. Initially, the voltage rises quickly at the beginning of a charge. After this initial rise, the voltage gradually increases as charging continues. As the charge of the battery slowly reaches full charge, the gradually increasing voltage may begin to climb even faster. When the voltage reaches its peak, the battery is said to be completely charged. If continued to charge, the voltage will decrease, and overcharging will occur (discussed in the next section, section 2.1.2.3). During charging, the temperature of the battery increases because the charge reaction is exothermic along with the generation of extra heat due to excess charge. In general, there are four indications of when to terminate the charging of a NiMH battery. Commercial chargers use a combination of these indications [2]. They are…

1. Negative change in voltage
2. Rate of temperature increase (usually around $1^{o}C$ per minute)
3. Temperature sensing (for maximum allowable battery temperature)
4. Timers (maximum allowable charge time)

Figure 14 shows the charging performance of a NiMH battery. As the battery reaches full charge and into overcharge, the rate of temperature increase grows, the voltage decreases, and the pressure inside the battery increases.

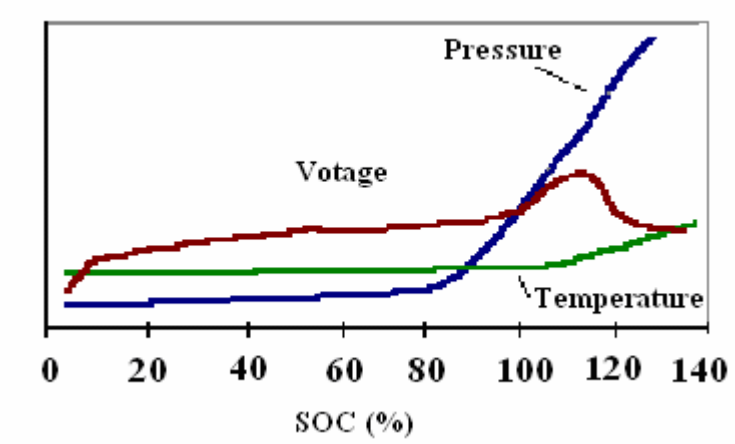

Figure 14: Charging Characteristics [5]

Similar to discharging, temperature and rate of charge have an effect on the charging performance. A higher temperature will cause the voltage curve to shift downward. This is due to the decrease of resistance (or increase in efficiency). As the charge rate increases the voltage curve will increase because more charge is being supplied to the battery at a higher rate.

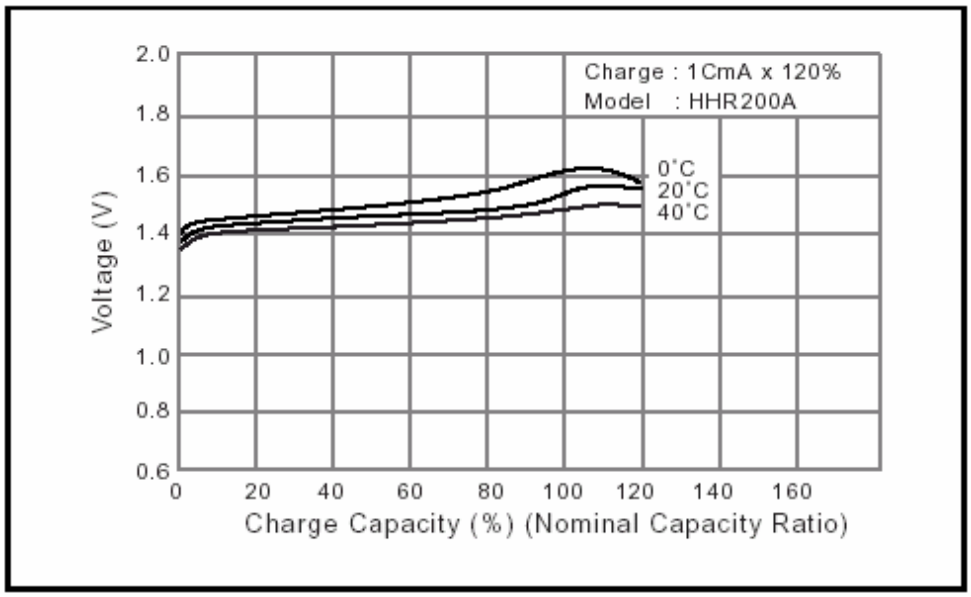

Figure 15: Temperature Effects on Charging [10]

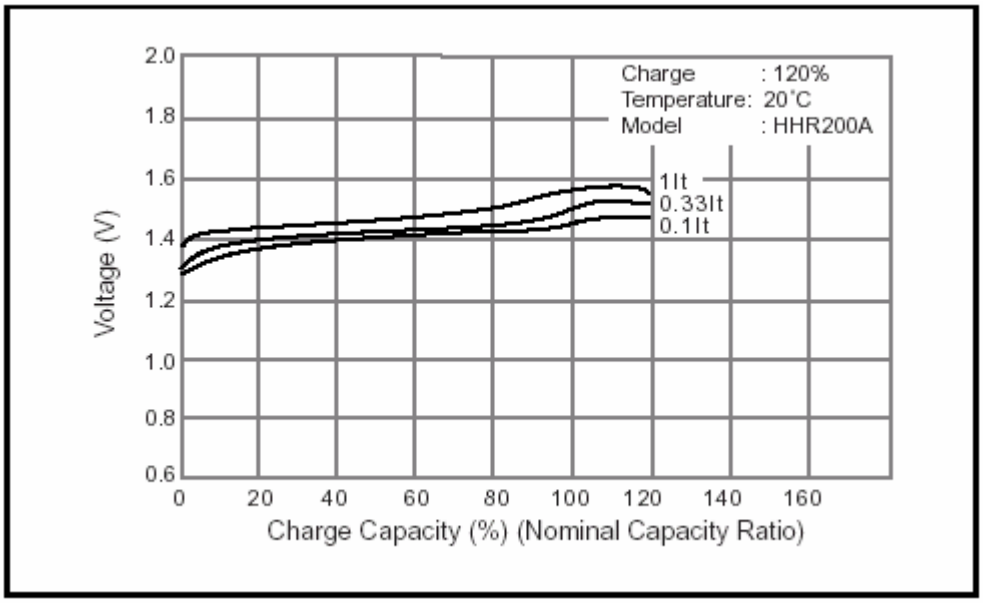

Figure 16: Charge rate effects [10]

Figure 17 shows the entire cycle of a NiMH battery based on SOC representing a typical charge and discharge profile.

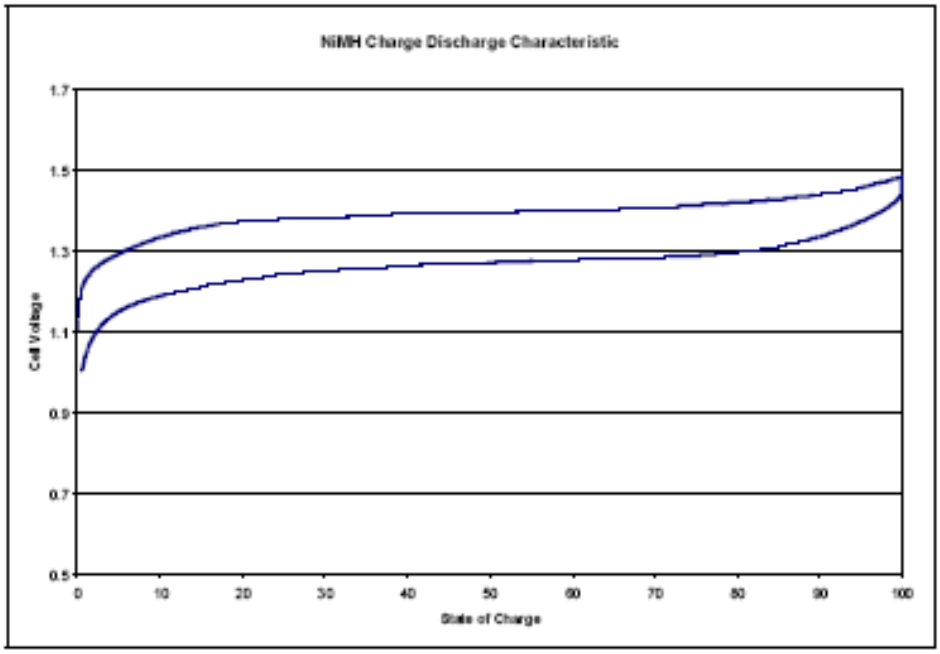

Figure 17: Charge and Discharge of NiMH Battery [9]

2.1.3. *ABUSIVE OPERATION*

The common abusive treatment on NiMH, and of all batteries in general, is overcharging and overdischarging. The battery can be severely damaged if precautions are not taken to avoid overdischarge and overcharge. The cell undergoes different chemical reactions that allow the battery to, in a sense, handle abusive conditions and limit severe and permanent effects [2]. These reactions, which can also be seen in Figure 10(cell reaction), are shown in Table 4. The reactions are oxygen recombination reactions.

Table 4: Overcharge and Overdischarge Cell Reactions

Overdischarge:
$2H_2O + 2e^- \leftrightarrow H_2 + 2OH^-$
Overcharge:
$4OH^- \leftrightarrow 2H_2O + O_2 + 4e^-$

For overdischarge, the "net result is no reaction but heat and some pressure are generated in the cell. The ability of the NiMH cell to tolerate overdischarge is very important for large series strings of batteries since capacity mismatches may allow some cells to be overdischarged" [9]. For overcharge, the result is also heat generation. The heat generation from the reaction equals the energy input. "This occurs at the expense of increasing the stored charge in the battery. If the rate of charge exceeds the rate of recombination, then an increase in cell pressure will result" [9]. Although the NiMH has the slight ability to tolerate moderate overdischarging and overcharging, especially for instances when batteries are connected in series and the possibility for correction due to capacity differences, it is strongly recommended to avoid if at all possible.

2.1.3.1. OVERDISCHARGE

The battery can only handle up to a certain point of discharging before it begins to have severe and permanent effects. Once all the charge in the battery has been removed, continuing a discharge will begin to reverse the electrodes in the battery. When a battery is permanently damaged due to overdischarging, the electrodes are completely reversed and hydrogen gas builds up inside the cell, often causing the battery to vent (release of gas). Usually, there is a specified lower voltage limit for discharging. This limit can vary from battery to battery, but a general limit for all NiMH is 0.9V/cell [1].

2.1.3.2. OVERCHARGE

As the battery charges, the reaction is exothermic, and heat begins to grow inside the battery. When the battery reaches full charge and charging continues, almost all the electrical energy is transformed directly into heat. This causes the temperature to rise even faster. The pressure inside the battery will greatly increase along with the temperature. The pressure continually increases as gas is generated during the charge reactions. These effects are results of overcharging. If overcharging persists, the pressure will grow enough to vent the battery, which results in poorer battery performance. If the battery does not have a safety vent, then the battery could explode [1].

2.1.4. *FAILURE MODES*

As in all chemical batteries, there are many modes of failure associated with the chemistry inside the battery. In general, these modes cause damage to the battery. Some damages can be rectified, while others remain permanent. The main modes of failure for NiMH batteries are the following:

1. Surface Corrosion of Negative Electrode [12]
2. Decrepitation of Alloy Particles [12]
3. Loss of Water in the Electrolyte (Separator Dry-Out) [9]
4. Crystalline Formation [2]
5. Cell Reversal [9]
6. High Self Discharge [2]
7. Shorted Cells [2]

Some of the failure modes occur when the battery undergoes abusive conditions, but others occur through normal cycling. Some of these failure modes can be restored through various procedures to prolong the battery's life. However, any combination of these failure modes can occur in the battery. The slow accumulation of the permanent damage of the battery due to these modes is considered battery aging.

Surface Corrosion of the negative electrode is generally the main cause of NiMH aging. The battery can be operated under ideal conditions through 'small' cycles (with a periodic full discharge to reduce memory effects) and still not be able to avoid corrosion of the negative electrode. This failure mode does not cause catastrophic failure, but it

does cause capacity loss. The active material of the metal hydride is very conductive, so corrosion at the surface results in a reduction of capacity, as well as, reduction of ability to supply power. The corrosion also has a side effect of reducing the content of water in the electrolyte, which is described later in this section [9].

Decrepitation of Alloy Particles often occurs along with surface corrosion. Normal aging of the battery will cause decrepitation of the negative electrode. This is not technically a failure mode by itself. It only increases the surface area of the electrode, which at first can increase conductivity by increasing the area available for the chemical reactions. However, it also increases the area available for surface corrosion. Some literature suggests that alloy decrepitation and surface corrosion of the negative electrode is the main cause of normal battery aging and can be quantified as a function of DOD with EIS [12]. This is discussed in section 2.1.5 'Aging of NiMH.'

Loss of Water in the Electrolyte can be caused by a number of conditions, such as surface corrosion, but is mostly encountered during abusive operation. Operating in abusive conditions whether it is overcharge, overdischarge, or improper temperature ranges can cause the pressure inside the battery to build and the gas to vent. Venting the gasses reduces the battery's ability for electrolysis, and thus reduces its power. Another contribution to loss of water in the electrolyte is diffusion through the case only if the case is plastic. This is not a problem with steel constructed casing [9].

The *Crystalline Formation* is the cause of battery memory. If the NiMH battery is not periodically discharged to 0% SOC, then crystals will form around the electrodes of the battery. A full discharge usually restores the electrode surface. However, if not properly maintained, the crystalline surface will grow and can damage the separator. If the growth reaches through the separator, the battery will simply short circuit and be rendered useless [2]. The figure below shows the crystalline formation on a Nickel Cadmium battery electrode. The crystals have grown from around 1 micron to 50-100 microns. After a pulsed charge, the crystals were reduced to 3-5 microns.

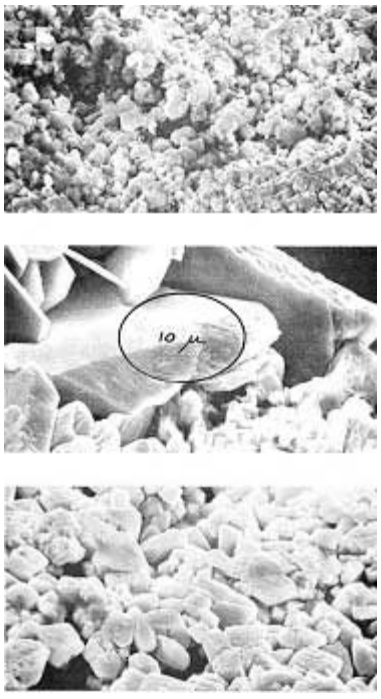

Figure 18: Crystalline Formation on Nickel Cadmium Electrode [2]

Cell Reversal only occurs through abusive operation, most notably, overdischarging. This is when the electrodes inside the cell become reversed in charge, rendering the battery unable to store and supply energy.

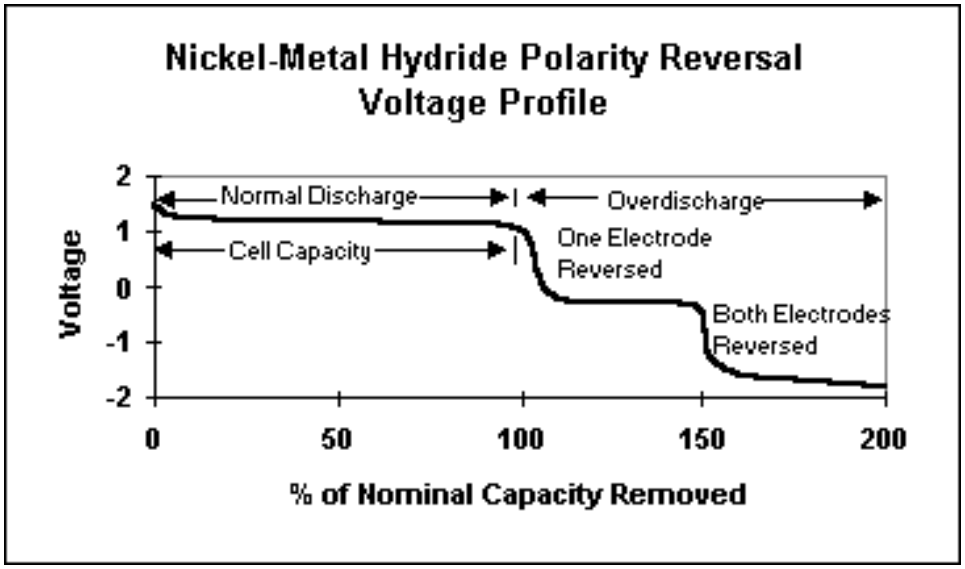

Figure 19: Cell Reversal through Abusive Discharging [13]

High Self Discharge will not cause catastrophic failure, unless it is to the extreme of an electrical short circuit. All batteries are affected by self discharge, NiMH being one of the highest. Elevated self discharge occurs along with the growth of crystalline formation. As the crystalline forms out from the electrode, it begins to mar the separator, thus allowing for an easier path from one electrode to the other [2]. Accordingly, the higher the self discharge, the lower the capacity of the battery.

Shorted Cells are generally rare and sometimes unexplainable. It has been suspected that foreign particles may have contaminated the separator during manufacturing causing the shorted cells of new batteries. As manufacturing processes improve, shorted new batteries have reduced in number. Cell reversal can also cause shorted cells when in series with other batteries. As mentioned above, the growth of crystals through the separator will also cause an electric short [2].

2.1.5. *AGING OF NIMH*

Battery aging generally means both or one of the following performance levels to depreciate: Power and Capacity. Aging occurs through regular cycling of the battery, calendar time, and abusive operation [9]. Any combination of the failure modes listed above causes the degradation of the battery. Much research has been done to relate battery aging characteristics to DOD and operating temperature.

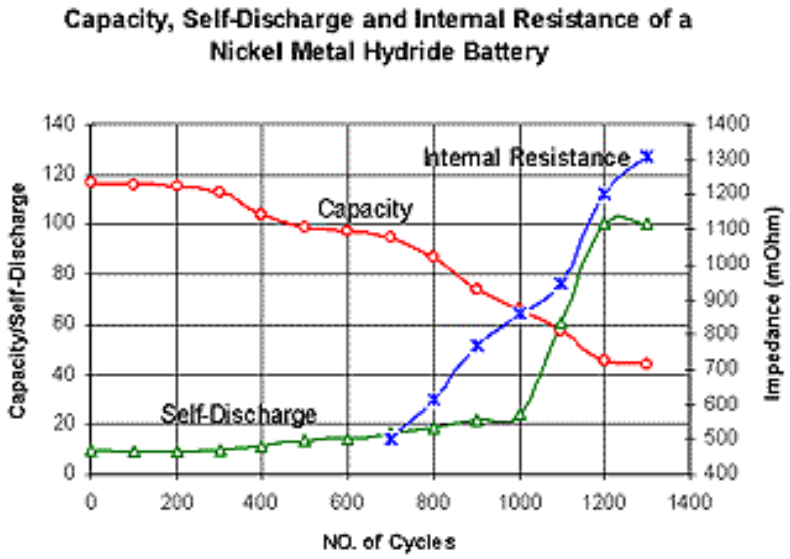

Figure 20: Typical Cycle Life of NiMH Batteries [2]

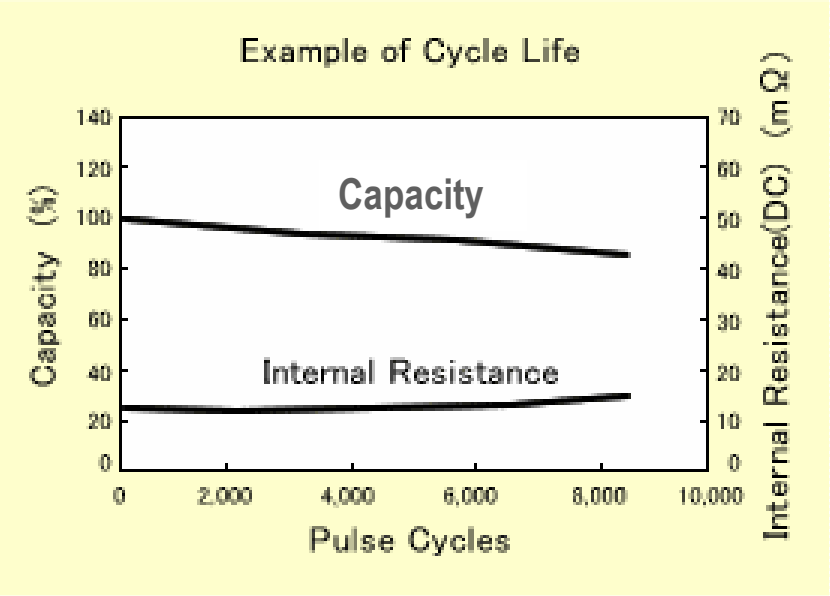

Figure 21: Typical Cycle Life of NiMH Batteries 2 [14]

2.1.5.1. DEPTH OF DISCHARGE

Figures 20 and 21 represent the normal aging of the battery with predefined and repeated cycles of the same DOD. Figure 22 shows how different DOD's on the battery will affect its cycle life. If the battery undergoes full discharges of 100% DOD, the battery will then only be able to provide a few hundred of these cycles.

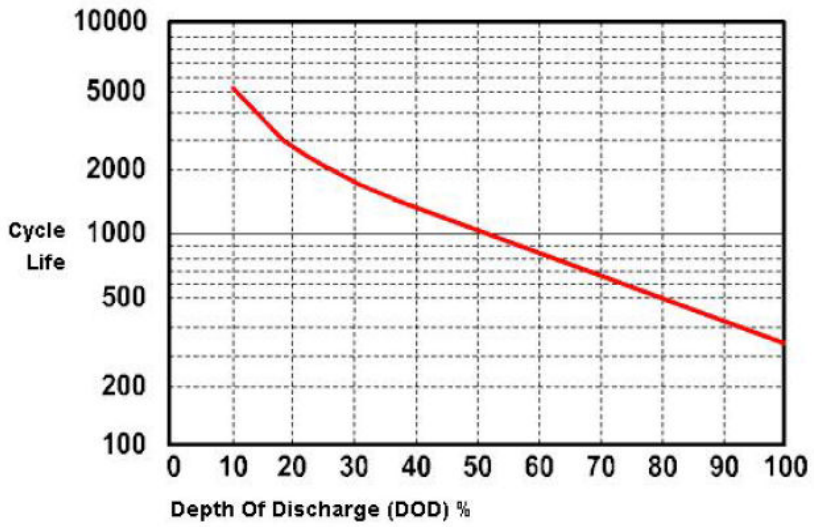

Figure 22: Depth of Discharge Effect on Cycle Life of NiMH Batteries [15]

2.1.5.2 TEMPERATURE

Operating temperature has a bitter-sweet effect on battery performance. Increasing the operating temperature will decrease the internal resistance of the battery, and thus increasing battery efficiency. However, increasing the temperature will also have adverse effects on battery life. Figure 23 shows how increasing the operating temperature can have a large impact on battery cycle life.

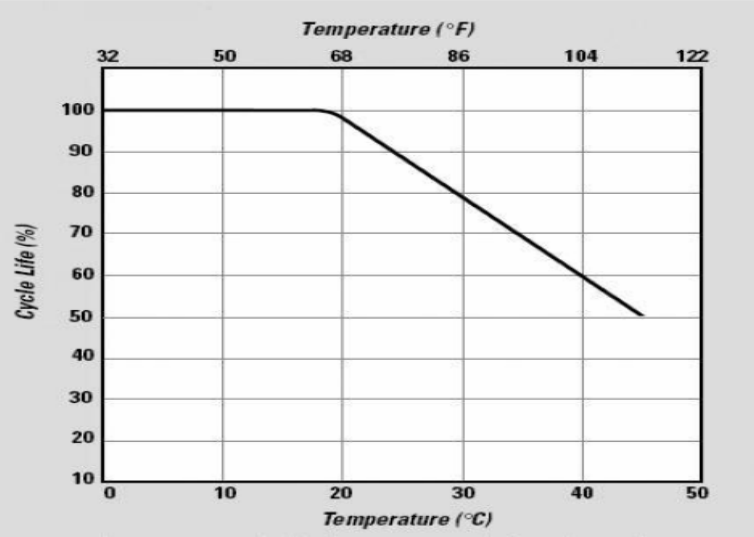

Figure 23: Temperature and Cycle Life of NiMH Battery [15]

2.1.5.3. DISCHARGE RATES

It is expected that the rate of discharging the battery will also have affects on a battery's cycle life. The battery stresses more when higher currents are demanded of it. Some literature suggests that the corrosion of the electrode, which is main cause of normal battery aging, is independent of discharge rate [12]. Other literature suggests the opposite in saying that higher discharge rates do have adverse effects on a cell's expected lifetime [15]. It is possible that drawing high current can cause uneven distributions of charge throughout the plates of the battery causing higher stress on the battery, since each plate does not have the same conductivity [14]. The research of this paper hopes to breach the possibilities of battery aging dependence on discharge rate.

2.1.5.4. CAUSES OF NORMAL AGING

Under the most typical circumstances, it has been shown that much of the aging is due to the surface corrosion of the negative electrode. Therefore, the main hindrance of battery

life is capacity loss. It is generally accepted that the battery has reached its end-of-life when it reaches 80% of its rated capacity. Likewise, the power fade of the battery is from the loss of water in the electrolyte during corrosion. The NiMH battery already has reasonably high power compared to other batteries and for their applications. Thus, the NiMH battery will be first limited by the capacity loss and not the power loss. Figures 24, 25 and 26 show through a scanning electron microscope the decrepitation of the alloy after cycling. As described above, the decrepitation allows for more corrosion of the electrode and thus more permanent aging.

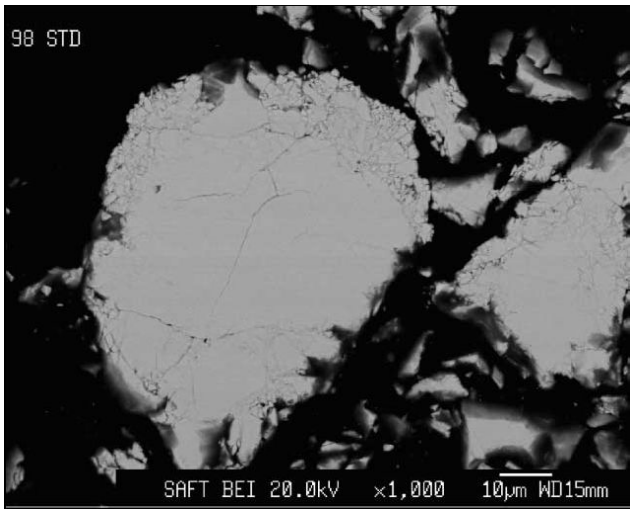

Figure 24: Initial MH Electrode Surface [12]

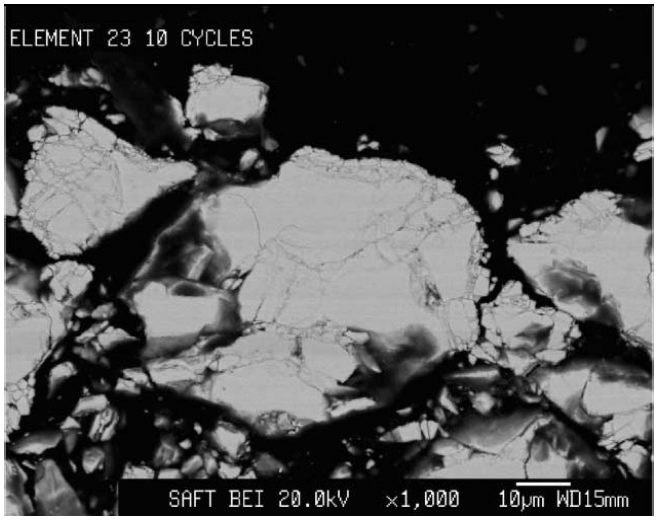

Figure 25: MH Electrode After 10 Cycles (9.6 Ah Discharged) [12]

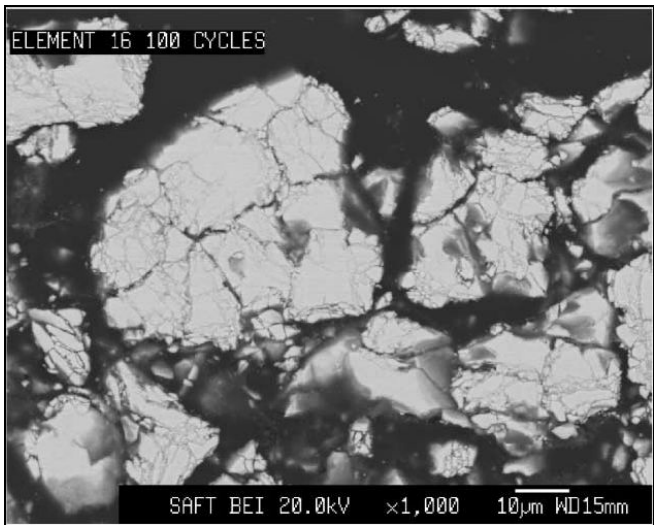

Figure 26: MH Electrode After 100 Cycles (96 Ah Discharged) [12]

2.1.6. *MOTIVATION*

The research presented in this thesis specifically attempts to transcend traditional aging research by characterizing NiMH aging directly to real HEV cycles. A set of basis cycles can be studied to quantify aging for real HEV operation. These basis vectors will then be characterized by how they age the NiMH batteries, thus attempting to create a method to predict aging of NiMH batteries in HEV applications.

2.2. LEAD-ACID

2.2.1. *BACKGROUND INFORMATION*

Lead-Acid batteries are the oldest rechargeable batteries in existence. The rechargeable Lead-Acid battery was invented by French physicist Gaston Planté in 1859. It is even speculated that the battery may be much older than this. Some believe that this lead acid chemistry was used by the Egyptians to electroplate antimony onto copper over 4300 years ago [2].

Even with the new high energy density batteries like NiMH and Lithium Ion emerging into the commercial markets, Lead-Acid batteries still dominate in automobiles as starter batteries and large uninterruptible power supply systems. The Lead-Acid battery is inexpensive and simple to manufacture. It has one of the lowest self discharge rates of all rechargeable battery systems. It has no memory, and is capable of high discharge rates. The Lead-Acid battery is limited by low energy density, and limited number of full discharges, along with an environmentally unfriendly electrolyte [2].

2.2.2. *BATTERY PERFORMANCE*

The cell operation of a Lead-Acid battery is slightly more complicated than that of the NiMH battery. Its electrolyte does enter into its full cell reaction, unlike the NiMH, which means the state of the electrolyte will affect the battery performance.

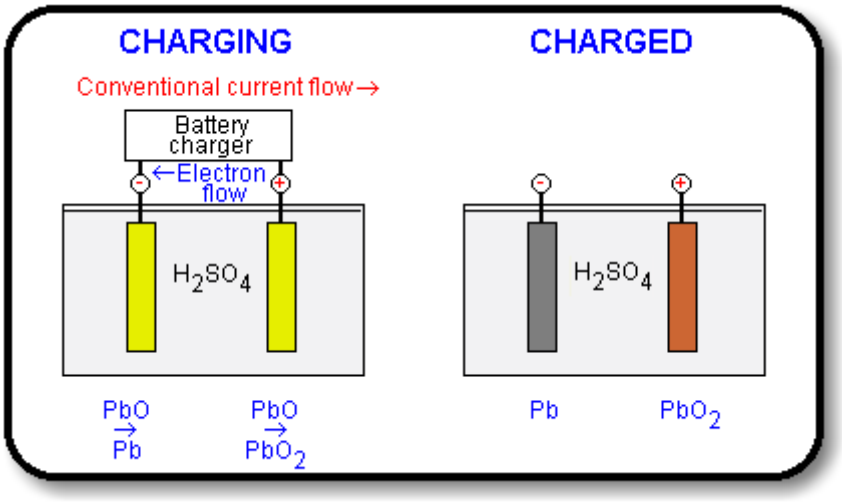

Figure 27: Charging of Lead-Acid Battery [16]

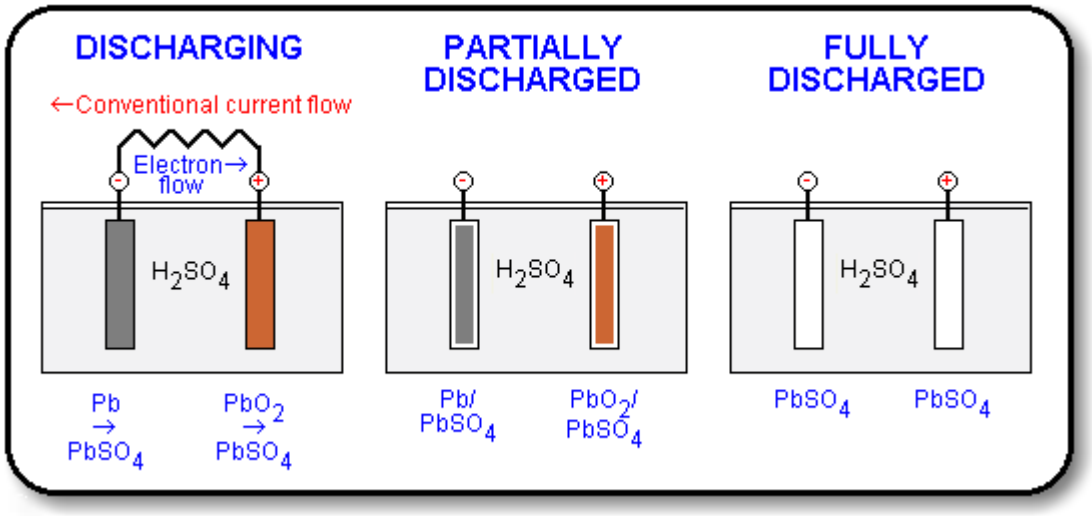

Figure 28: Discharging of Lead-Acid Battery [16]

2.2.2.1. DISCHARGE PERFORMANCE

The Lead-Acid battery has a very acceptable discharge profile for rechargeable batteries. As the battery discharges, there is an initial drop and partial recovery in voltage known as the coup-de-fouet, and then the voltage gradually decreases with time. Towards the end of the discharge as the state of charge of the battery reaches very low values, the voltage declines very rapidly, which can be called 'knee' of the profile. To compare with NiMH,

the discharge performance is very similar in profile if one removes the coup-de-fouet phenomenon; however, the Lead-Acid battery does not maintain as flat a voltage level as the NiMH. Figure 29 provides a typical discharge of a Lead-Acid battery.

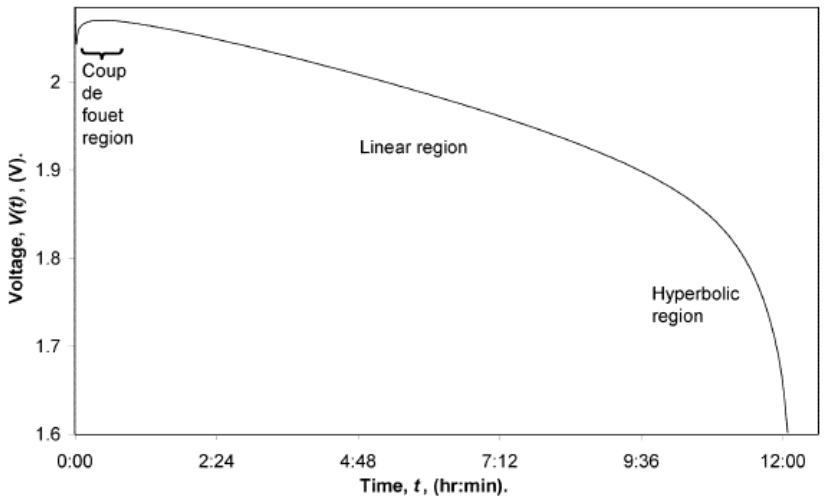

Figure 29: Typical Discharge of Lead-Acid Battery [17]

The discharge profile of these batteries is also dependent on temperature, and discharge rate much like that of NiMH; as the temperature changes, the performance of the battery changes. Figures 30 and 31 provide examples of discharge performance with different temperatures: as the temperature decreases, the capacity of the battery decreases.

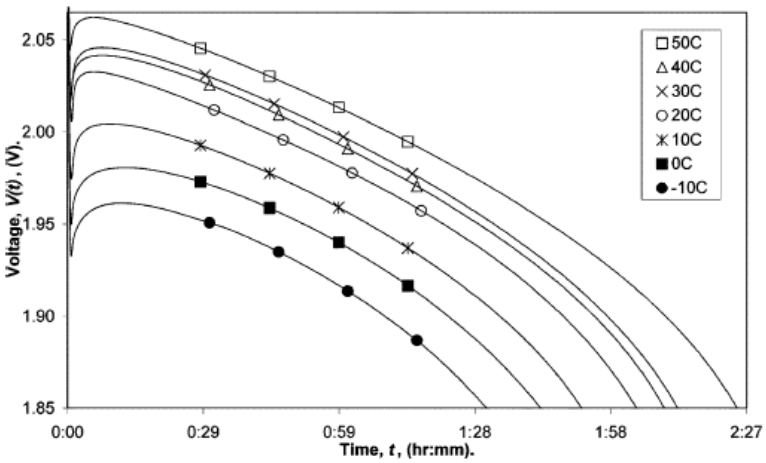

Figure 30: Temperature effects on lead-acid battery discharge [17]

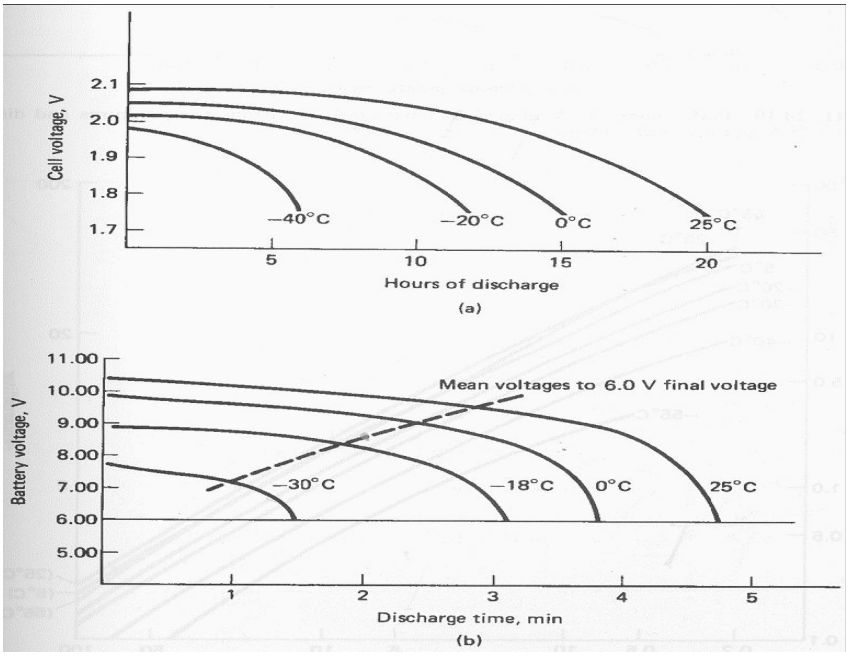

Figure 31: Temperature effects on lead-acid battery discharge 2 [18]

The discharge rate of the battery affects the voltage curve in a similar fashion. As the discharge rate increases, the voltage curve shifts downward much like the NiMH battery.

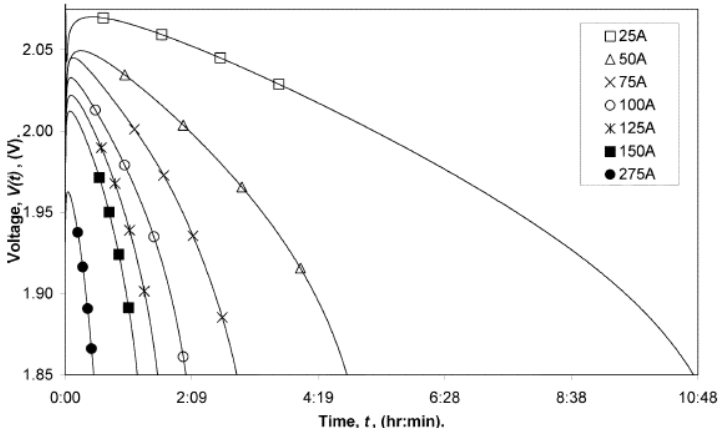

Figure 32: Discharge Rate Effect on Discharge Performance [17]

2.2.2.1.1. *THE PEUKERT EFFECT*

For Lead-Acid batteries, however, there is not a linear relationship with the discharge rate and capacity. For NiMH, the C-rate is a very good indication of the amount of time one could deliver charge. The Lead-Acid battery encounters what is known as the Peukert Effect with higher discharge rates. This is not to say the Peukert Effect does not affect NiMH, it is just practically negligible for that battery with loads under 1C. For example, if one discharges the Lead-Acid battery at 1C, it will take less than 1 hour to discharge completely. Generally, one has to discharge at as low as 0.05C in order to proportionally relate the time and the rated capacity of the battery. Table 5 provides some example discharges of a Lead-Acid battery.

Table 5: Estimated Discharge Time of a 10Ah Lead Acid Battery [2]

Discharge current	C-Rate	Discharge time	End of discharge
0.5A	0.05C	20h	1.75V/cell
0.1A	0.1C	10h	1.75V/cell
2A	0.2C	5h	1.70V/cell
2.8A	0.28C	3h	1.64V/cell
6A	0.6C	1h	1.55V/cell
10A	1C	0.5h	1.40V/cell

The Peukert Effect can be portrayed through an equation relating available capacity and discharge current. It is most commonly modeled as an exponential function where each battery type has its own Peukert constants to be inserted into the equation. Lead-Acid batteries generally have a Peukert Number around 1.4 [2]. The closer the number is to 1, the less Peukert Effect on the battery.

Table 6: Peukert Equation [4]

Peukert Equation:
$$Q = K \cdot I^{1-n}$$

Q is the capacity, and I is the current. K and n are the battery characteristic constant and the discharge rate sensitivity exponent, respectively. The equation quantifies the how the apparent capacity of the battery decreases disproportionately to a discharge rate increase [4]. It also can be used to describe the internal resistance of the battery based on its efficiency. A value close to 1 indicates efficient battery performance with little losses

and thus a lower internal resistance [2]. Figures 33 and 34 show the Peukert Effect on discharge and capacity. Figure 33 shows voltage curves shifting downward due to discharge rate. Due to the Peukert effect, the 1C discharge does not take 1 hour to completely discharge the battery. It only takes about half-an-hour since the battery is not as efficient at the higher rate. This inefficiency can be expressed through the effective capacity provided through the discharge. If one looks at the final value of time, and multiplies by the discharge rate, the capacity discharged does not equal the rated capacity. Figure 34, provides an example for the change in effective capacity due to the Peukert Effect on NiMH batteries. A similar effect also applies to Lead-Acid batteries.

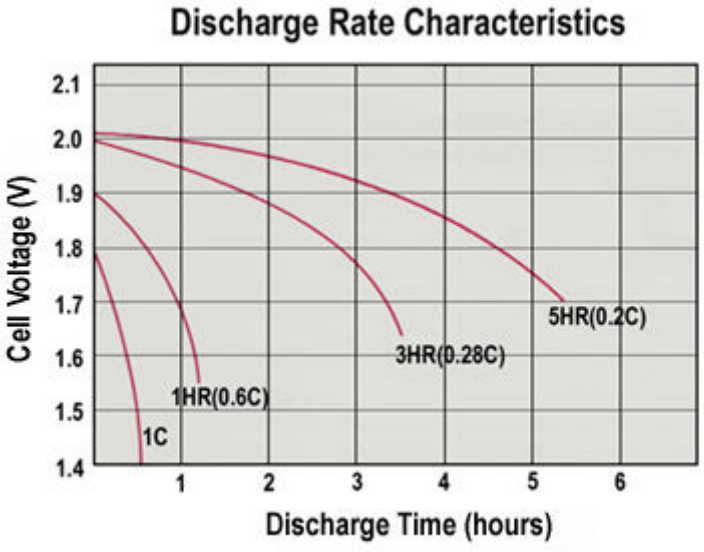

Figure 33: Peukert Effect on Lead-Acid [2]

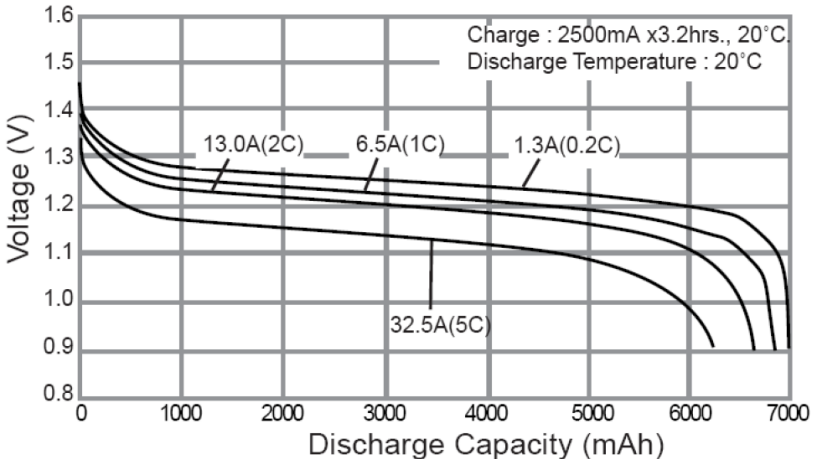

Figure 34: Peukert Effect on NiMH (6.5Ah) [19]

2.2.2.1.2. *COUP-DE-FOUET*

The initial dip that occurs in the Lead-Acid battery's discharge is called the coup-de-fouet. It usually occurs when the battery is on a long-term float charge and then suddenly applied to a load [8]. A float charge, also known as a trickle charge, is very common in operating lead-Acid batteries. It is a charging technique that keeps the Lead-Acid battery continually at full charge by charging it at the same rate the battery self discharges. The discharge process converts lead dioxide into lead sulfate. This chemical reaction is better facilitated when the lead sulfate molecule is generated. In other words, during the initial moments of discharge, the reaction is slightly less efficient than when the lead sulfate molecules are created [8]. Thus, an initial voltage drop is seen in the discharge, and then it recovers as the chemical reaction becomes more efficient with the generation of lead sulfate.

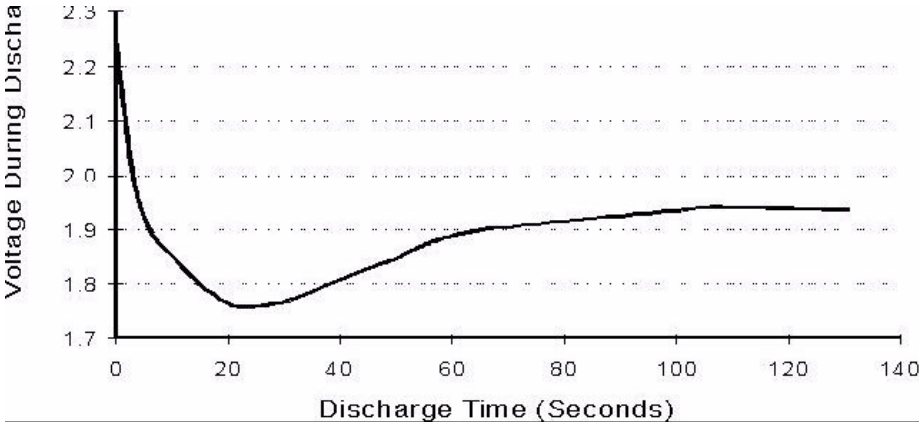

Figure 35: Voltage Dip known as the Coup-de-fouet [8]

2.2.2.1.3. *SURFACE CHARGE*

This battery characteristic does not describe the discharge or charge performance of the battery, but cannot be ignored in discussion of Lead-Acid batteries. Surface charge occurs more on Lead-Acid batteries than that of NiMH and most other batteries. It is simply the build-up of charge on the surface of the electrode as the battery either charges or discharges. For research that deals with rapid dynamic testing, surface charge can be quite cumbersome. It has the ability to make a good battery appear bad, and a bad battery appear good through open circuit voltage measurement. If one measures the voltage of the battery directly after a charge, then the voltage will appear very high and possibly above 'overvoltage' criteria. This is because of the charge build-up on the electrode. It is recommended to wait at least 4-12 hours for the charge build-up to dissolve, and then measure the open circuit voltage. Additionally, the higher the charge or discharge rate, the larger accumulation of surface charge will be.

2.2.2. *ABUSIVE OPERATION*

The Lead-Acid battery is well known for its tolerance of abusive conditions. The Lead-Acid battery is reasonably forgiving on temperature extremes; however, higher temperatures will shorten life [2]. Even when operating the battery in reasonable temperature regimes, there are certain conditions that can damage the battery. Much like NiMH batteries, discharging past a certain limit will damage the battery, charging past a certain limit will damage the battery, and improper float charging will damage the battery. Battery damage will drastically shorten the cycle and calendar life of the battery and is to be avoided.

2.2.2.1. OVERCHARGE

Since the Lead-Acid battery has such a long history, there are some basic, almost fool-proof methods, for charging the battery. One method, which is often used by commercial battery chargers, is a multi-stage charge method that initially controls the charge current, and then switches to control a voltage limit. At first the battery will rapidly charge with a reasonably high current until it reaches a specified voltage, then the charger will switch to a controlled voltage and the battery will slowly charge to full capacity. Figure 36 depicts this process. Often the battery will be placed on float charge until it is used.

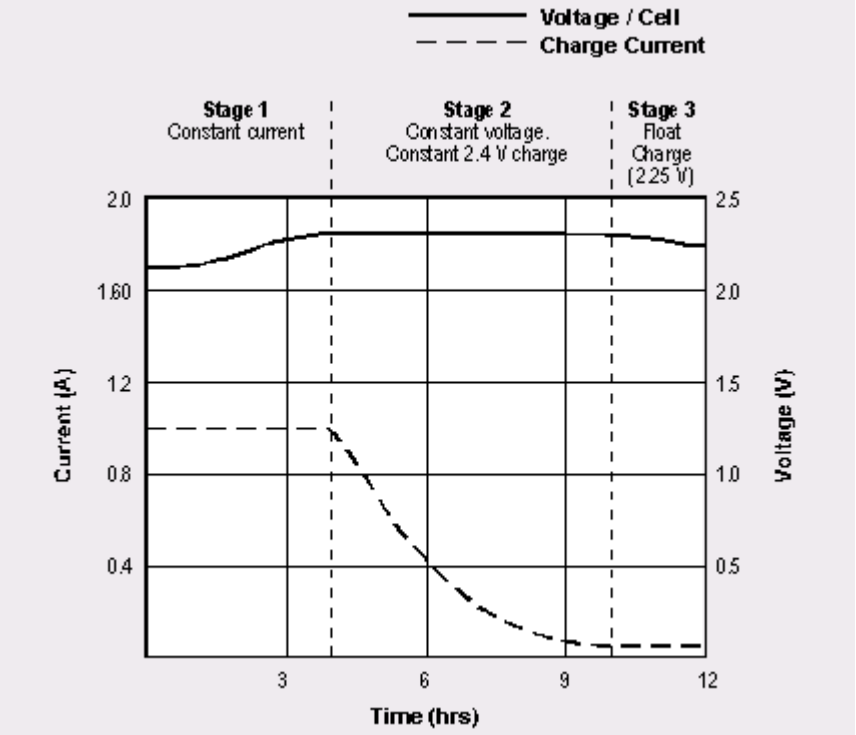

Figure 36: Multi-Stage Charge Method [2]

Another method involves just the use of a power supply. One can charge a Lead-Acid battery with a constant voltage threshold and limit the current to a maximum ampere level. Other processes include pulse charge methods which some believe reduce the amount of cell corrosion during charging [2].

With any charge method, the limits are applied to prevent overcharging. Overcharging will cause cell corrosion at the electrodes which will cause permanent damage [2]. Some pulse charge techniques claim to reduce corrosion, but the effectiveness has not been widely accepted. Overcharging for a Lead-Acid battery comes in two forms: current and voltage. Charging at too high of a current will cause more corrosion and overcharging, and likewise charging at too high of a voltage will do the same. Manufacturers will

specify their recommended charge procedure. Overcharging accelerates failure modes of the battery, which can lead to gassing. These failure modes, including grid corrosion, are discussed in Section 2.2.3.

2.2.2.2. OVERDISCHARGE

The Lead-Acid battery should be limited at a specified voltage to terminate a discharge to prevent cell damage. Regular operating conditions generally place this limit at 1.75V/cell [2]. Thus, for a 12V battery, a discharge should terminate at 10.5V. Going beyond this limit will begin to overdischarge the battery. Such abuse can cause cell reversal, or even short circuiting of the battery. These failure modes will be discussed in more detailed in subsequent section 2.2.3 'Failure Modes.'

2.2.2.3. FLOAT VOLTAGE VARIATION

Float voltage is a fixed voltage limit that allows a fully charged battery to charge at the same rate it discharges. The battery is thus 'floating' at full charge. Variation of the float charge is closely related to overcharging. If the float voltage is too high and charging occurs at a faster rate than the self discharge of the battery, then overcharging occurs. Additionally, if the float charge is not equal to the self discharge of the battery, then this is known as undercharging and can damage the battery. Undercharging can lead to sulfation which leads to capacity loss and permanent damage. This sulfation is different from the sulfate that forms during normal discharging.

2.2.3. *FAILURE MODES*

The failure modes associated with the Lead-Acid battery are very similar to the modes associated with the NiMH batteries. The Lead-Acid battery does have, however, a few more modes of failure. Some of these failures are not catastrophic and can nearly be fully restored. The main modes of failure for the Lead-Acid battery are the following:

1. Corrosion of Battery Components [8] – positive grid, negative strap
2. Loss of Water in the Electrolyte (Dryout) [2]
3. Loss of Active Material [2]
4. Sulfation [2]
5. Cell Reversal [8]
6. High Self Discharge/ Shorted Cells [2]
7. Hydration [8]
8. Thermal Runaway [8]

Corrosion of the positive grid contributes to most battery degradation. This failure mode takes place through normal operating conditions, but will accelerate if the battery is operated in abusive conditions like high temperature and overcharging. Corrosion can also occur at the negative strap, but is generally rare. *Corrosion of the negative strap* occurs in absorbed glass matt VRLA batteries. The negative strap is often not completely immersed in the electrolyte and is generally exposed to a hydrogen environment in the void space above the negative plates. Since the negative plates are often depolarized, the

negative strap can corrode and fracture causing premature failure of the battery. Some manufacturing processes now wrap the negative strap in absorbed glass matt to prevent corrosion of the negative strap. Corrosion of the battery components leads to both loss of capacity and power because the build up of corrosion reduces the surface area available for the active material to interact with the electrolyte [8]. This effect is noticed more profoundly in loss of capacity since it greatly reduces the capability to store charge.

Loss of water in the electrolyte has generally the same effect for Lead-Acid batteries as it does the NiMH batteries and most any other chemical batteries. It reduces the conductivity of the chemical reactions, which generally means an increase in internal resistance and consequently a loss of power. Since the electrolyte plays a large role in the reactions inside the Lead-Acid battery, it also accounts for loss of capacity. If the battery undergoes venting, then there will be less water in the electrolyte. Water loss can also occur by diffusion through a plastic battery casing. Vented Lead-Acid batteries can be accessed to restore the water supply in the electrolyte, but VRLA batteries cannot be refilled. Many call this failure mode *starved electrolyte* since it is 'starved' of water. The corrosion process reduces the amount of water in the electrolyte since it is used in the corrosion process [8].

Loss of active material on the positive electrode will accelerate the loss of capacity. This generally only occurs in overcharging, when excessive gassing may knock active material off a partially corroded positive plate [8].

Sulfation occurs through the discharge process and is broken down through the charge process. If the battery undergoes abusive conditions, sulfation can become permanent. Higher discharge rates also increase the growth of sulfation. Operating at high temperatures, leaving the battery on a low state of charge, or simply at open circuit for extended periods will increase sulfation. It is generally not a problem unless it crystallizes into an inactive form which cannot be re-broken through charging. Permanent crystallization is possible in any circumstance in which sulfation occurs. Sulfation can lead to both failure modes. Since it removes the available surface area for the chemical reaction it will effectively increase the battery's internal resistance. It will usually permanently manifest itself as a loss of capacity since most sulfation is removed during charging and a reduction in charging efficiency will reduce the ability to store energy.

Cell reversal is very rare with Lead-Acid batteries since they are generally very tolerant to abusive operation, but it is still possible. Cell reversal could happen through a very abusive overdischarge process, but mostly occurs if the cells inside the battery do not match. A weak cell will discharge more quickly and could cause reversal if discharged too low.

High self discharge is also not common in Lead-Acid batteries because they remain to be one of the least self discharging batteries available [2]. A Lead-Acid battery only self discharges at a rate of approximately 5% a month which is much slower than the nickel-based and lithium technologies. Repeated deep cycling of the battery will increase the

rate of self discharge. Other failure modes like crystalline formation due to sulfation that mars the separator could cause high self discharges and a short circuit. Additionally, if the negative strap corrodes and falls over the top of the separator and connects to the positive plate, then it will result in an electrical short circuit [2].

Hydration is the process of lead compounds from the plates dissolving in the water of a discharged cell to form lead hydrate, which is then deposited in the separators. This will cause multiple short circuits between the plates. Hydration is caused by overdischarging, or leaving the battery in a discharged condition for an extended time [8].

Thermal Runaway is the process where the battery destroys itself through internal heat generation. This can occur through overcharging of a float charge. As the battery naturally heats up through charging, more current is needed to keep the float voltage at a set level. The additional current will then provide more gas generation, which results in more heat generation as the gas undergoes the recombination process. The battery temperature will continue to increase, eventually destroying itself by overheating [8]. A thermal runaway diagram is presented Figure 37.

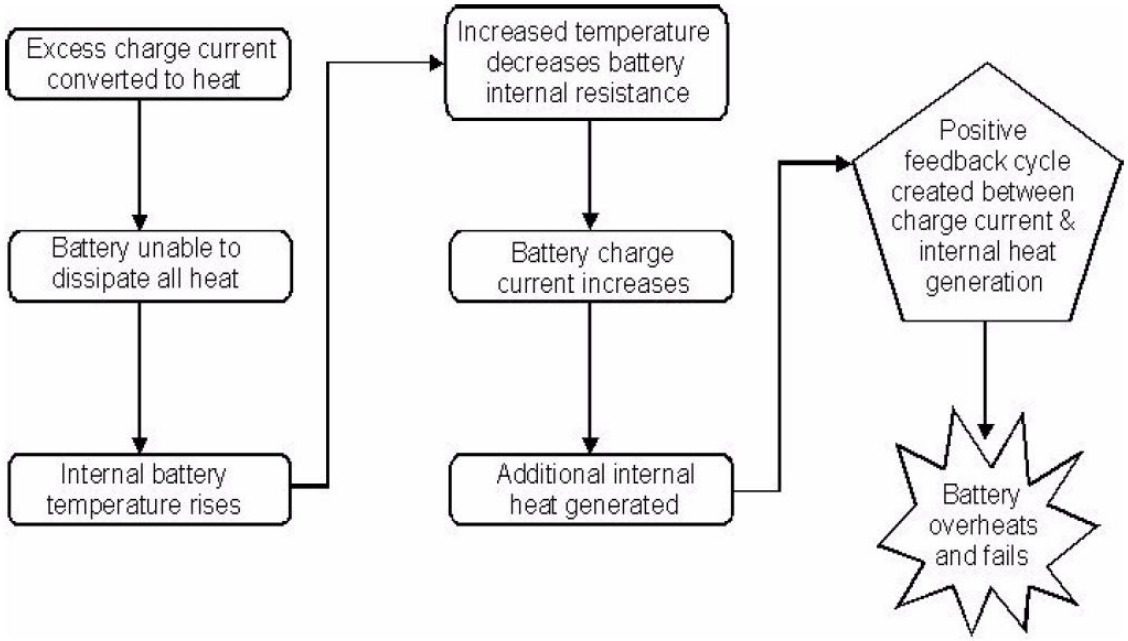

Figure 37: Thermal Runaway Sequence [8]

2.2.4. *AGING OF LEAD-ACID*

The Lead-Acid battery is destined to wear out even under ideal conditions and operation. There is no guarantee to how long the battery will provide energy no matter how gently the battery is operated. It can be guaranteed that the life of the battery will be shortened if operated in abusive conditions. There has been much research done on the aging of Lead-Acid batteries. Loss of power is not a major considered for Lead-Acid batteries since they are designed to supply high power applications. Most research focuses on the loss of capacity of the battery since this is most often encountered first. Typically, a battery is assumed at the end of its life when it drops below 80% of its rated capacity although an automotive Lead-Acid battery is still functional at 80% capacity for its intended purpose. Aging of the battery is closely related to the battery's DOD, and operating temperature. Ideal performance of the Lead-Acid battery can actually operate

higher than its rated capacity if properly maintained. Figure 38 describes the ideal battery life for a Lead-Acid battery.

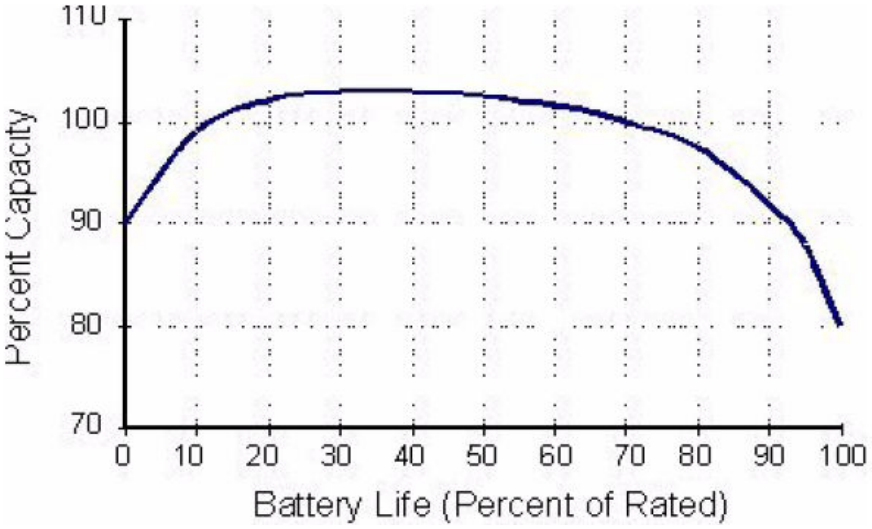

Figure 38: Ideal Battery Life [8]

2.2.4.1. DEPTH OF DISCHARGE

In general, the Lead-Acid battery is not designed for deep cycling purposes. In fact, the sealed Lead-Acid battery will probably only provide a couple hundred cycles of deep discharges. As the DOD increases, the cycle life of the battery decreases. Any combination of failure modes listed above can age the battery, but it is mostly the growth of grid corrosion that makes the depth of discharge variable age the battery.

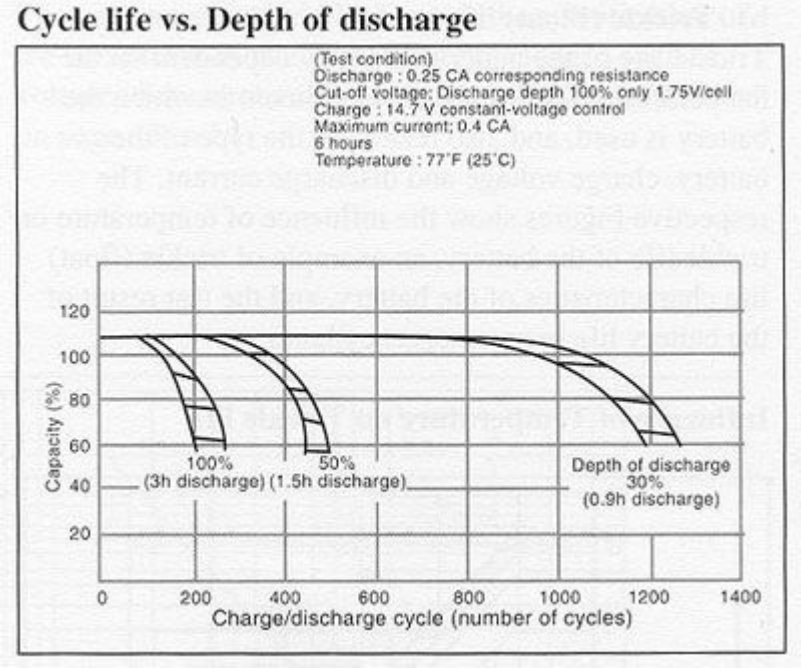

Figure 39: Cycle Life of Sealed Lead-Acid Battery [20]

2.2.4.2. TEMPERATURE

The operating temperature becomes an aging factor mostly because it can increase the effects of the failure modes described above. Temperature will increase the corrosion process, thus increasing the degradation of the battery components. Higher temperature will help the battery run more efficiently, at the price of aging the battery faster.

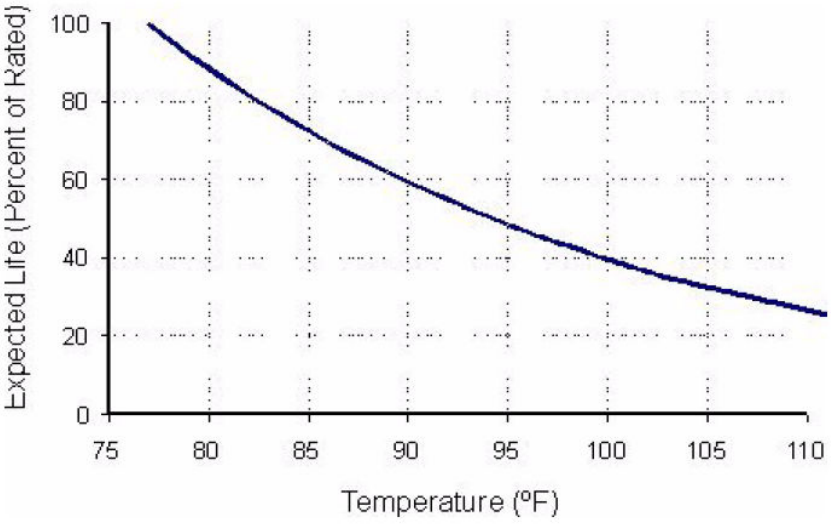

Figure 40: Temperature Effect on Expected Life [8]

2.2.4.3. DISCHARGE RATE

Much like that for NiMH batteries, there is not much research that has looked into the direct relationship of discharge rate and cycle life for the Lead-Acid battery. It is known that the discharge rate will increase sulfation in the battery as well as increase other possible failure modes. It is also suspected that the discharge rate will age the battery much like that of DOD. A larger discharge rate will stress the battery more much like the larger DOD stresses the battery more. It is one of the goals of this research to investigate the effect of discharge rate on aging of the battery.

2.2.4.4. CAUSES OF NORMAL AGING

Even if the battery performs ideally and is operated under ideal conditions, it will eventually fail. As briefly explained before, the main cause of battery failure is loss of capacity. Most research has determined that this loss of capacity is strongly related to the

positive grid corrosion of the battery, with the addition of loss of water from the electrolyte due to the corrosion process.

2.2.5. *MOTIVATION*

One goal of this research is to conduct experiments in order to further the characterization of aging in Lead-Acid batteries. More specifically, it is hypothesized that the battery will undergo different aging modes based on the operating conditions. If the battery is subjected to different and specific load demands, then it is expected to age differently. Most aging research focuses on capacity loss since the majority of batteries reach this end-of-life criterion before power loss. However, in real world conditions, it is possible for the battery to lose its power capabilities before a substantial amount of capacity is lost. In other words, the car battery nay have the ability to store and provide charge, but may lose the ability to supply current during cranking. Thus, when the car is running, all on-board electrical devices will operate normally. The battery only fails when the engine needs to start. Understanding the effects these specific cycles have on aging will provide insight towards aging during real world operation.

2.3. ELECTROCHEMICAL IMPEDANCE SPECTROSCOPY

Electrochemical Impedance Spectroscopy is a unique tool for evaluating dynamic battery performance. It is essentially a measure of the battery's internal resistance as a function of frequency. Similar methods include DC step responses, but EIS is not suspect to long relaxation times and non-linearity [1]. This method is based on the classical transfer function where the impedance is a ratio of the sinusoidal input and response. The input is

an AC signal of small amplitude and the response being the voltage. Thus, through basic Ohm's Law, the impedance of the battery can be determined. If the signal and response are measured through a broad frequency range, many dynamic characteristics of the battery's impedance can be determined.

When this spectrum is acquired, electric circuit models can be evaluated to whether or not they accurately depict the battery performance. These models consist of combinations of resistors and capacitors as an attempt to relate chemical batteries to traditional electrical circuits. This is where this research will focus its attention since evaluating an equivalent model can help determine aging characteristics. If one imagines an electrical circuit with a simple resistor, the EIS test can describe the resistor state of health. If this resistor increases its resistance over time, the EIS tests will be able to capture this change. Thus, the same holds with battery aging. The EIS tests will help capture the aging of the battery through its increase in internal resistance.

2.3.1 *EIS BASICS*

The EIS system can either be potentiostatic or galvanostatic. The first is a system that inputs a sinusoidal voltage and measures the current response. The latter is a system that inputs a sinusoidal current and measures the voltage response and is the type used for this research. The impedance can then be determined with this response based on Ohm's law.

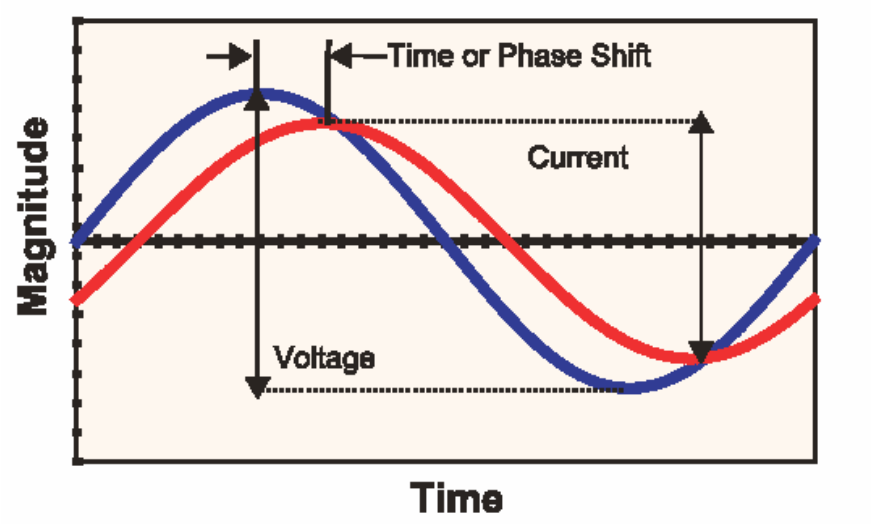

Figure 41: Current and Voltage as Functions of Time [21]

Table 7: Ohm's Law [1]

Direct Current – Resistance:
$R = \frac{V}{I}$
Alternating Current – Impedance:
$Z = \frac{V_{ac}}{I_{ac}}$

The impedance is then plotted along a range of frequencies to help describe battery behavior. The plots that are used to show this spectrum are a Bode Plot and a Nyquist Plot.

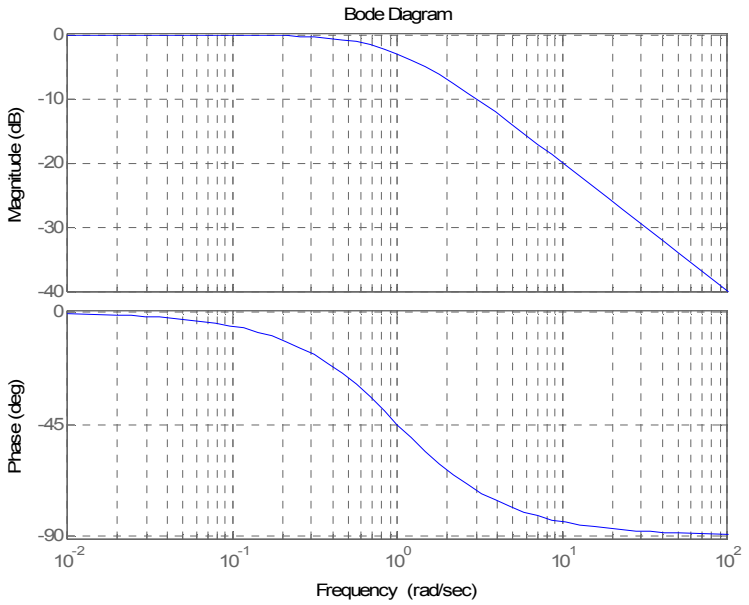

Figure 42: Sample Bode Plot (First Order System) [1]

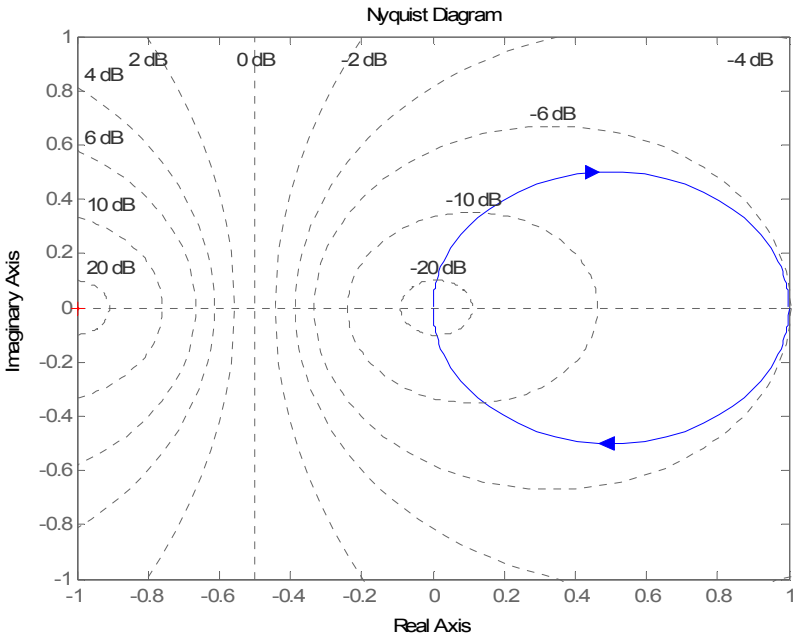

Figure 43: Sample Nyquist Plot (First Order System) [1]

2.3.2. *BATTERY MODEL OVERVIEW*

EIS is used in this way to help create electrical circuit models for chemical batteries. By developing the impedance spectrum through EIS, a circuit model's impedance can be compared to the chemical battery. [1] created an electrical model for the NiMH battery using EIS and also describes how those model elements change the impedance spectrum. Most NiMH electrical models are based off the Randle's Circuit Model, which consists of two resistors and a capacitor. After further trials, most researchers generally come up with a second order model to better characterize the NiMH battery.

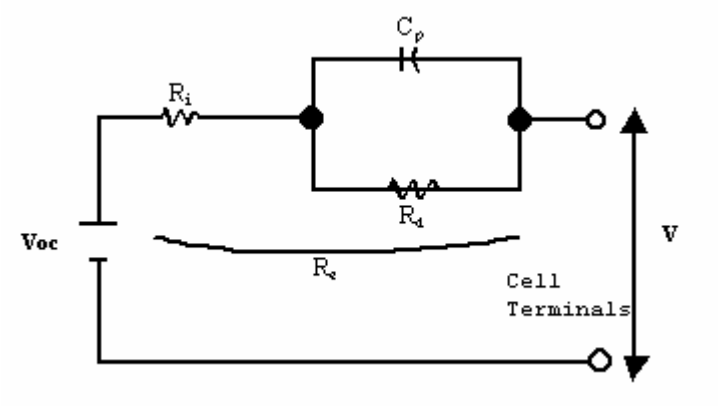

Figure 44: Randle's Model [11]

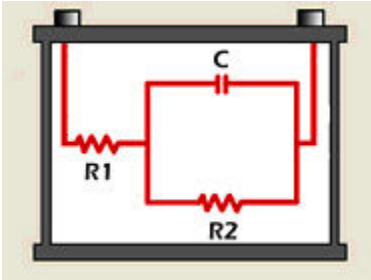

Figure 45: Visualization of Battery with Randle's Circuit [2]

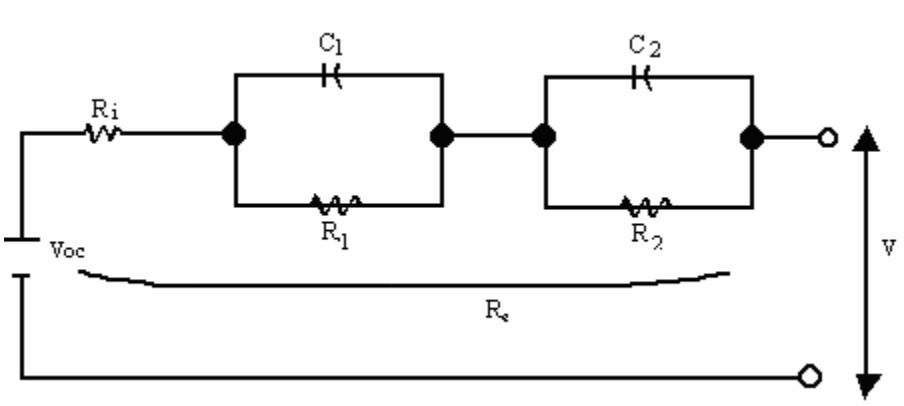

Figure 46: Second Order Model [1]

Some models even include a special impedance element called the Warburg Impedance. This element allows for an even better fit to NiMH battery spectrum. [1] found the Second Order Model with a Warburg Impedance to be the best approximation of the NiMH battery spectrum. Figures 47 and 48 show the model, and the fitted spectrum.

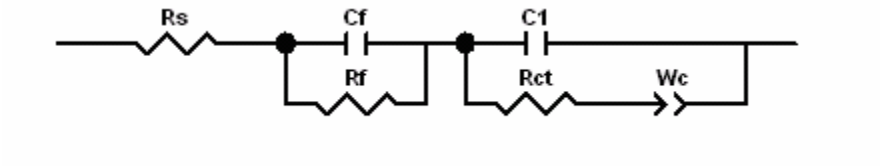

Figure 47: Second Order Model with Warburg Impedance [1]

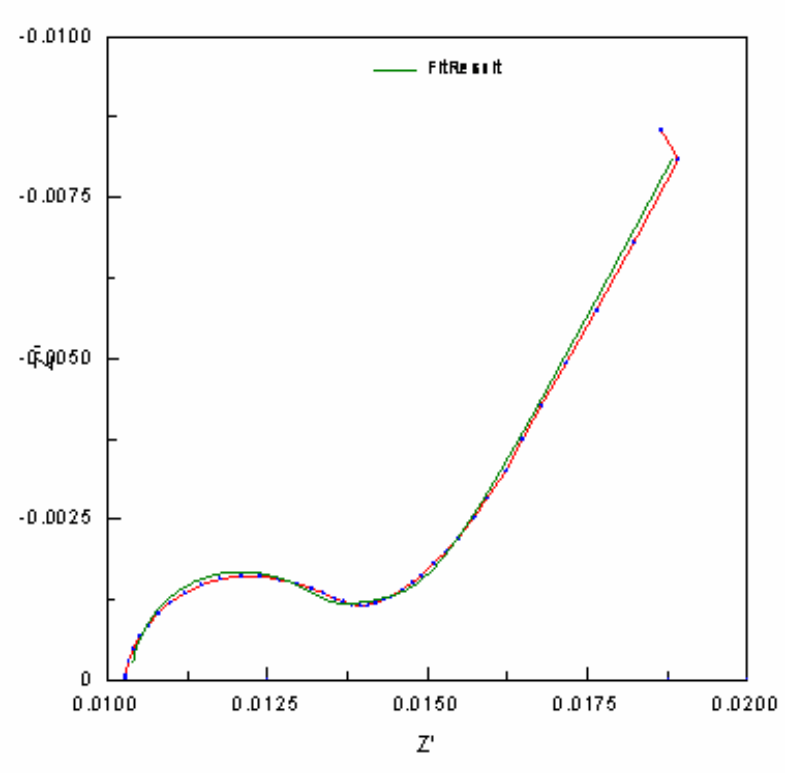

Figure 48: Resulting fit of second order model with Warburg impedance on Nyquist Plot [1]

The modeling helps describe the internal components of the battery. At high frequencies, the capacitors in the model act as an open circuit, thus allowing the impedance spectrum to be nearly represented by only the series resistance. The resistors themselves can physically represent the conduction of the electrolyte, sulfation, etc. Knowing these impedance characteristics can allow for prediction of future battery performance. Some manufacturers have developed algorithms that approximate the battery's performance based on an EIS test. Figure 49 shows how well the EIS (in this chart called 'Spectro') can predict the cold cranking amps of a Lead-Acid battery; the figure also provides a comparison with AC conductance testing.

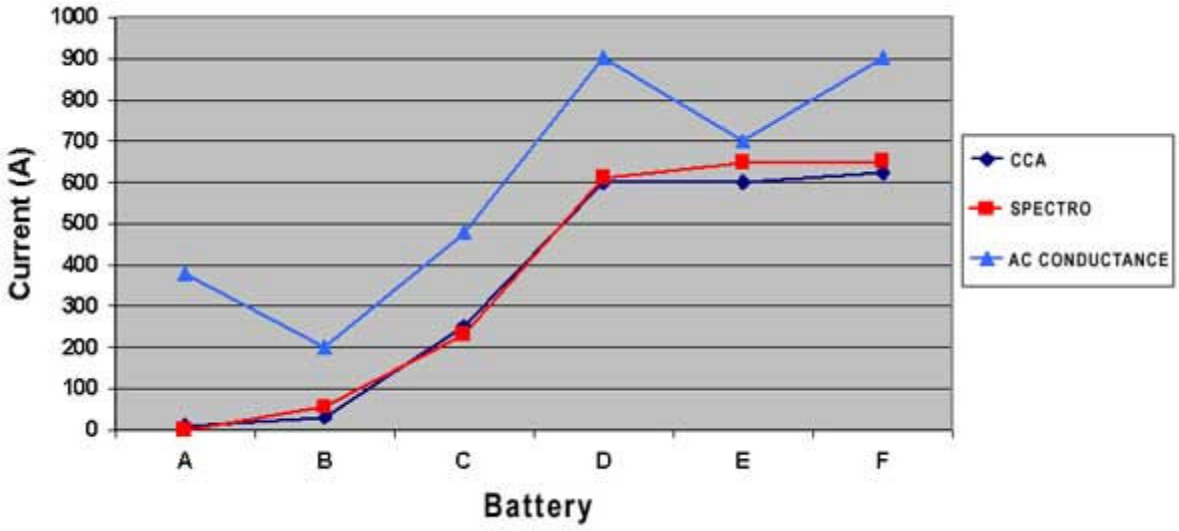

Figure 49: EIS Predicting CCA [2]

One of the most important indications of battery state of health is capacity. EIS can not directly assess the capacity of the battery because there is no simple relationship between impedance and capacity. Figure 50 shows the inability to relate impedance with capacity by plotting a battery's cold cranking ability along with its capacity.

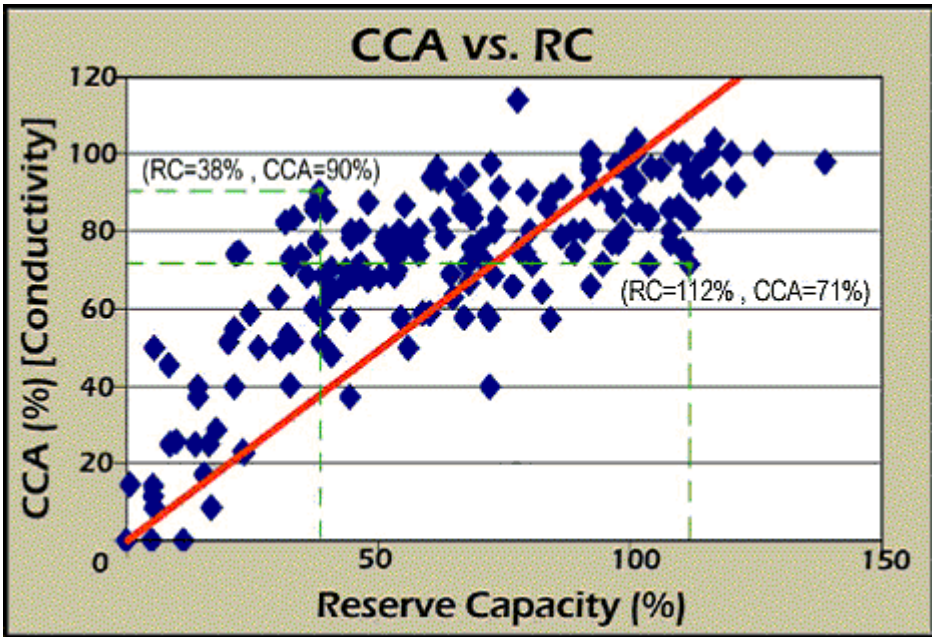

Figure 50: CCA vs. Capacity [2]

However, some manufacturers have done extensive research to create models that will approximate the reserve capacity of a battery through EIS. These approximations are found to be reasonably accurate, as can be seen in the Figure 51, especially for a rapid battery test when considering the only true way to determine capacity is through a long and deep discharge of the battery.

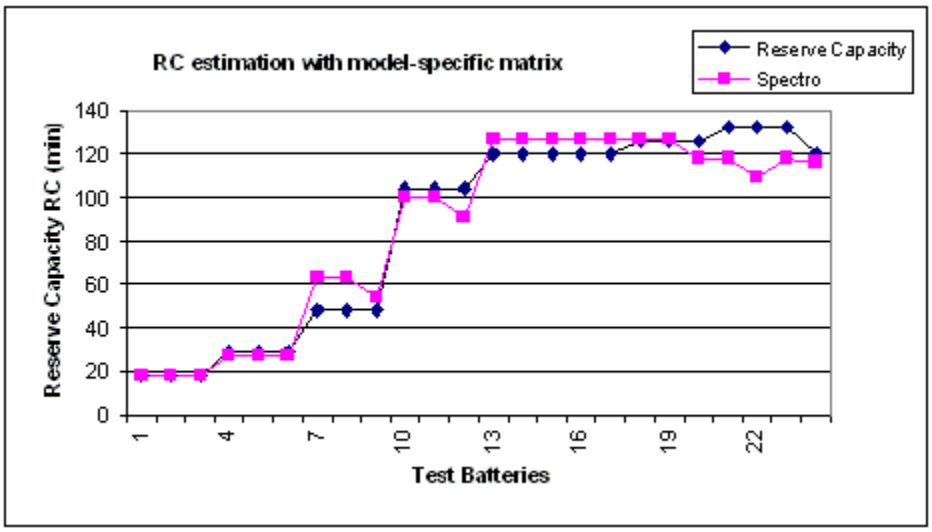

Figure 51: EIS Predicting Capacity [2]

2.3.3. *BATTERY AGING WITH EIS*

Not only does EIS have the ability to help generate and validate electrical models, it can also be used to describe battery aging. As the battery ages, its internal resistance will increase. This increase can be seen in the impedance spectrum. By plotting the original spectrum over the aged spectrum, it is easy to see the shift in the curve representing the increase in impedance.

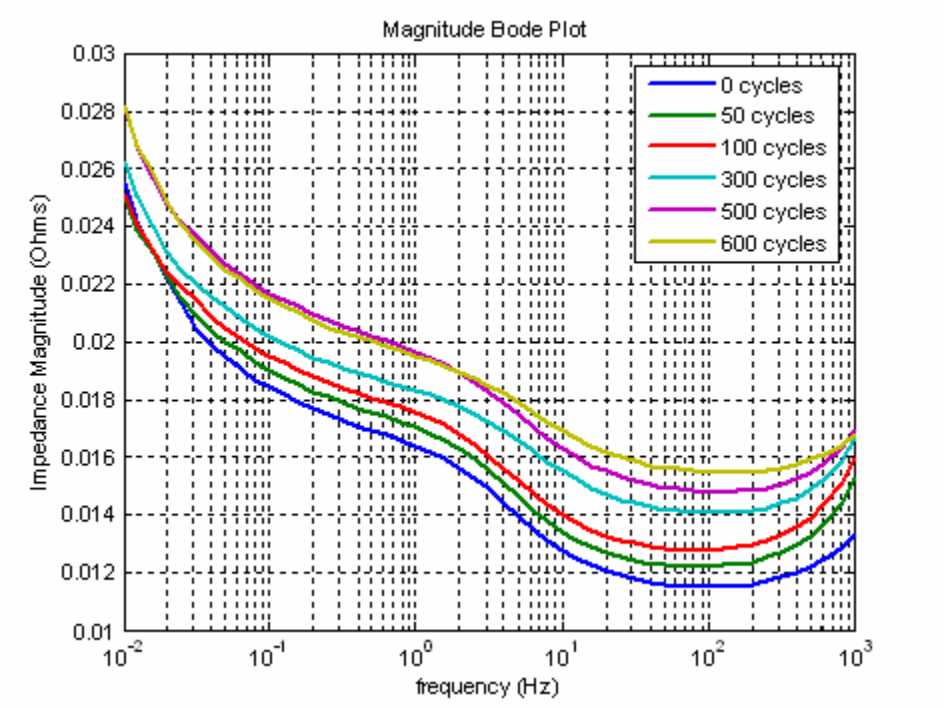

Figure 52: Bode Plot - Increase in Impedance Magnitude Showing Aging [1]

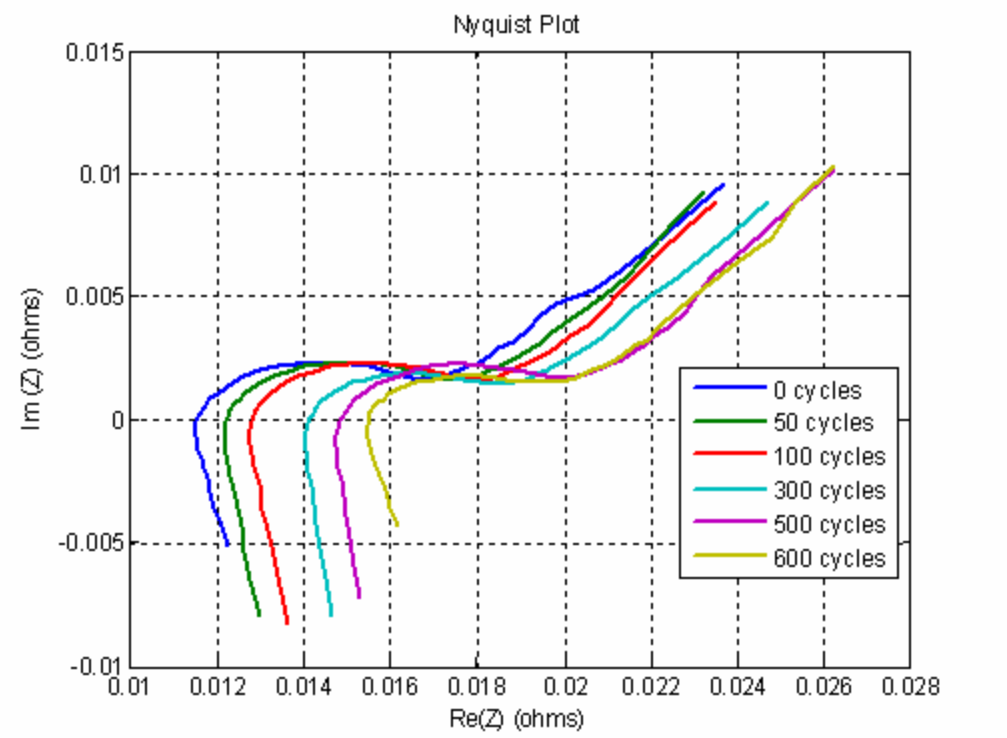

Figure 53: Nyquist Plot – Increase in Impedance Showing Aging [1]

EIS can also be used to describe aging in more detail. [12] uses EIS to quantify the aging mechanism of corrosion and decrepitation. The model developed for this NiMH spectrum was also a second order model, but without the Warburg impedance.

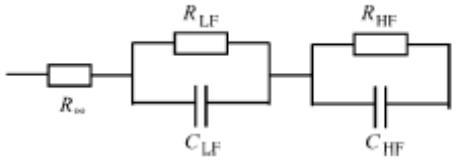

Figure 54: Second Order Model after [12]

With this model, [12] determined a relationship between some of the circuit elements and the decrepitation of the electrode. Moreover, the ratio of the initial resistance R_{LF} over the actual (aged) resistance R_{LF} was found to be "an accurate method for alloy decrepitation evaluation" [12].

EIS continues to become a very reasonable means of describing battery aging. It is also conceivable that if one could implement a low-cost on-board version of this diagnostic tool, it has the potential of becoming an on-board diagnostic method in HEV's. This would allow the owner to easily asses the battery's state of health and determine residual life of the battery.

3. BATTERY AGING AND PROGNOSIS APPROACH

The generation of basis cycles from real battery operation is an attempt at diagnosing and predicting battery life. This next section will provide the methodology for creating this basis cycle set that will be studied and used in predicting battery life. This approach was developed in conjunction with both Dr. Giorgio Rizzoni, Director of the Center for Automotive Research, and Lorenzo Serrao, a PhD candidate in Mechanical Engineering. Here are some relevant references:

1. Serrao, L., Chehab, Z., Guezennec, Y. and Rizzoni, G., "An Aging Model of Ni-MH Batteries for Hybrid Electric Vehicles", Proc. IEEE Vehicle Power and Propulsion Conference, Chicago, Peer Reviewed, September 2005.
2. Chehab, Z., Serrao, L., Guezennec, Y., Rizzoni, G., "Aging Characterization of Nickel – Metal Hydride Batteries Using Electrochemical impedance spectroscopy", Proceedings of IMECE2006, 2006 ASME International Mechanical Engineering Congress and Exposition, November 5 - 10, 2006, Chicago, Illinois, USA

3.1 PROGNOSTICS BACKGROUND

Many applications require that their systems undergo health monitoring diagnostics in order to asses the system's reliability for the application. Where system monitoring is quite common, prognostics technology is just emerging. Most current prognostic theory comes in the form of structural engineering where a system's life under cyclic loading can be predicted to avoid catastrophic failure from fatigue. For instance, the Palmgren-Miner rule [22, 23, 24] predicts fatigue failure through crack propagation by adding the damage of the current crack propagation as a function of its life to date. This 'additive law' is essential in approximating the cumulative damage on the system and thus predicting future damage from the same loading. The accumulation of damage is factorized as a product of the function of the current damage, $\varphi_1(\vartheta)$, and a function of

the excitation amplitude, $\varphi_2(p)$, where p is the excitation amplitude, and ϑ is the damage variable.

$$\frac{d\vartheta(n)}{dn} = \varphi_1(\vartheta)\varphi_2(p) \qquad 1$$

Many systems are effectively nonlinear when estimating damage evolution, and must be examined thoroughly to determine a reasonable relationship. Before the damage can be studied, the variables that cause the damage must be identified and experimentally validated. Additionally, these variables must provide some means of parameter extraction that will reliably correlate with the damage variable as it changes with the life of the system. This process can be extremely difficult, especially with a nonlinear system where the initial conditions have high importance, and must be conducted through sets of experiments with carefully controlled conditions.

The above 'additive' relationship will be applied to battery aging. The damage variables that affect aging have been reviewed earlier in the report and include the battery's internal resistance. DOD, discharge rate, operating conditions, etc are then vectors representing p, the excitation amplitude in relationship. It is this research's approach to utilize a similar relationship described in the Palmgren-Miner rule to battery aging prognosis.

3.2 BATTERY AGING PROGNOSIS METHODOLOGY

The current manufacturer supplied data on battery life is not sufficient for estimating battery life in a useable context. The supplied data is a representation of the battery's

decreased cycle life as a function of DOD. This information can not be easily translated to actual battery life degradation because of the fact that this information was developed solely through predetermined load cycles that do not represent real world operation. Figure 22 in section 2.1.5.1 provides a sample of manufacturer supplied battery cycle life information for NiMH.

This information is usually obtained through a simple signal, usually a square wave. The square wave can easily be adjusted to investigate a different DOD by simply changing the period of the signal or its amplitude. While understanding the battery cycle life dependence on DOD, it does not come close to representing what really happens inside a vehicle. Figure 55 provides a simple representation of what a NiMH battery could see inside an HEV.

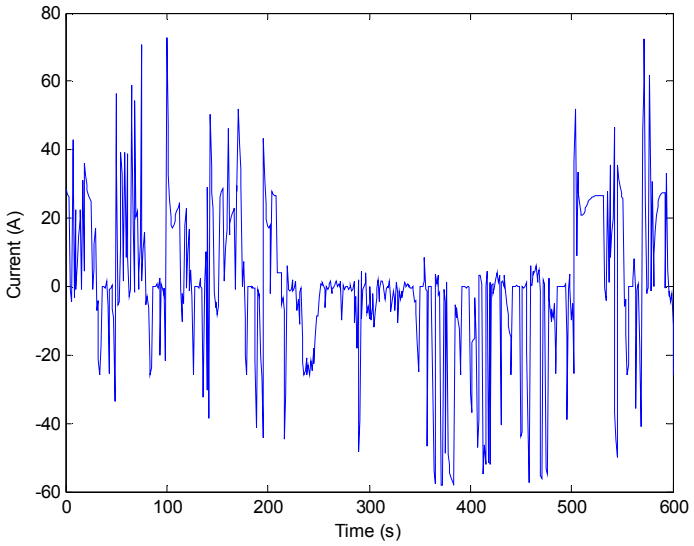

Figure 55: Typical Current of NiMH in an HEV

As one can see, this in no way relates to a square wave. The current profile is quite dynamic with many sharp peaks and valleys. The challenge then becomes creating some method for not only determining the aging effects through real operation, but also creating a means of predicting the remaining life of the battery.

The approach through this research will be based on the 'additive law' described above. The damage accumulated in the battery from one cycle or interval of operation will add cumulatively with the previous damage already inherent to the battery from previous cycles or intervals of operation. This law then allows for an approximation of remaining life based on the aging effects of the current and previous data by defining a total life that is decreased from every cycle or interval of operation to which the battery is subjected and assuming the same operating conditions for the future.

The first step is to identify the damage variables, as briefly mentioned above. These variables are discussed in the previous sections that age the battery. The variables that will be considered with the highest weighting are the DOD, the operating temperature, and the shape of the current profile which inherently includes the discharge rate. This last variable is the element that is significant in determining the aging of the battery from previous damage as well as predicting subsequent aging. It is important to note that it is assumed that the shape of the profile has an effect on battery aging. Relating once again to mechanical fatigue, the system will undergo more stress from a larger load. If this idea is represented through a battery cell, the cell will undergo more stress from a higher discharge rate, and consequently the shape of the current profile could then also have an

effect on the stress of the battery cell. In order to investigate this relationship through representations of real world operating cycles, a set of basis cycles will be generated and tested for their aging or damage effect on the battery.

In summary a proposed aging model will be dependent on DOD, discharge rate, operating temperature, and profile shape. Each profile shape will be investigated for its aging effect on the battery along with the effects in changing the profile's DOD, discharge rate, and the operating temperature. In a sense, each profile will then provide one 'map' of aging based on those other variables. Repeating this process for each representative basis cycle will provide a comprehensive aging model that can then be used to diagnose battery aging as well as predict its remaining life.

The model proposes to assume that each profile will have an effective total life on a battery. That is to assume if the battery was subjected to this profile at the same DOD, discharge rate, and temperature over the battery's entire life, then the resulting life, L_k, is the amount of total charge in Amp-hours the battery was able to provide over its entire life. Each profile would then have a different L_k, which would fluctuate based on the DOD and temperature of the profile.

$$L_k = f\left(profile, T_k, DOD_k\right) \qquad 2$$

The resulting damage or aging on the battery can then be represented with the 'additive law.' The amount of amp-hour aging undergone at a particular profile could be represented as a percentage of the battery's actual life based on the total amp-hour life for

that particular profile under those operating conditions. Thus a residual battery life, Λ_{res}, could be calculated through the simple equation.

$$\Lambda_{res} = 100\% - \sum_{k=1}^{N} \frac{\int_k Idt}{L_k} \qquad 3$$

where L_k, is the total life from that particular profile, and the integral is the amount of amp-hours applied to the battery for that profile.

Through aging diagnosis tests, the aging of each profile can be quantified and a comprehensive model can be created. If one was to use this process with the predetermined square wave profile that is typical of a manufacturer's data, the process would follow the diagram below…

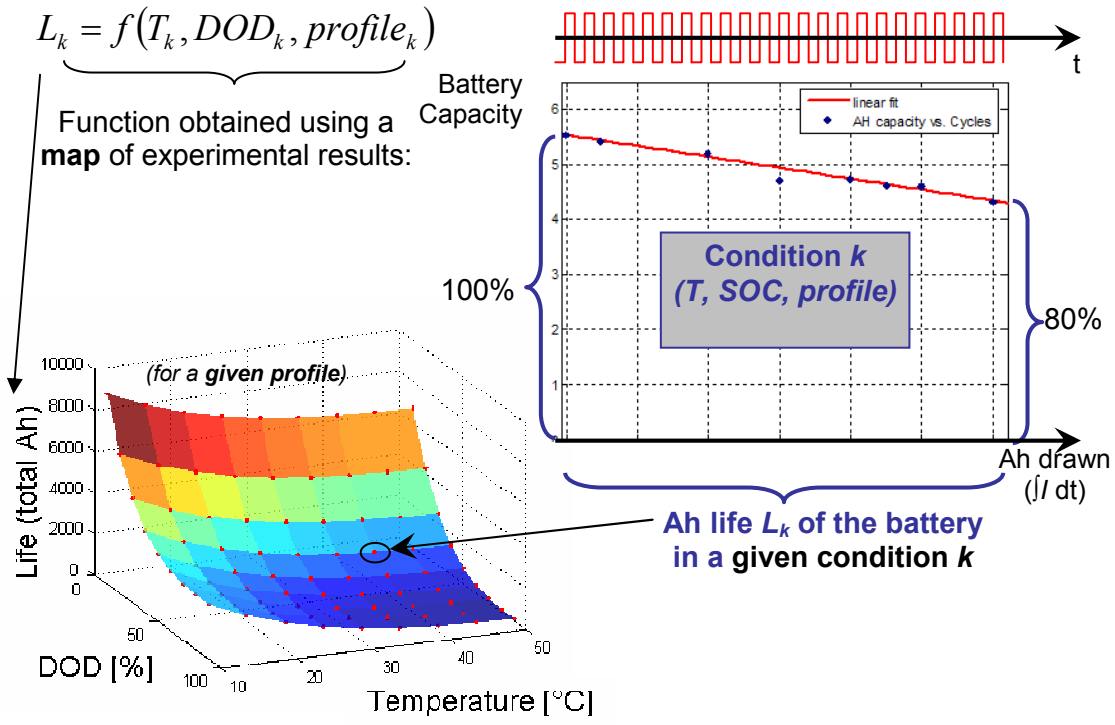

Figure 56: Square Wave Profile in Aging Model Methodology

The surface plot on the lower left is just an example of what each profile would create when adjusting the other parameters of DOD and temperature. First, a profile, L_k, is created and conditions are set. It is aged continuously with intermittent aging diagnosis tests applied to determine the battery's state of health after a certain number of cycles or total Amp-hours. One aged battery through those conditions would then represent one point for the three dimensional surface that represents the aging due to one given profile.

To expedite the process, the profiles to be investigated will be a basis set that statistically represents real world operation. This will limit the number of profiles that will need to be studied to diagnose and predict aging. The process is described in the Figure 57.

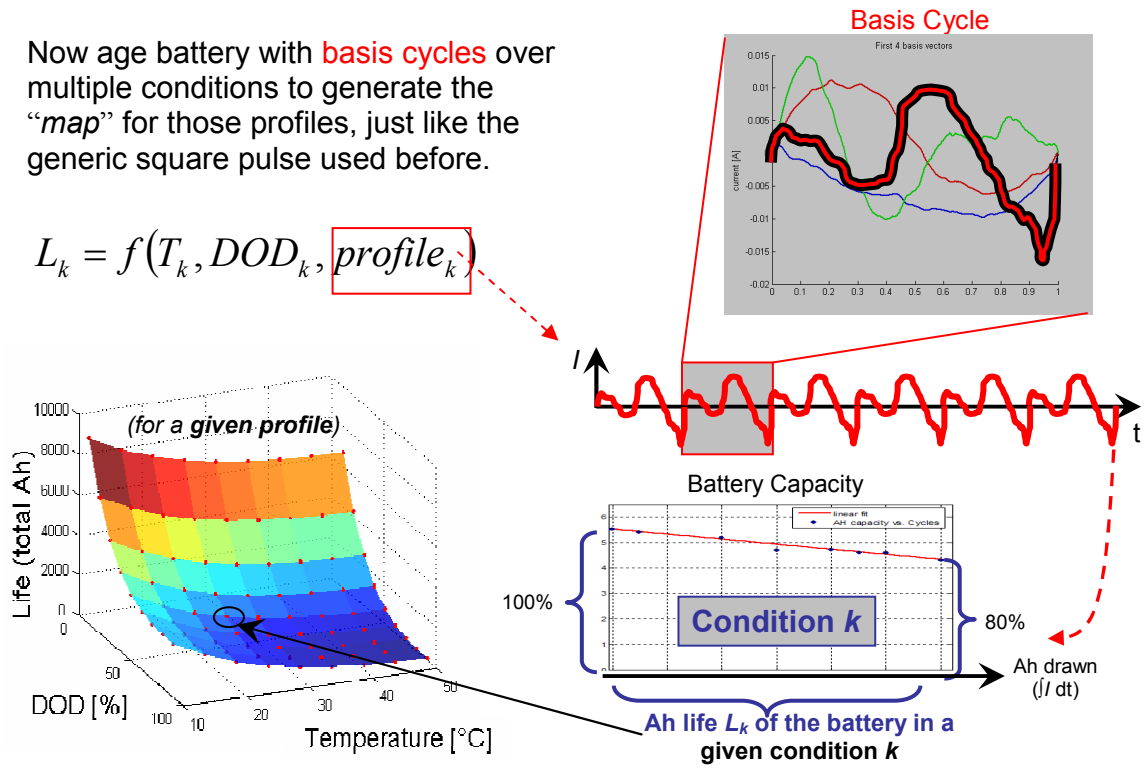

Figure 57: Aging Model Methodology

4. Lead-Acid Experimental Methodology

This section describes the methodology for Lead-Acid battery aging. Two specific profiles that are intended to cause the two common failure modes for this battery type are discussed. Aging the battery through these profiles will provide insight into the creation of a comprehensive aging model for Lead-Acid.

4.1 Background Review

The dominant failure modes of the Lead-Acid battery involve either capacity loss or power loss. Most research and experience suggest that capacity loss is the more frequent failure mechanism of the two. However, power loss is still encountered, and it is the goal of this research to help determine the methods that cause these failure modes. To visualize the differences between the two, one should imagine once again the water tanks. For a battery with power loss, the battery is still capable of supplying all the rated energy, but can not supply the high amount of current. To relate to a water tank, imagine a tank that is full but can only be emptied one drip of water at a time.

Figure 58: Battery as a Water Tank with Power Loss [2]

Alternatively, a battery that has capacity loss can still deliver high amounts of current but can not deliver the rated amount of energy. As a water tank, it would be able to provide a strong stream but there would be rocks inside the tank limiting the amount of usable water inside.

Figure 59: Battery as a Water Tank with Capacity Loss [2]

In order to determine the methods that cause these battery failures and also distinguish between the two, this research has developed specific discharging cycles that will try to cause these specific failures independently from the other. The first discharge cycle consists of high discharge rates with a very small amount of removed energy. The second discharge cycle has very small discharge rates with very deep and large amounts of removed energy. It is hypothesized that the latter will cause a more profound capacity loss, and the former will cause a more profound power loss. If this is the case, then more advancements and testing can be done to help prevent these failures in future batteries.

4.2 PROCEDURE

The approach to studying the common failure modes of the Lead-Acid battery involves cycling the battery with two different loading profiles. These profiles are herein called the *Power Cycle*, for power loss aging, and the *Energy Cycle*, for capacity loss aging.

4.2.1 POWER CYCLE

The battery is connected to a constant impedance load, and allowed to discharge as high as possible based on that impedance. This is repeated for a number of times at a fixed duration. The battery is then recharged with a power supply, and the process begins again. After a number of aging cycles have been applied, aging tests will be administered to record the battery's age, or state of health. These tests will be discussed in more detail in section 4.2.3 'Aging Diagnosis Tests.'

The aging cycle of the power test is simply repetition of rapid but shallow discharges, followed by a slow charge. Figure 60 shows this profile.

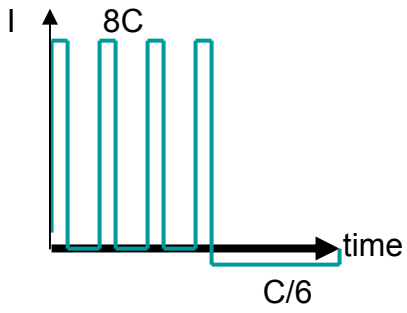

Figure 60: Power Cycle

The rapid discharge will be repeated 40 times before the re-charge. The discharge is provided by connecting the battery to the impedance load and commanding the relay connector to complete the circuit. The user will specify how long to discharge along with the number of pulses, which will control when the relay connector disconnects the circuit and ends the discharge. The charging begins with the power supply after the repetitive discharges have ended. The software will determine through integration of the current and time response, how long to charge the battery with a user specified amount of current. The current for this profile was determined to be C/6 for charging, and about 8C for discharging. The algorithm below describes this process.

Power Cycle Aging Algorithm:

1. Take a 75% SOC battery based on its V_{oc}.
2. Stabilize at 113^{o}F or 45^{o}C
3. Discharge the battery through the impedance load for 5 seconds and rest for 5 seconds.
4. Repeat step 2, 40 times.
5. Charge with C/6 to replace charge.
6. Repeat from step 2, 32 times (or based on scheduling).

4.2.2. ENERGY CYCLE

The aging cycles for this test consist of long deep discharges at low discharge rates with long and slow charge currents to replace the charge. After a predetermined number of discharges and charges, the battery will undergo aging tests to assess its state of health.

The aging cycle for the Energy Cycle is represented below in Figure 61. The slow rates make the cycling of this test very long, so it too will be automated.

Figure 61: Energy Cycle

In order to automate this profile, the system records again the voltage level and the time. The battery is discharged by the electronic load at a user specified rate, in this case C/2, until the battery reaches 10.5 volts. To aid in control, another relay connector is used to ensure immediate connection and disconnection of the circuit. After the discharge, the relay connector connects the battery in circuit with the power supply in order to charge the battery. The power supply is programmed by the user to charge at a specific rate, once again C/6 for this case, and is commanded by the software to charge for the same time the battery was discharged. The algorithm below helps describe this procedure.

Energy Cycle Algorithm:

1. Take a 75% battery based on its V_{oc}.
2. Stabilize at 113^{o}F or 45^{o}C.
3. Discharge at C/2 rate until 10.5 volts.
4. Charge at C/6 to replace charge for same amount of time in step 2.
5. Repeat from step 2, 20 times (based on scheduling).

The number of times to repeat the aging cycle is determined mostly through scheduling. Additionally, aging the battery at a higher temperature will increase the rate of aging. This will shorten the time to obtain results.

4.2.3. AGING DIAGNOSIS TESTS

In order to assess the aging of the battery, aging tests must be conducted periodically between cycling. The aging tests used in this research involve a simple industry standard capacity test, an impedance spectrum measurement, a real engine cranking capability test, and a large signal response test. By comparing these tests along the battery's cycle life, the battery's aging can begin to become quantified.

The capacity test remains the only true means of aging assessment, or state of health. It is widely accepted as the industry standard for assessing battery health because it is easily relatable to a new battery. The capacity test is a long test that also requires laboratory conditions like the control of temperature. Since it is the best way to assess battery life, and it is a very long test, it leads little possibility for 'on-the-fly' on-board vehicle assessment.

The capacity test procedure is relatively simple. It is only a complete discharge of a fully charged battery. The discharge rate is very slow in order to avoid the Peukert Effect as much as possible. For this research, the capacity test will be conducted at room temperature and a discharge rate of C/20 is utilized. Before the capacity test can be

conducted, the battery must be fully charged and at room temperature. Thus, there are also procedures for acquiring these conditions before battery testing can begin.

To stabilize a battery at room temperature, or any other temperature, it simply consists of resting, or 'soaking', the battery in that temperature for an extended period of time. The time for soaking should be sufficient enough that the battery electrodes are at the desired temperature. For lead-acid batteries, this time period can take more than 24 hours. Assuming the battery is being operated under a temperature other than room temperature, the battery has to soak at room temperature for 24 hours before aging tests can begin. If aging tests are desired to be at a certain hot or cold temperature, the battery should soak an additional 16 hours while in the desired temperature after soaking for 24 hours at room temperature.

Temperature Stabilization:

1. Soak the battery at 23^{o}C for 24 hours to stabilize at room temperature
2. If other temperature is desired, soak for additional 16 hours at desired temperature.

This research must maintain consistency in the battery conditions in order to accurately assess and compare the battery aging. To determine different states of charge, one must first take a fully charged battery and discharge it to the desired SOC level. In order to fully charge a 12V Lead-Acid battery, the procedure calls for a 24 hour charge with two different steps. The first step involves a voltage threshold with a current limiting power

supply. The second step involves a simple and very small supply current, which is generally called a float charge.

Charge to 100%SOC:

1. Stabilize battery at room temperature.
2. Apply 16V threshold while limiting the current to 25A. Continue for 23 hours.
3. Apply a C/200 charge current for 1 hour.

After this procedure, the battery is considered fully charged and temperature stabilized and aging assessment can begin.

Capacity Test:

1. Stabilize fully charged battery at 23^{o}C.
2. Discharge with C/20 until terminal voltage reaches 10.5V (0% SOC).
3. Record time taken to reach 10.5V.
4. Capacity = (C/20) * time
5. Do not leave battery at low SOC, recharge to at least 50% SOC.

This research also uses EIS to assess the battery's aging. EIS remains a high potential for 'on-the-fly' on-board vehicle battery assessment because it uses a very small signal and is a much faster test than a capacity tests.

EIS Test:

1. Stabilize 75% SOC battery at 23°C.
2. Conduct frequency sweep with EIS equipment (Solartron)

There are several reasons for using a 75% SOC battery instead of a fully charged battery. The primary reason is that the Solartron (EIS Equipment) has trouble with voltages above 13V, and a fully charged battery is generally above $13V_{oc}$. Another reason is that an aged battery might not be able to continually reach above 13V for the test. The only way to consistently measure aging is to keep the same V_{oc} as the battery ages. Using a lower SOC as the test level will help ensure its repeatability as the battery ages.

Similar to the EIS test, a large signal response test is applied to investigate the battery parameters at larger signals than the EIS test. These signals, or loads, will range from 10-60 Amps, whereas the EIS can only consistently test the battery impedance below 10 Amps. This is due to the fact that the SOC of the battery changes as the battery discharges, which in turn changes the batteries internal resistance. The EIS test then becomes too long of a test to assume a constant SOC during the discharge. The large signal response test is essentially a series of current steps which will provide a means for estimating the battery parameters at different levels of current. This test's protocol is the same as the EIS test.

Large Signal Response Test:

1. Stabilize a 75% SOC battery at 23°C.

2. Conduct staircase load and record voltage and temperature response

The last test will only provide information for one characteristic of the battery and only through comparison. A cranking test will provide a consistent means of comparing the internal resistance of the battery as it ages through its peak current. The cranking test is conducted by placing the battery in an engine and cranking the engine while recording the voltage and current responses. The test will also be conducted at three SOC's and three different temperatures in order to obtain data for investigating their effects.

Cranking Test:

1. Stabilize battery at desired temperature and SOC.
2. Connect battery to test cell engine.
3. Start the ignition while recording voltage, current, and RPM signals (10kHz).
4. After engine cranks and settles to idle, turn off engine and end test.

5. INSTRUMENTATION

5.1 TEST BENCH DESCRIPTIONS

The purpose of the test benches is to conduct reliable aging experiments on lead-acid batteries. The test benches will also be automatic since the tests will take large amounts of time. This in turn requires the test benches to be very safe because of the high possibility that they will be running unattended. These test benches are located at The Ohio State University's Center for Automotive Research (CAR) and the main purpose is to simulate aging on lead-acid batteries.

It is important to note that the Lead-Acid test benches are adaptations from the previous battery aging bench at CAR for NiMH. The next section will describe the previous NiMH test bench, and then the changes made to that bench to create the two new Lead-Acid test benches.

5.1.1 NIMH AGING TEST BENCH STRUCTURE

The previous test bench structure used for other batteries in which the lead-acid battery benches are modeled includes a power supply, an electronic load, a data acquisition system, and a computer. Both the power supply and the electronic load are programmable and are currently controlled through a LabView interface. The current systems run directly from Matlab along with the data acquisition system.

The programmable load, or electronic load, provides the load current to be applied to the battery. Conversely, the power supply provides the charge profile. The system allows

for the creation of a current profile in Matlab which can then be applied physically to the battery through the power supply and electronic load. In other words, the power supply and load work together to create a user defined profile.

An additional member of the test bench structure is the environmental chamber. The battery aging is to be conducted at different temperatures to test the dependence of aging on temperature. Therefore, an environmental chamber that can control temperature and humidity will simulate the climate that is desired for aging. The battery will simply be aged through the user defined profiles while inside the environmental chamber. Figure 62 provides a picture of the previous battery aging system. Figure 63 provides a picture of the environmental chamber. Figure 64 provides a schematic of the previous system's physical connections.

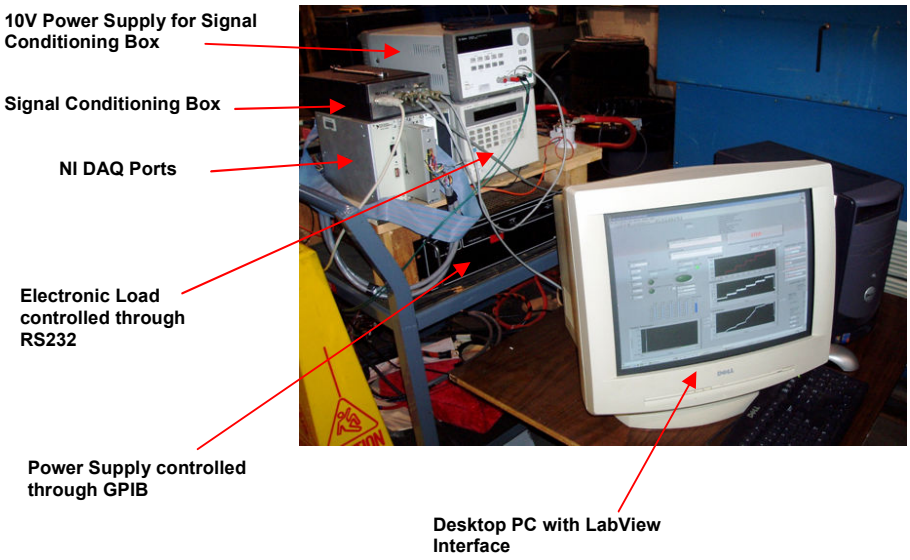

Figure 62: Previous Battery Aging Test Bench

Figure 63: System with Environmental Chamber

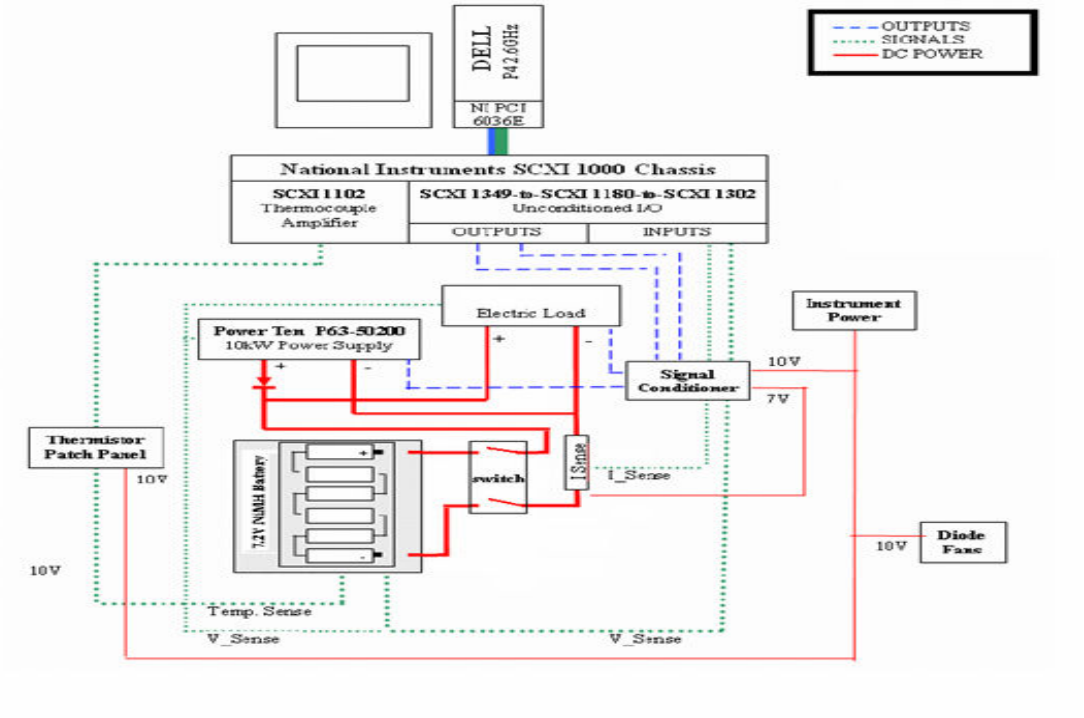

Figure 64: Schematic of Test Bench [1]

5.1.2 Lead Acid Test Bench Structures

The current battery test benches are modeled off the previous system, but are adapted to the specific aging cycles desired for the project: the Energy Cycle and Power Cycle.

5.1.2.1 Energy Test Bench

The Energy Test demands a long slow discharge of the battery. In fact, the desired discharge current is C/2 which means one discharge will take approximately 1.5 hours. After the discharge, a charging current of C/6 is used to replace the charge. This means that one cycle of aging will take at least 4 hours without resting for a fully charged battery. The test bench for this test needs to be capable of automating this process so that it can be repeated continuously to save time.

Even though the process needs to be automated, there is not much adaptation needed from the previous system to make this possible. For this system, a power supply and an electronic load are needed for the discharge and charge regimes. However, the user does not input a current profile, they will only need to specify the constant current amplitude, which is C/2 for the discharge, and C/6 for the charge. As with the previous system, voltage sensors, current sensors, and thermocouples will be used to monitor the battery performance and conditions.

This test requires a simple feedback loop for control. It demands that the discharge should be stopped when the battery reaches its lower voltage limit. For lead-acid

batteries, the lower voltage limit is generally accepted as 10.5V, which is when the battery is considered to be fully discharge. Moreover, the system reads the voltage as the battery discharges, and then commands the load to end the discharge when the battery's voltage reaches 10.5V.

To replace the charge removed from the battery, one must know the amount of time the battery was just discharged. If one knows the time and rate of the discharge, then to replace the charge one only needs to specify the new current rate for a longer time to charge equivalently the same amount. Therefore, the test bench must contain an internal clock that will keep track of the time the battery is being discharged to be fully automated. Then the power supply is then commanded to provide the new current rate for the appropriately calculated time length.

Since the cycles must be repeated automatically, certain safety aspects must be implemented. One safety aspect that is similar to the previous system is the temperature measurement. The test bench can be set to turn off if the battery's temperature reaches above a specified value. Likewise, the same can be implemented by the user for current and voltage.

Table 8: System Components for Energy Test

Components	**Model/Make**	**Usage Notes**
Electronic Programmable Load	Agilent N3301A	Load Current
Power Supply	40V/40A Sorenson DHP Series	Supply Current
DAQ card	NI SCXI-1000	DAQ system
Desktop PC	Dell	
Current sensor	Honeywell 225A Sensor	Record Current
Voltage Sensor	Voltage Divider (1:2)	Record Voltage
Thermocouples	Omega SA1XL-K-72-SRTC	Battery temperature monitoring
Temperature chamber	Cincinati Sub-zero CTH-27-2-2-H-AC	Battery temperature control
Software	Matlab	Interface and Analysis

5.1.2.2 POWER TEST BENCH

The Power Test demands high, short discharge rates and the replacement of charge after the high discharge. The desired current for this test is essentially the maximum current the battery can provide. In general, this test should be able to discharge at nearly 500A for approximately 5 seconds. This discharge is then repeated a number of times, and then the battery is recharged. The time to conduct the pulse discharges and replace the charge

is estimated to be less than one hour. Thus, the Power Cycle is able to apply more aging cycles per day than the Energy Cycle, and does not need to run overnight.

This test bench has a few more adaptations to the current system than the Energy Test. First, this test bench does not require a programmable electronic load. In order to allow the battery to discharge at its highest rate, the battery needs only to be connected to a small resistance. Figure 65 shows the resistors that will be connected in parallel to create a small enough resistance for a nominal current of 500A. Second, like the Energy Test, a feedback loop is needed to replace the charge removed. For this test, one does not know exactly what the response of the battery will be. The current the battery is able to provide will vary depending on the battery's conditions and age. Once again, voltage, current, and temperature are measured to monitor the battery's conditions and response. In order to replace the charge, the current during discharge is integrated along the time domain. This will provide the exact amount in amp-hours of the removed charge. The power supply is then commanded to provide the same amount of amp-hours but at a slower rate, which replaces the charge removed from the battery.

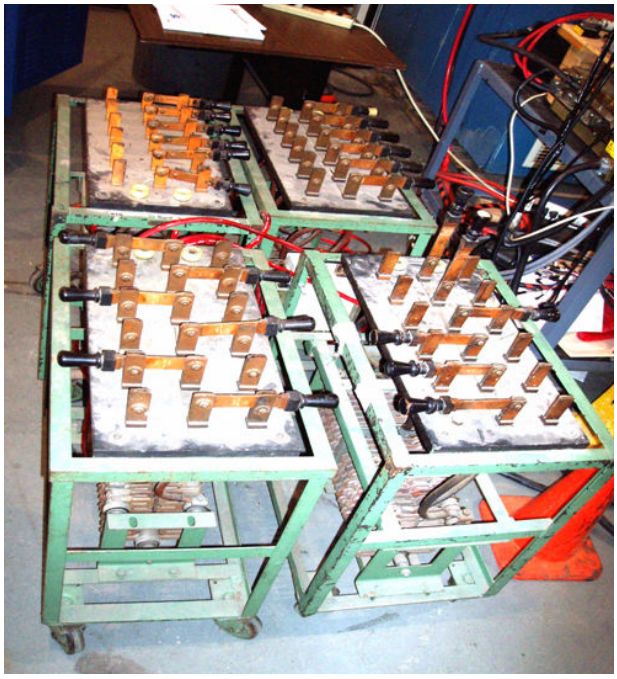

Figure 65: Power Test Resistors

Since the current for this test is very high, additional safety measures are needed. To avoid damaging the battery temperature, current, and voltage limits will be set to turn off the system if the limits are reached. Also, the resistors are located away from any possible contact to avoid injury.

Table 9: System Components for Power Test

Components	**Model/Make**	**Usage Notes**
Impedance Load	N/A - see above	Resistive Load
Power Supply	10W 50V/200A PowerTen	Supply Current
DAQ card	NI SCXI-1000	DAQ system
Desktop PC	Dell	
Current sensor	LEM Hall Effect 500A	Record Current
Voltage Sensor	Voltage Divider (1:2)	Record Voltage
Thermocouples	Omega SA1XL-K-72-SRTC	Battery temperature monitoring
Temperature chamber	Cincinati Sub-zero CTH-27-2-2-H-AC	Battery temperature control
Software	Matlab	Interface and Analysis

5.1.2.3 CRANK TESTING EQUIPMENT

The testing procedure calls for intermittent crank testing, which is simply the starting of an engine with the battery. This test is used for aging diagnosis, since the amount of current the battery will be able to supply will change as it ages. The engine used for this test is a 2-Liter IVECO Diesel Engine that is mounted in a test cell area at the Center for Automotive Research. This engine is concurrently being utilized for exhaust and emissions testing. The advantage for using this engine for the cranking tests is the fact that it will demand a high current from the battery due to its initial inductance and is always kept at room temperature, which will ensure consistent results.

There are three variables that need recorded for this test: the battery current, the battery voltage, and the engine RPM. The battery current is measured from a Fluke Current clamp rated at 1000A with a resolution of 1mV/1A. The battery voltage is divided in half by a voltage divider and sent directly to the Data Acquisition card. The engine RPM is estimated from the ECU of the engine. A Dell Laptop equipped with LabView and a NI DAQCard-1200 is used to sample and record the signals. Figure 66 provides a diagram of the set-up.

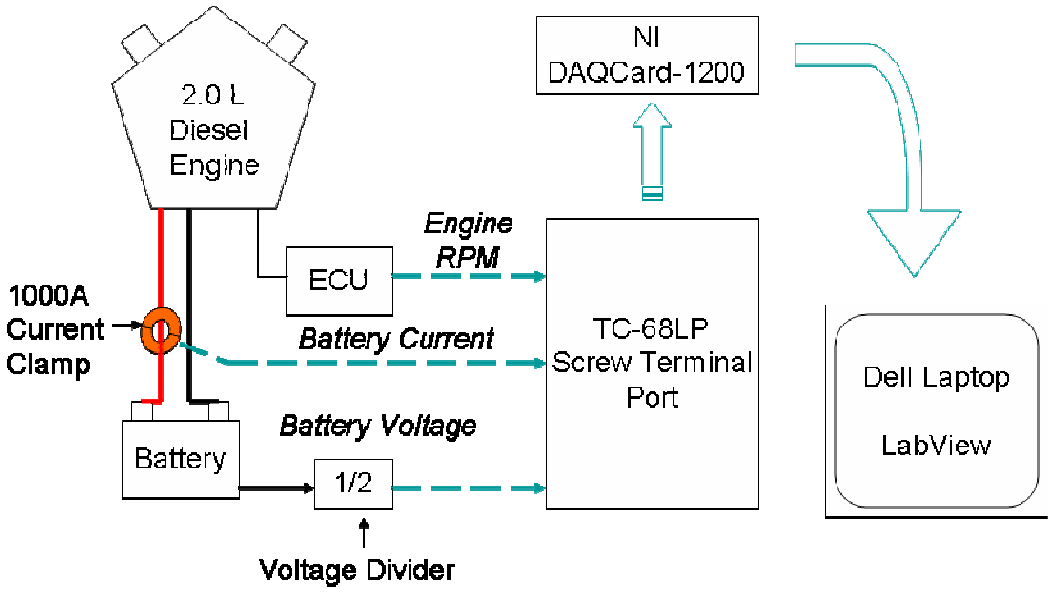

Figure 66: Crank Test Set-Up

5.2 SOFTWARE

The software for the Energy Cycle and the Power Cycle test benches is designed by B.J. Yurkovich, a student at the Center for Automotive Research. The current benches are not yet fully automated as described in the instrumentation above, but do collect all the

signals necessary for analysis. This automation will be done in the future, but for now, the software simply saves and plots in real-time the battery data.

The Energy Cycle is operated manually by specifying the current applied to the battery both from the supply and load. The software used for the acquisition of data and as an interface for the user is a Matlab VI. This program, dubbed 'DAQ Collector' receives the signals from the voltage divider, the current sensor and the amplified thermocouples. The program also allows the user to specify a channel that can be plotted in real-time. Additionally, the program allows for the user to specify the sampling rate and the scaling of the channels. Figure 67 provides a view of the interface for the program.

Figure 67: MatLab VI for Data Acquisition

The Power Cycle test bench utilizes the same program for acquisition, but this bench is semi-automated. For discharging, a contactor is needed to accurately time the pulse discharges. The program used for the pulse discharges sends a user-specified time sequence to operate the contactor which connects the battery to the resistors allowing for the battery to discharge. When the battery undergoes the charging regime, the same program as in the Energy Cycle is utilized. Figure 68 provides a visualization of the Power Cycle control and acquisition for discharges.

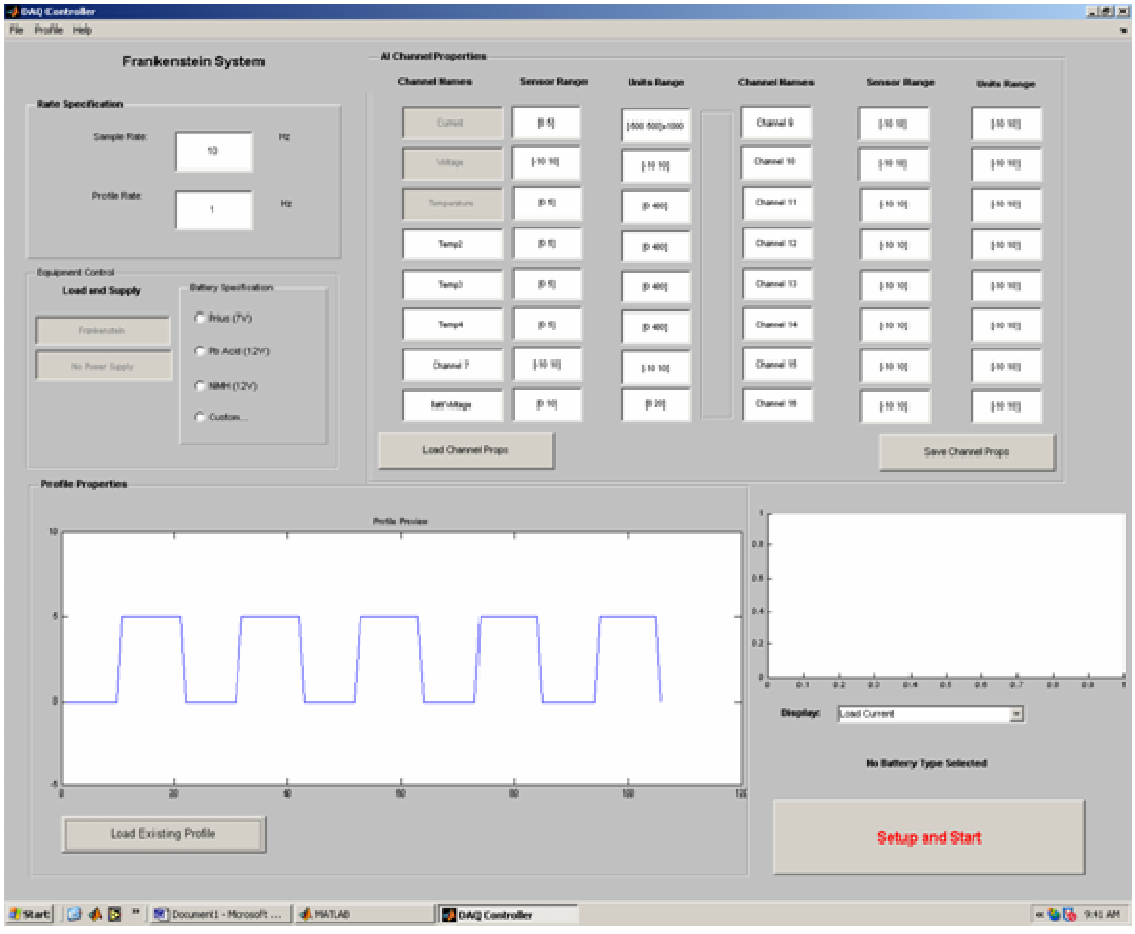

Figure 68: Matlab VI for Power Cycle Discharges

At some point in the future, these programs will be manipulated to control the loads and supplies remotely. The data acquisition aspects of these programs will remain the same, but the computer will be able to control the electronics with user-specified values of current.

6. BASIS CYCLE GENERATION

The approach for creating the comprehensive aging model calls for the generation of a set of statistically representative basis cycles. This section describes the process for extracting those cycles from real driving data.

6.1 WAVEFORM DECOMPOSITION

The generation of the basis cycle set stems from a large real world driving data set. The current from the battery is recorded, and the vehicle is left to operate while the data is collected. The driving patterns are dependent on the vehicle owner with the understanding of obtaining as many different driving scenarios as possible that include highway, neighborhood, rush-hour, etc. With this large data set, enough information is obtained to generate the basis cycle set.

This large data set is split into 'mini-cycles' where each mini-cycle is simply all the data between two zero crossings. This is represented in Figure 69. Each mini-cycle is then put into a matrix where each column then consists of one mini-cycle. In order to create a square matrix each column is interpolated to have the same number of data points as the largest mini-cycle.

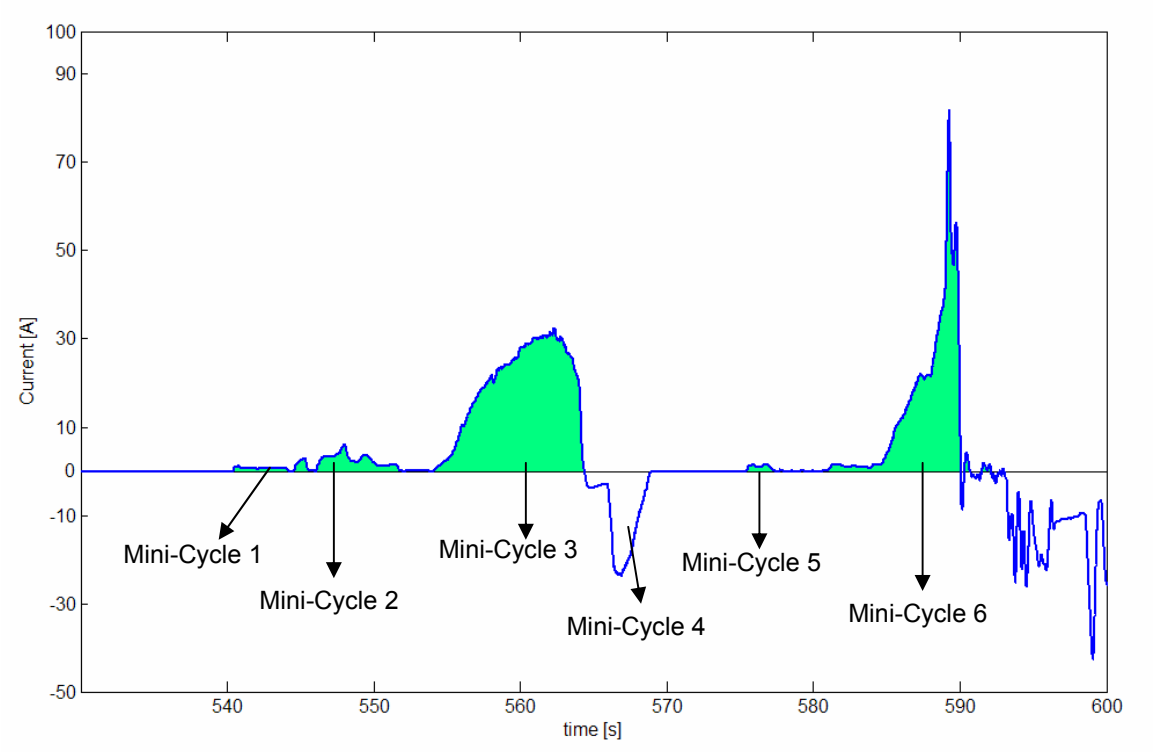

Figure 69: Mini-Cycles

The mini-cycles are then normalized against their length (time) and their amplitude, thus preserving their shape which is the most important aspect to analyze in creating the basis cycle set. For example, a few mini-cycles are shown in Figure 70 with their normalized shape.

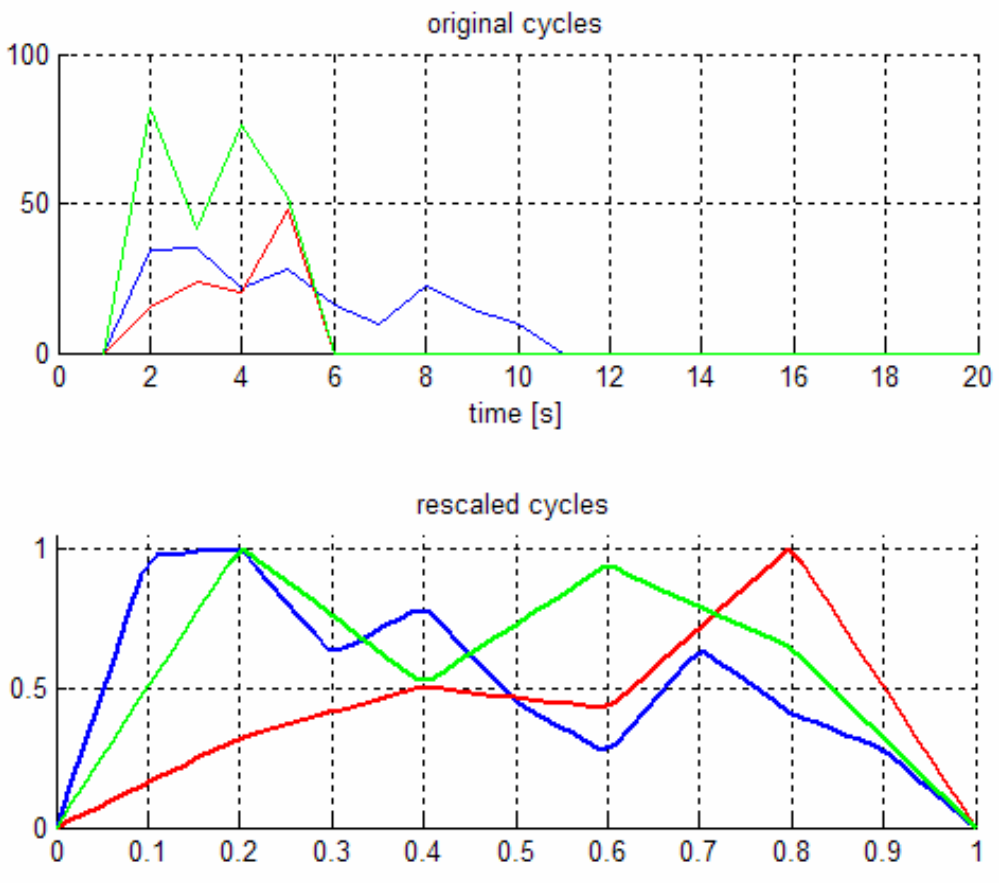

Figure 70: Normalized Mini-Cycles

Once the matrix is manipulated in this fashion, a decomposition can be performed in order to find the orthonormal basis for the matrix. This is done simply in Matlab by using the function `orth()`. A basis set is then created where the original mini-cycles can be reconstructed through the basis cycle set through an appropriate weighting of each basis cycle. The formula below represents this reconstruction where the first column of the matrix is, I^{c1}, the basis cycle set is B, and the weighting for each i^{th} basis cycle is k.

$$I^{c1} = \sum_{i=1}^{S} k_{i,1} \cdot B_i$$

The results from this function provide a large set of basis cycles. In order to restrict the number of cycles to be analyzed, only the first few with the most significance will be analyzed. The basis cycles that will provide the best reconstruction are the cycles that provide the best degree of approximation. The approximation is determined through error analysis.

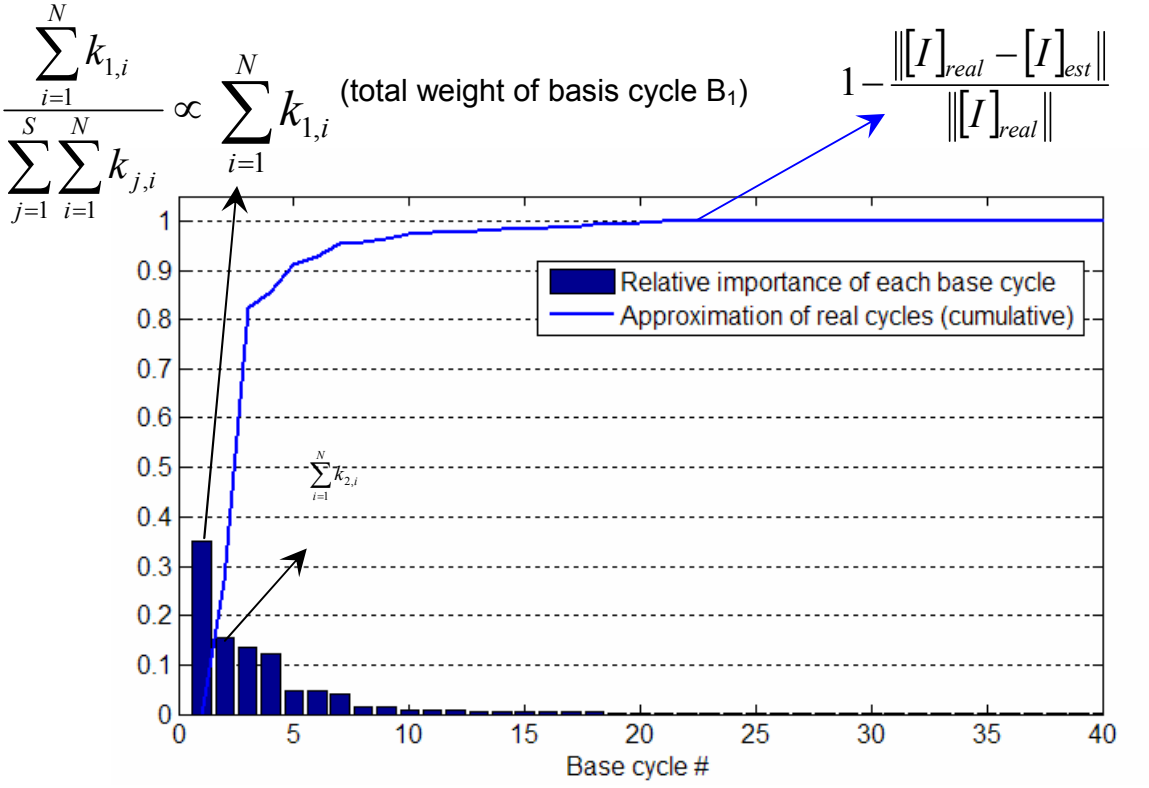

Figure 71: Degree of Approximation for Each Basis Cycle

Therefore depending on the degree of approximation desired, only a few basis cycles need to be used in order to statistically reconstruct the mini-cycles with over 90% accuracy.

6.2 Basis Cycle Set for NiMH

Following the above procedure, the basis cycle set for NiMH is shown in Figure 72. Based on the degree of approximation, the first four vectors could statistically recreate the mini-cycles with approximately 97% accuracy. Such a small basis cycle set will prove to simplify the aging model greatly in future research.

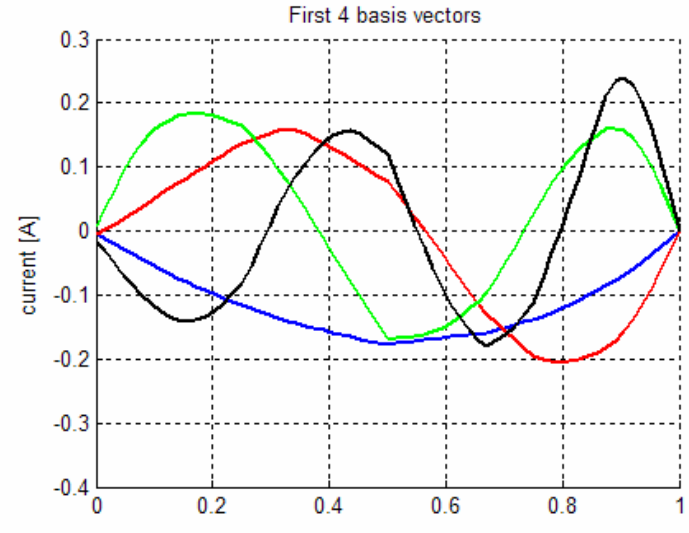

Figure 72: Basis Cycle Set for NiMH

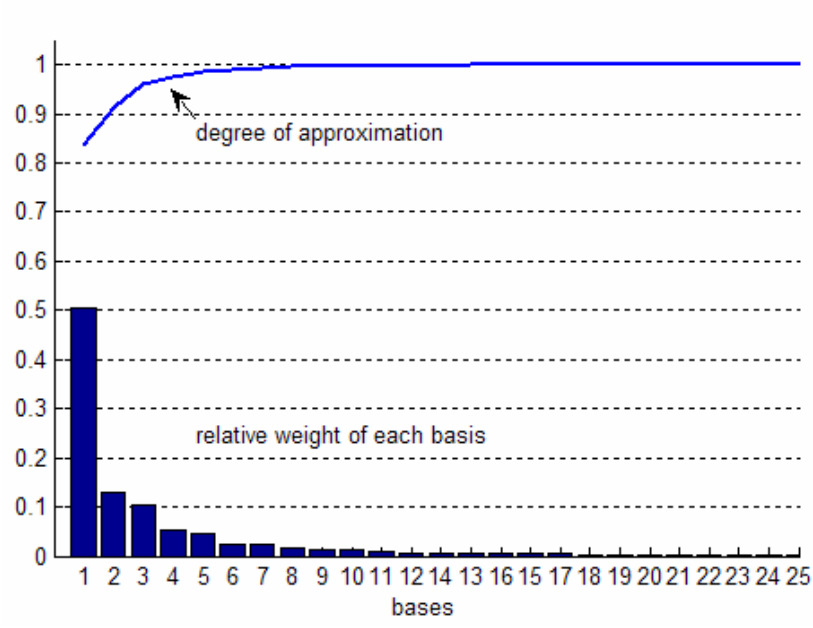

Figure 73: Degree of Approximation for Basis Cycles of NiMH

Investigating the reconstruction of the first mini-cycle showed a reasonable recreation with the first four basis cycles. If the first eight basis cycles are used, the reconstruction becomes even tighter.

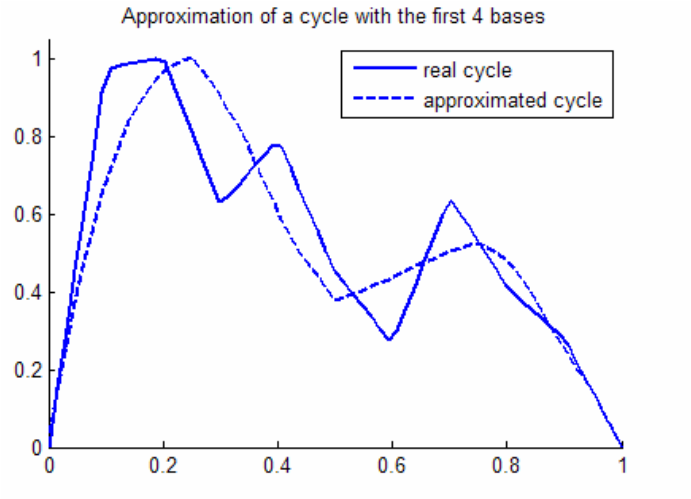

Figure 74: Mini-Cycle Reconstruction with 4 Basis Cycles

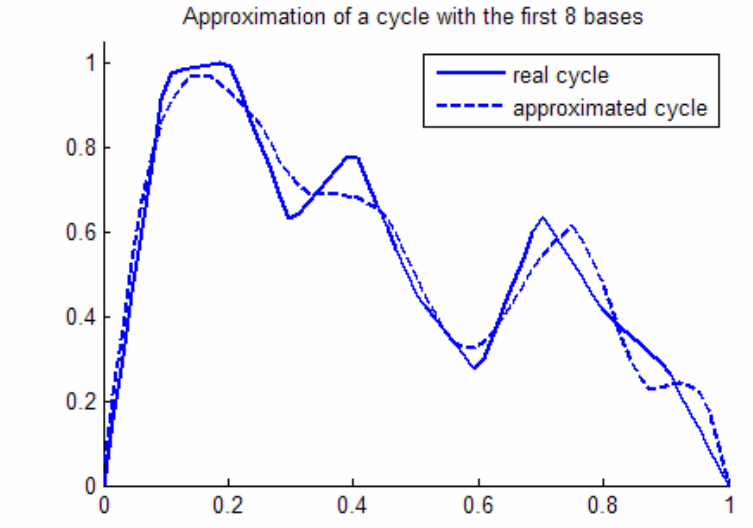

Figure 75: Mini-Cycle Reconstruction with 8 Basis Cycles

Further analysis is conducted by investigating the differences that might arise in separating discharge and charging mini-cycles independently instead of having them in the same matrix for decomposition. This analysis provided similar results in the shape of the basis cycle set. For any case investigated, the basis cycles seemed to represent harmonics which could prove to make analyzing and creating the aging model simpler since there are no cycles that contain large spikes or other more complicated shapes.

6.3 Basis Cycle Set for Lead-Acid

Research is ongoing at the Center for Automotive Research at The Ohio State University, for the generation of a Lead-Acid Basis Cycle Set. A large driving data set is currently being acquired which will inevitably be used in the determination of the basis cycles. It will be interesting to see the data set since a Lead-Acid battery operates differently in a conventional automobile as compared to a hybrid battery in an HEV. The only loads the Lead-Acid battery tends to encounter in a regular car are transient loads from the on-board electronics and the starting of the engine. The basis cycle set for this battery chemistry and operation should be quite different from the set obtained for NiMH in an HEV.

7. BATTERY CHARACTERIZATION AND MODELING RESULTS

The purpose of the battery model refinement is to adapt the current model slightly to allow for battery results for battery prognosis. The refinement process will also consider multiple techniques in determining a new electric circuit model for the battery. The two techniques to be utilized for this model are large signal response analysis and electrochemical impedance spectroscopy.

Battery modeling is the process of representing an electrochemical cell by a simpler electrical circuit of resistors and capacitors. This representation is not trivial, not just because it is inherently difficult to estimate a complicated chemical process through a simple series of resistors and capacitors, but also because these parameters, the resistors and capacitors, are known to change as the battery's conditions change.

7.1 ELECTROCHEMICAL IMPEDANCE SPECTROSCOPY MODELING

The use of electrochemical impedance spectroscopy (EIS) provides the most convenient process of investigating many circuit models for the battery. The equipment used is a Solartron 1280B, and the software is Zplot and ZView for Windows. The process inputs a certain frequency of either current or voltage, an aspect that is determined by the user, and measures the impedance at that frequency. The software then allows for an attempt at fitting any circuit model created by the user to the spectrum measured. This process is applied for open circuit analysis, and closed circuit analysis. The method used for the fitting analysis is the Complex Non-linear Least Squares Levenburg-Marquardt method.

The user creates a representative circuit model in the software, and then the least squares method attempts to fit the model to the impedance spectrum.

7.1.1 Open Circuit EIS Modeling

The first tests conducted are tests with a lead-acid battery at open circuit. To do these tests, the battery is simply connected to the EIS Solartron and the frequency sweep is applied. Figure 76 provides the nyquist and bode plots of the impedance spectrum for a lead-acid battery at open circuit.

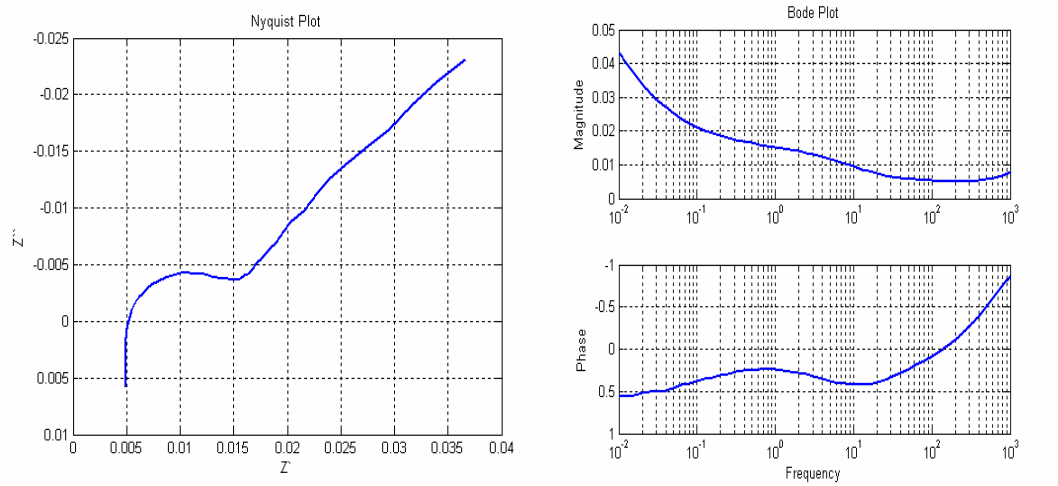

Figure 76: Impedance Spectrum for Battery at Open Circuit

The open circuit analysis must be investigated at different states of charge of the battery since the battery parameters are known to change with the battery state of charge (SOC). The open circuit analysis is then applied at three different states of charge, and multiple model fittings are attempted at each state of charge. The states of charges tested are 50%, 75%, and 100%. Figure 77 provides an example of a third order Randle Model fitting to

a battery at 100% SOC, or fully charged. All other SOC's provided similar shapes with the same results for the order and type of the model.

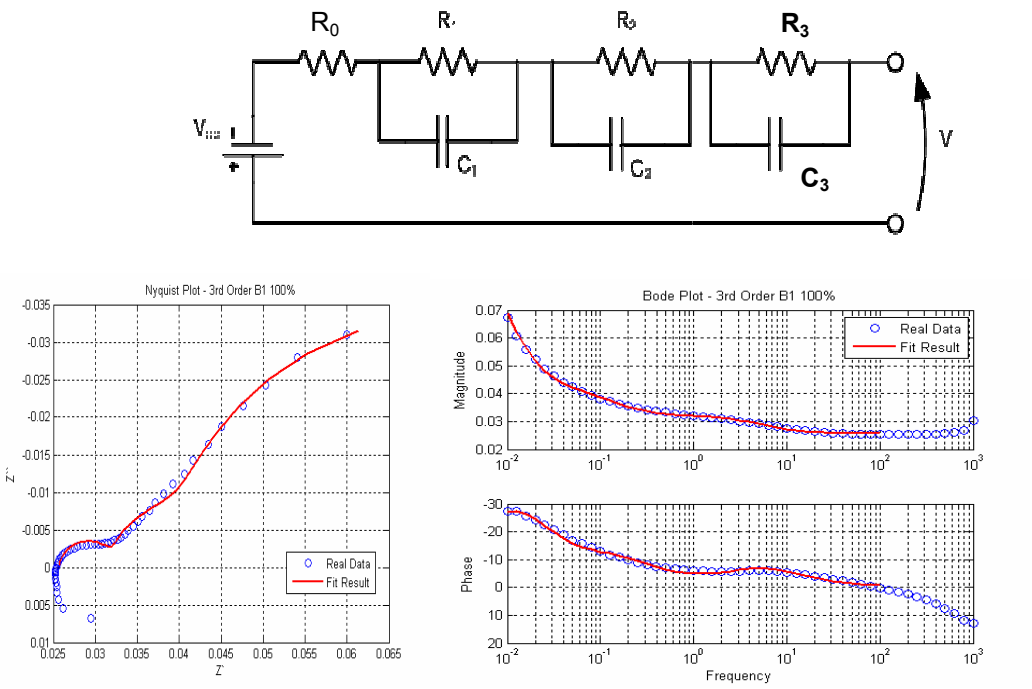

Figure 77: 3rd Order Randle Model Fit to a 100% SOC Battery

The best fit model for the battery at open circuit proved to be a first order Randle model with a Warburg Impedance. This impedance element is a special constant phase element that provides a linear slope in the complex plane. The Warburg is especially difficult to model in the time domain, which means it would not be advantageous for battery prognosis simulations if the refined battery model contained a Warburg impedance. The Warburg impedance can be represented by the equation below.

$$\text{Warburg Impedance:} \quad Z = \frac{1}{T(j\omega)^{\mathrm{p}}} \tag{4}$$

where T is the length or magnitude and p is the angle in the complex plane. If p is 0.5, then the equation changes to $Z = \frac{1}{T\sqrt{j\omega}}$ and the angle is 45°. T corresponds to the diffusion of charge based on the material thickness.

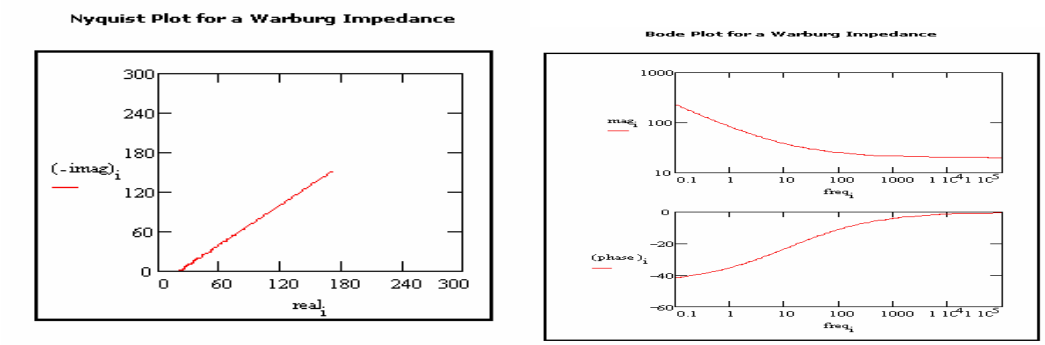

Figure 78: Warburg Impedance

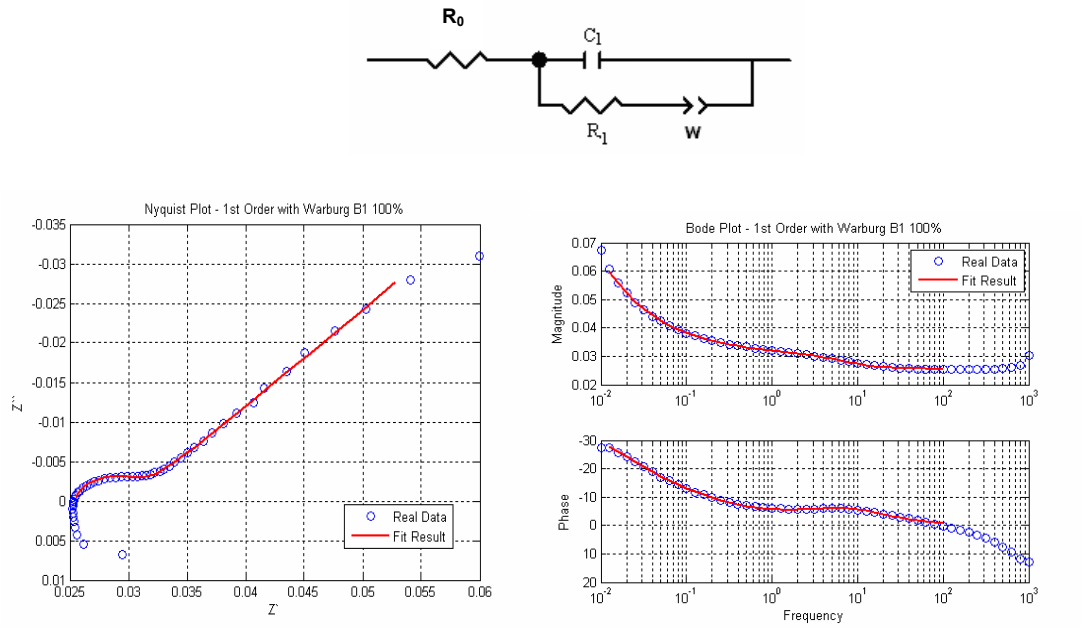

Figure 79: 1st Order Randle Model Fit of 100%SOC Battery

The open circuit modeling investigates six different models for fitting. The models include linear Randle Models from first order to fourth order, and two Randle Models, first and second order, that include the Warburg impedance. As stated above, the first order Randle Model with the Warburg is the best fit for batteries at open circuit. This result, however, may not be the most advantageous since the purpose is to simplify battery prognosis through simulations and other analysis due to the difficulty in representing the Warburg in the time domain. This leads to the conclusion that the best model for battery prognosis is a third order Randle Model.

EIS testing at different battery states of charge allows for an easy approach to studying the battery parameter's dependence on its state of charge. The results show that as the battery SOC decreases, the internal resistance increases. This can be seen in the shift of the EIS curves to the right, which represents an increase in the series resistance of the battery equivalent circuit.

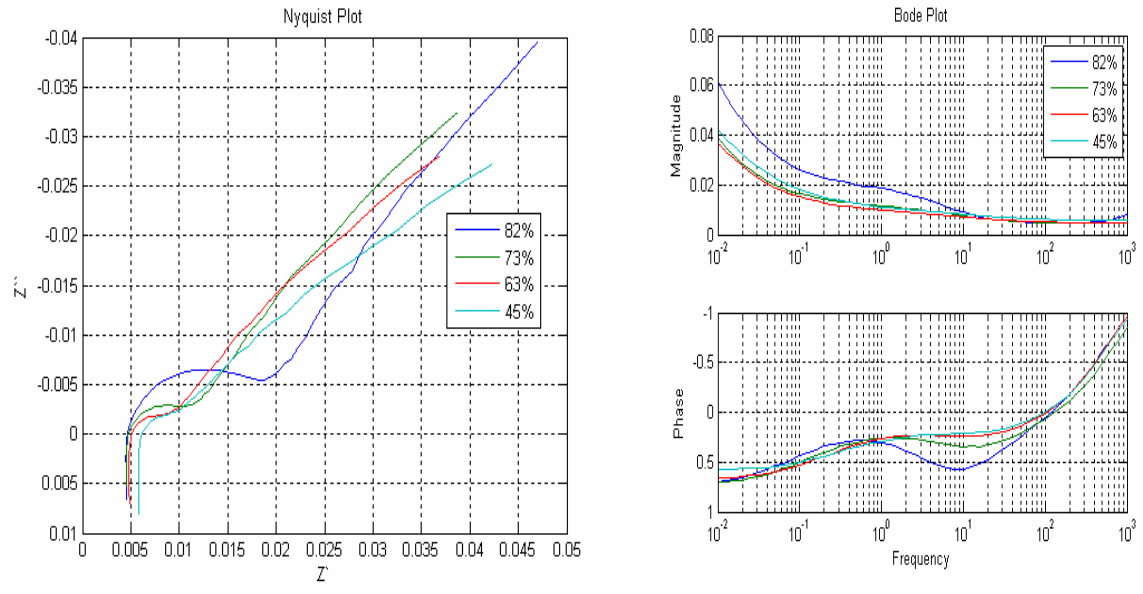

Figure 80: EIS and SOC

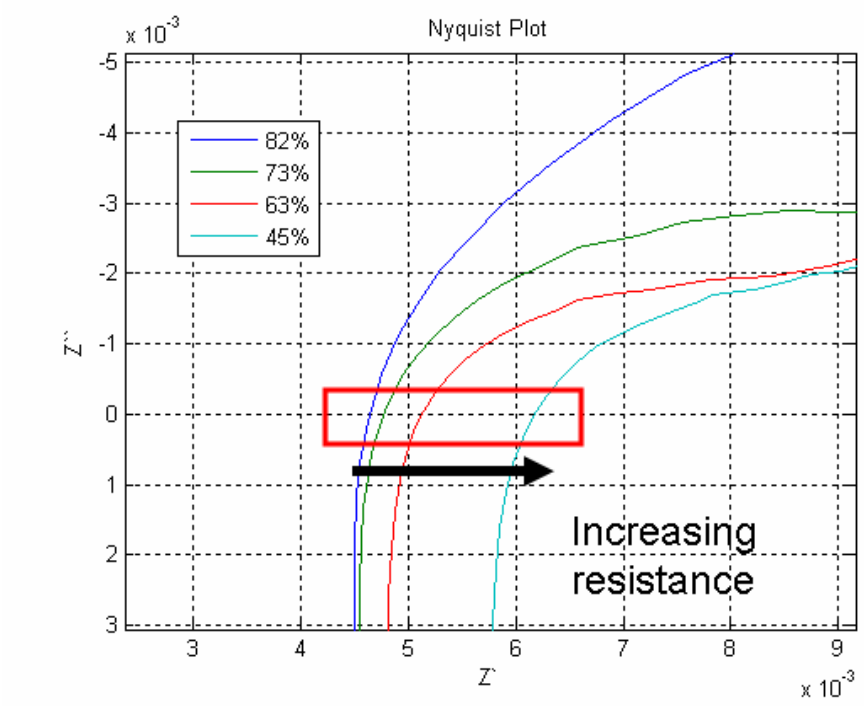

Figure 81: Real Axis of Nyquist Plot

The slight change in shape shows a dependence on SOC for all the other parameters in the circuit. This shows the non-linearity of the system even further.

7.1.2 Closed Circuit EIS Modeling

The same procedure is conducted again, but while the battery is operated in circuit. It is possible to obtain a frequency spectrum while the battery is being charged or under load which provides further information for determining a final battery model. In any case, investigating the impedance spectrum of a closed circuit battery may be more effective than open circuit since all battery prognosis simulations will be for situations while the battery is operated. The battery is thus tested at three currents, 1A, 5A, and 10A, for both charging and discharging.

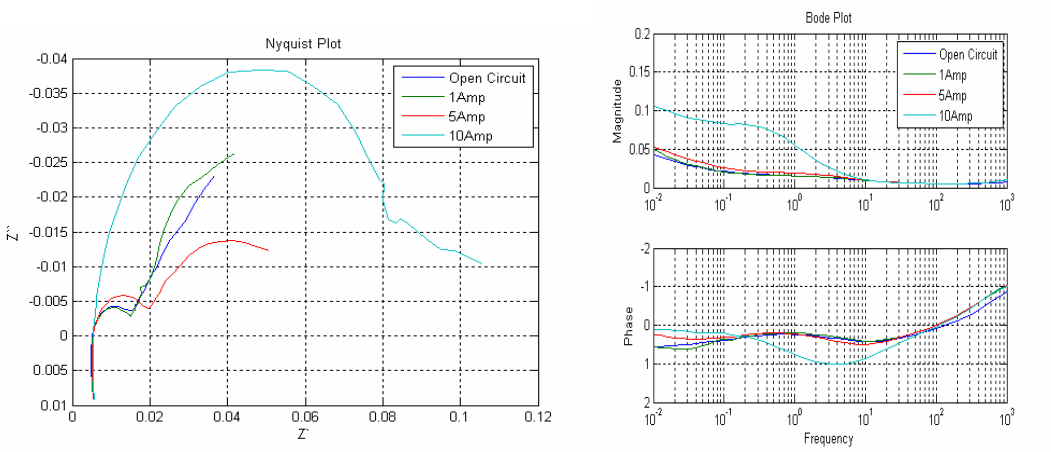

Figure 82: Charge Comparison

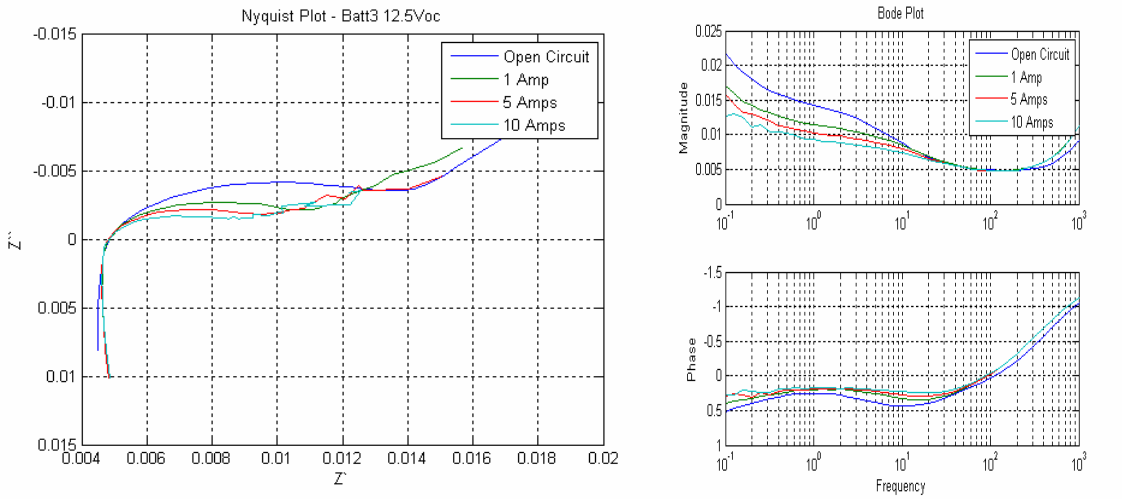

Figure 83: Discharge Comparison

For closed circuit modeling, the Warburg impedance is less effective in fitting the charging regime because most of the spectrums did not have the linear 'tail' in the complex plane. Once again a third order Randle Model provided the best fit for all of these scenarios. The charging regime shows a trend towards more of a fit to a 1st Order Randle model since its spectrum seems to grow towards a semi-circle. As the charging rate increases, the spectrum becomes more and more relatable to a semi-circle. The

discharging regime shows a trend in the size of the spectrum. As the discharging rate increases, the spectrum response seems to maintain its shape while shrinking in magnitude.

The trends shown above prove that the battery's parameters are in fact dependent on discharge rate. Therefore, it is correct in applying it as a factor and variable in the comprehensive aging model. The next step is to try and understand this trend further; however, EIS cannot provide sufficient testing results for larger discharge rates. In order to study this further, large signal modeling is utilized.

7.2 LARGE SIGNAL RESPONSE MODELING

The large signal response modeling provides another method for refining the battery model. This method allows for comparison and allows for better modeling of the battery for operation since the EIS modeling is really only sufficient for small signals. This modeling investigates the battery response to different large signals, for charge and discharge, and once again tries to fit a circuit model to the response.

7.2.1 MODIFYING ORIGINAL METHOD

The original battery model (from previous research at CAR) is based on this method, and the refined model is an adaptation to this method. The large signal to be applied consists of a staircase current profile, which will provide a sufficient set of responses to characterize the battery. The original model, however, seems to need adjustments to this staircase profile, as well as, adjustments to the parameterization method.

To begin, the staircase of current is developed specifically for the size of the battery capacity. Moreover, the time the current is to be applied depends on the battery capacity. The entire staircase will only discharge the battery approximately 5% of its rated capacity. This constraint is imposed because of the dependence of the parameters on the battery's SOC. If we limit the change of SOC, then we can effectively neglect the dependence of parameters on SOC. Each step within the staircase is a different current level, which will then provide a different response. The parameters are then determined at each step on the staircase by assuming constant SOC and temperature along the step. The result is a set of responses for one staircase where a set of parameters will characterize each step. An example staircase current profile can be found in the Figure 84.

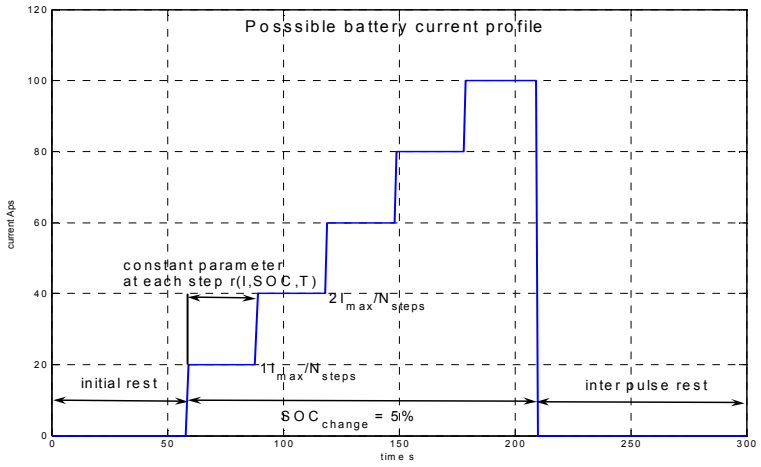

Figure 84: Staircase Profile for Large Signal Modeling [4]

As briefly mentioned above, this staircase profile needed to be modified to better approximate the battery parameters. One modification for the staircase profiles is to

include more steps in the staircase to obtain more responses. Another modification considered is to stagger the step levels. Since the battery in a vehicle is found to operate around 20A more than any other current level, it could be advantageous to have more current steps around the 20A level. Figures 85 and 86 help show these modifications.

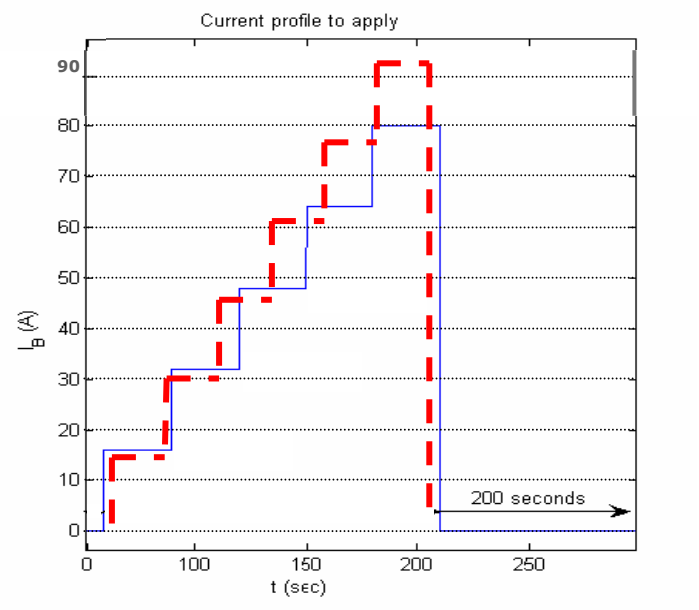

Figure 85: Additional Steps in the Staircase

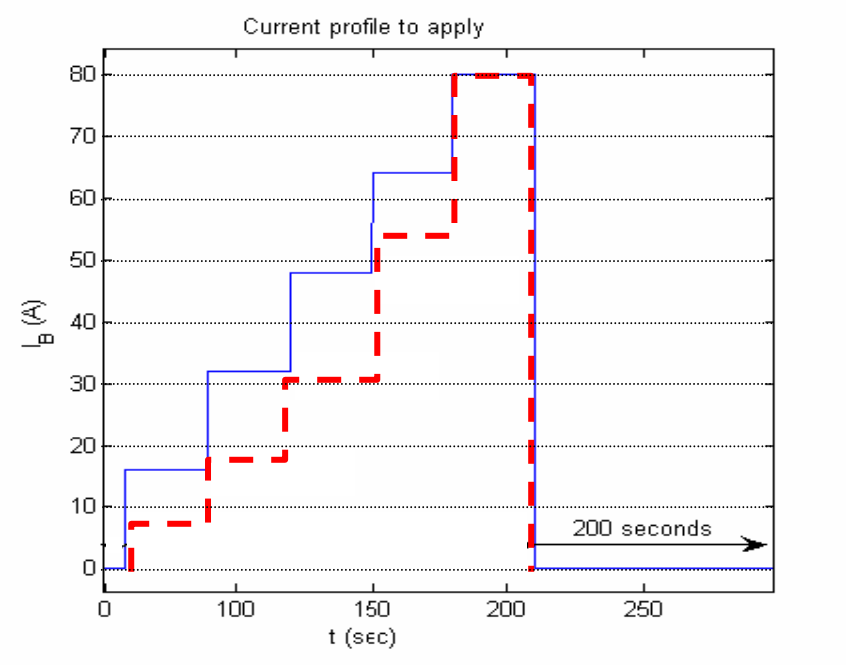

Figure 86: More Steps Concentrated around 20A

The final staircase to be used for the aging batteries is depicted in Figure 87. This staircase consists of steps between 0 and 60 Amps separated equally in 10 steps. This limit of 60 Amps is a hardware limit, but through preliminary testing, it was found that 60 Amps with 10 steps should provide more than enough information for aging characterization. Included in this profile is a charging staircase that applies three steps of 1, 5, and 10 Amps. The charging staircase is applied for two reasons. The first is that it allows the entire profile to be charge sustaining. The second is that if there is a future desire to investigate the response from charging regimes, the results from this profile will allow for the further research.

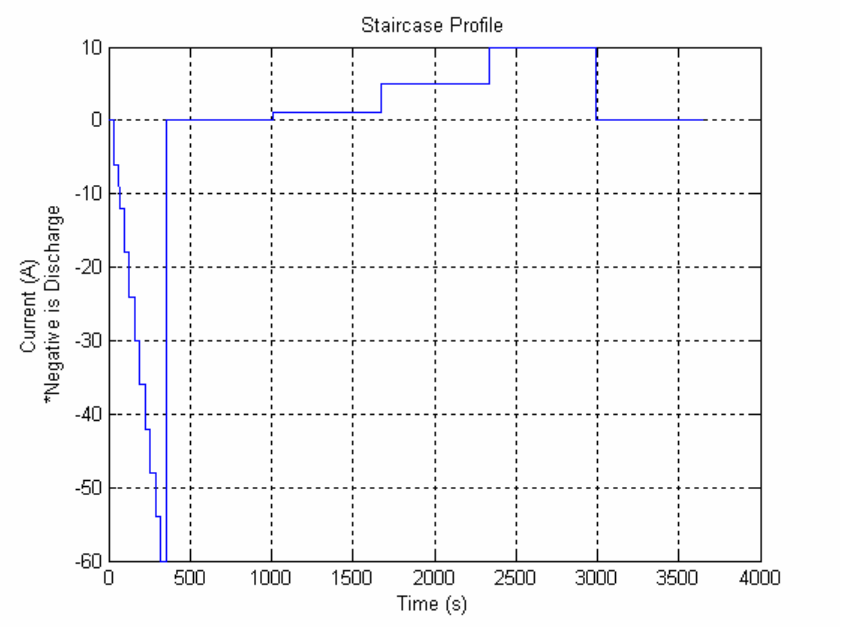

Figure 87: Staircase Profile for Large Signal Analysis

7.2.2 STAIRCASE RESPONSE ANALYSIS

Applying the current profile in Figure 87 will generate a voltage response from the battery. This voltage response can then be used to estimate the battery parameters which will be fit to a similar equivalent circuit from the EIS results. These parameters can then be used as another means to understand and quantify aging. This research will only investigate the discharge regime for parameterization.

The first step in the analysis is to represent the battery as an equivalent circuit much like the approach for EIS. The first equivalent circuit that will be used for this response analysis will be that of the 1st Order Randle Model. If a 1st order system is analyzed, the set of equations becomes the following…

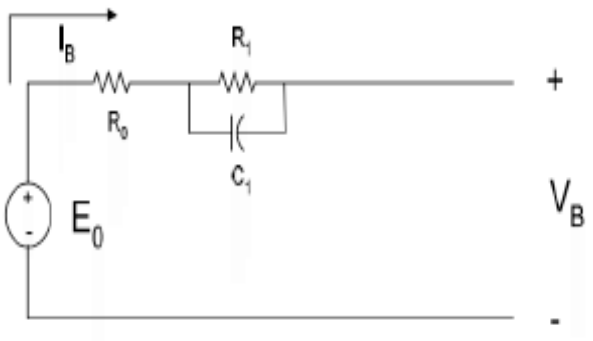

Figure 88: 1st Order Randle Model

KVL:

$$V_B = E_0 - V_{C_1} - I_B R_0$$

KCL:

$$\frac{dV_{C_1}}{dt} = -\frac{V_{C_1}}{R_1 C_1} + \frac{I_B}{C_1}$$

Initial Capacitor voltage:

$$V_{C_{1_0}} = E_0 - I_{B_0} R_0 - V_{B_0}$$

where *KVL* and *KCL* are Kirchhoff's voltage and current laws, respectively. These relationships provide the foundation for estimating the parameters within the equivalent circuit. If the battery's open circuit terminal voltage, E_0, its current, I_B, and its closed circuit voltage, V_B, are known, then the parameters R_0, R_1, and C_1 can be determined. Through a constraint minimizing function in Matlab called fmincon, the parameters are found and a fitting is provided in Figure 89. Each step of the staircase is parameterized individually with this procedure and the parameters are listed in Table 10.

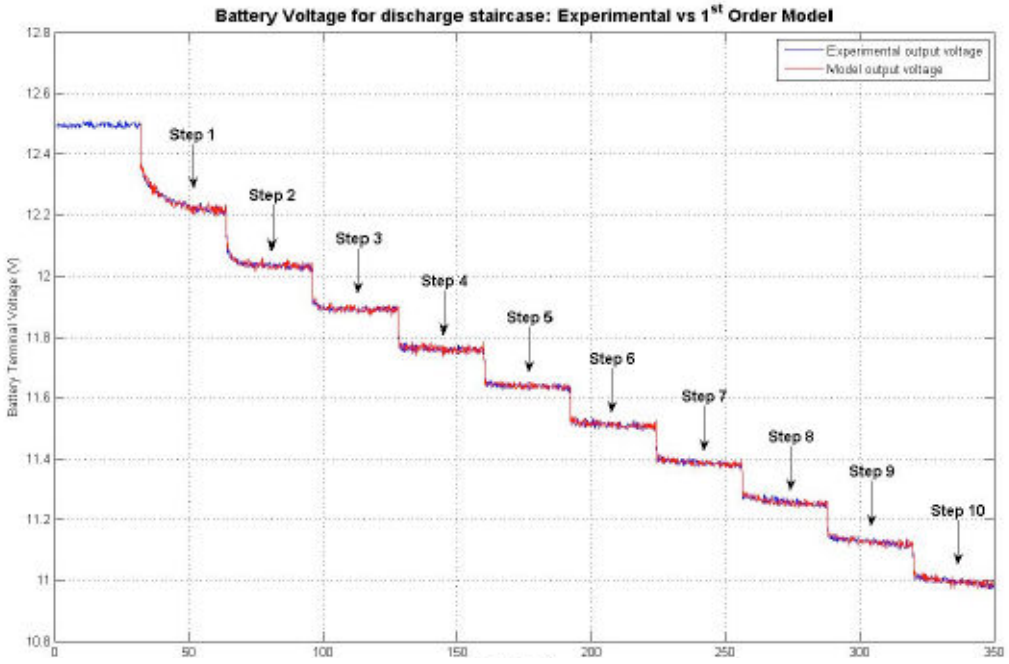

Figure 89: Experimental vs. Model Response of Staircase

Table 10: 1st Order Parameters

1st Order	Current	R0	R1	C1	T1	RMS error	Max error
Step 1	0 - 5.8A	0.0249	0.0241	324	7.81	0.0122	0.0516
Step 2	5.8 - 11.8A	0.0174	0.0222	109.4	2.43	0.0109	0.0293
Step 3	11.8 - 17.8A	0.0163	0.0177	77.6	1.37	0.0096	0.032
Step 4	17.8 - 23.8A	0.0231	0.0079	1055	8.33	0.0107	0.0318
Step 5	23.8 - 29.8A	0.0162	0.0129	1027	13.25	0.0086	0.0243
Step 6	29.8 - 35.8A	0.0168	0.0108	1028	11.10	0.0095	0.0312
Step 7	35.8 - 41.8A	0.0161	0.0106	1040	11.02	0.008	0.0234
Step 8	41.8 - 47.8A	0.014	0.0121	1040	12.58	0.0084	0.0221
Step 9	47.8 - 53.8A	0.0168	0.0088	1112	9.79	0.0094	0.0322
Step 10	53.8 - 59.8A	0.0165	0.0088	1263	11.11	0.0094	0.0276

(R-Ohms, C-Farads)

The function is largely dependent on the initial conditions including the starting voltage level which is the open circuit voltage. As mentioned previously in the report, the open circuit voltage is directly associated with the SOC of the battery. Similarly, the internal resistance of the battery is dependent on the SOC and the temperature. It will be important to estimate the open circuit voltage based on the SOC and vice-versa. Section

7.4 of the report discusses creating a voltage map that describes the relationship between SOC and open circuit voltage.

A more visual depiction of the response and parameterization can be found in Figure 90. It shows the relationship of the parameters at each current step with the voltage response. The initial drop of the response is largely dependent on the series resistance of the circuit. The subsequent transient response is due to the capacitor storing charge. The consequence is an exponential decay with a time constant of R_1C_1.

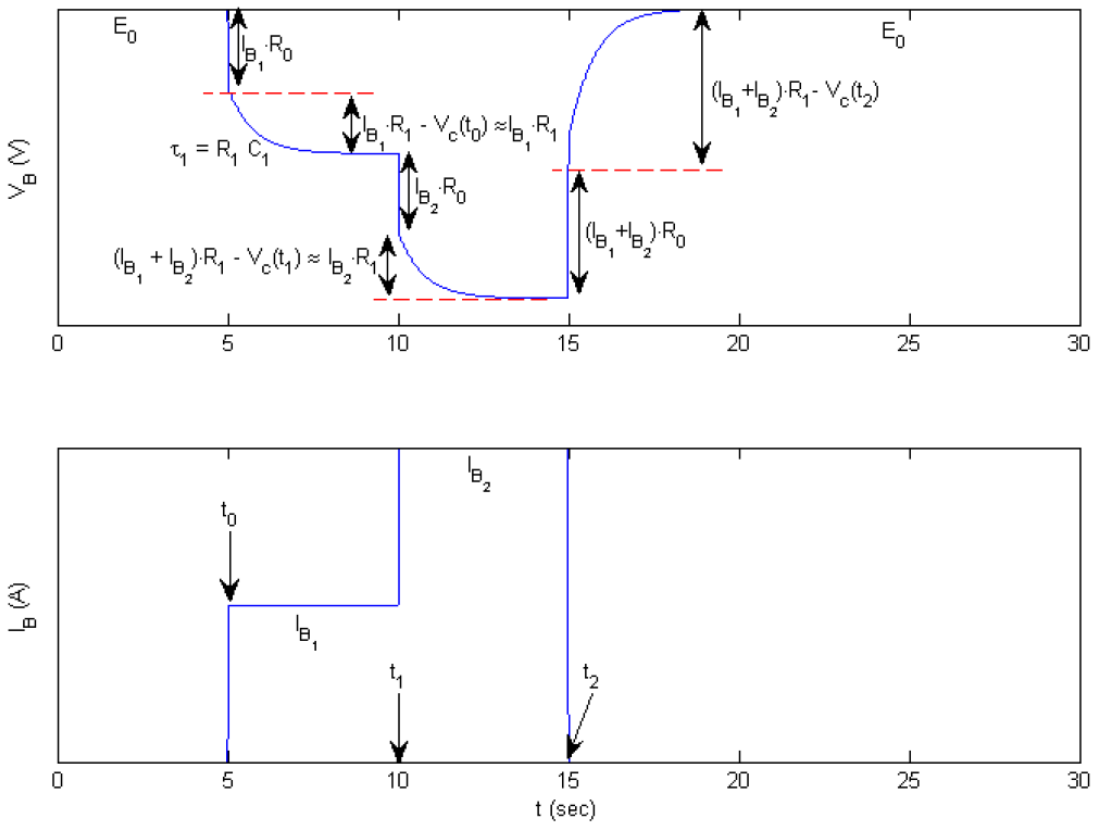

Figure 90: Parameter Extraction from Voltage Response [4]

This process is conducted intermittently throughout the battery's aging in order to study the aging affects on the circuit parameters. More data is needed before a final model can be determined, but currently a 1st Order model is quite reasonable in comparison to the experimental response.

7.3 Large Signal Response and EIS Comparison

The differences between the two methods above can be seen in the equivalent circuit models. The EIS analysis shows that a 3rd Order Randle Model is needed to fit with reasonable accuracy the entire frequency range, whereas a 1st Order model can only fit within a certain range of the spectrum. Additionally, a 1st Order model can fit the entire spectrum but only with a Warburg Impedance element. The Large Signal Response analysis shows that a regular 1st Order Randle Model is sufficient in fitting the battery response. This makes it quite clear that these test methods are inherently different, and will prove difficult in correlation.

In an attempt to compare and correlate the two methods, a third battery is tested extensively through both the EIS and Large Signal methods. Since the EIS method investigates the frequency response of the battery at low signals, the Large Signal Response needs to be manipulated to do the same, but with large signals. This can be done by altering the time length of the steps as well as the height, or change in current, of each step. This will, in a sense, excite the battery through different frequencies, and the response can be analyzed.

A staircase profile is created to investigate any differences the battery response might have to differences in the change of current level, while keeping the time step constant.

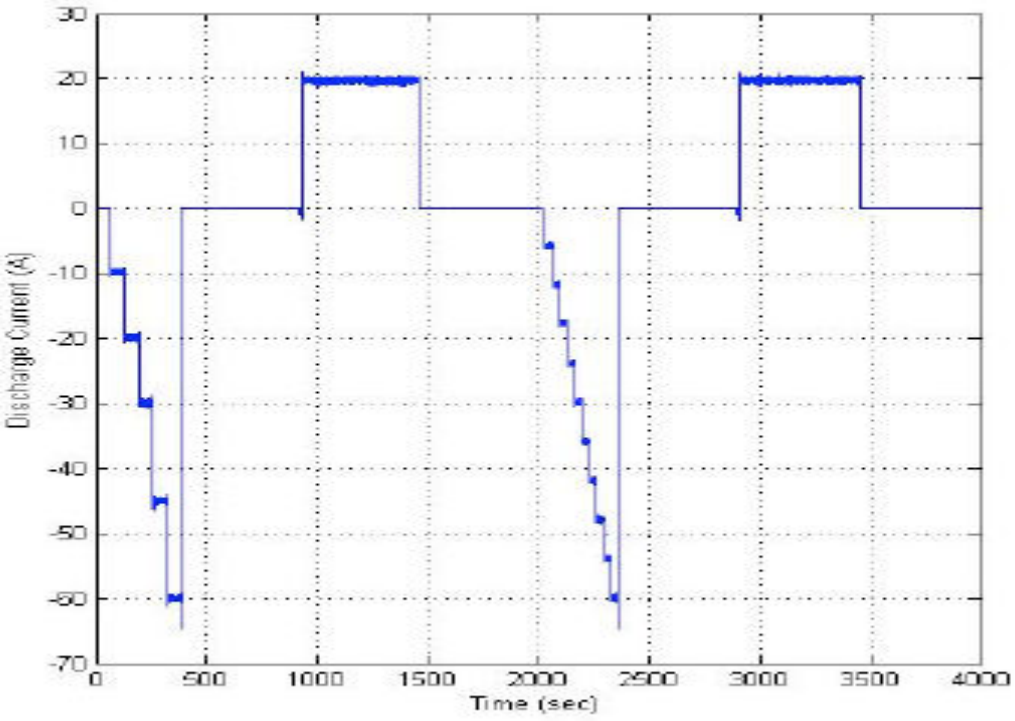

Figure 91: Dynamic Staircase Profile

The response from this staircase allows further investigation on the dependence of the battery parameters with current levels and the change in current levels. The parameters at each step can then be plotted as a function of current level and this function can be extrapolated and compared to small signal responses like EIS. For this profile, the model fitting needed to be at least second order.

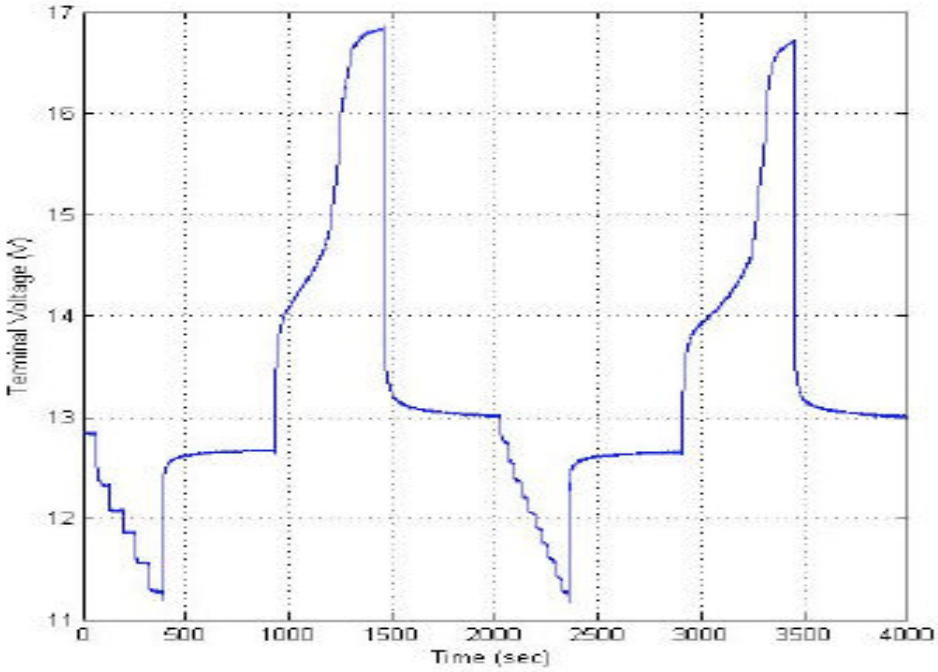

Figure 92: Battery Response to Dynamic Profile

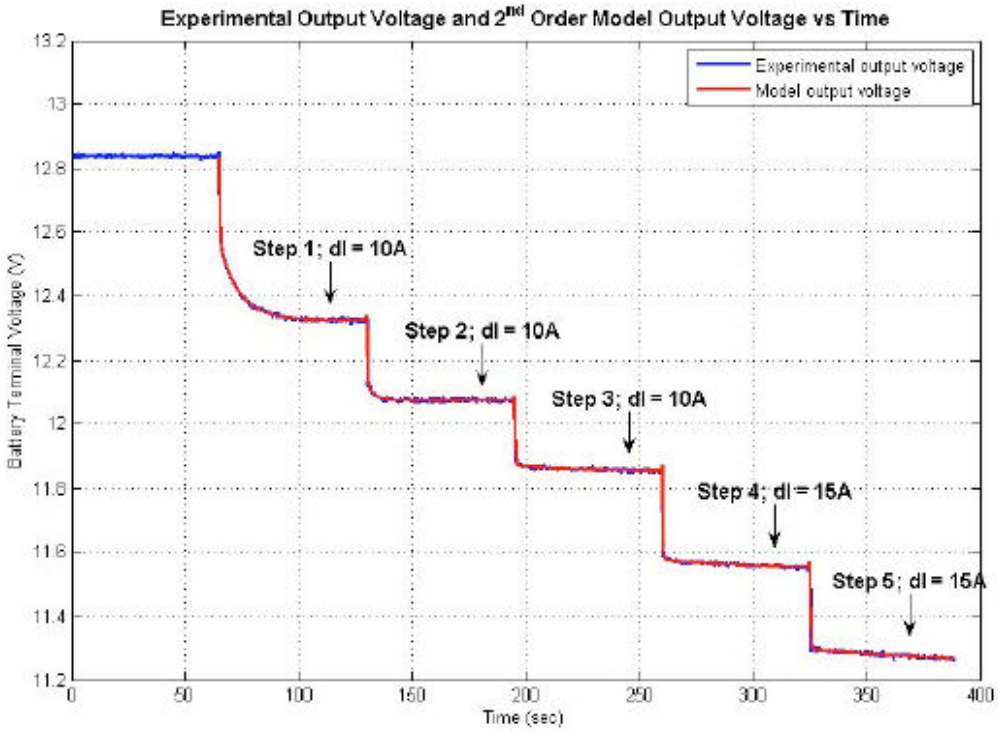

Figure 93: Second Order Model Fitting to Battery Response

Table 11: Battery Parameters from Model Fitting

2nd Order	R0*	R1	C1	T1	R2	C2	T2	E0	RMS error	Max error	E0i	E0lb	E0ub
Step 1	6.67E-05	9.43E-04	9436	8.90	5.74E-05	3774	0.217	12.314	0.0042	0.0341	12.829	5	20
Step 2	6.67E-05	0.003	1014	3.04	6.13E-04	405.7	0.249	12.002	0.0045	0.0464	12.314	7.314	17.314
Step 3	6.67E-05	0.0231	1505	34.77	5.50E-04	601.8	0.331	11.141	0.0046	0.0431	12.002	7.002	17.002
Step 4	6.67E-05	0.0185	2601	48.12	2.80E-04	1040	0.291	10.701	0.0051	0.0634	11.141	6.141	16.141
Step 5	6.67E-05	4.60E-02	1246	57.32	8.78E-05	3114	0.273	8.49	0.0055	0.0701	10.701	5.701	15.701
* Constrained to within 50% of first order value								Average:	**0.00478**	**0.05142**			

(R-Ohms, C-Farads)

More research is needed to investigate the differences between EIS and Large Signal Response modeling. The non-linearities of the battery parameters will be studied using these methods, and the results will be compared to provide further insight on the differences in model results for these tests.

7.4 ENGINE CRANK TESTING

Another means of investigating the internal resistance of the battery is by placing the battery under a high current demanding load. The battery is then placed in connection with a 2-Liter IVECO Diesel Engine, and used to crank and start the engine. An engine is the perfect load for this test since it requires a high current to overcome its large inductance. To avoid any inconsistencies during testing from any environmental factors on the engine, the engine is conveniently located inside a temperature controlled test cell, which will ensure consistent results for the crank testing.

This crank testing is conducted at three different SOC's at three different temperatures. The battery SOC's chosen were 90%, 75%, and 65% of the nominal capacity. To obtain these SOC's the battery is settled at specific open circuit voltages at room temperature based on the linear relationship between SOC and V_{oc} (Section 7.4) Once the battery is deemed to be at the desired SOC, the battery is placed in the environmental chamber at

the desired temperature for more then 16 hours. The 16 hour limit ensures that the electrodes have reached the desired temperature. The three temperatures for this test are 72°F, 0°F, and -22°F. The battery voltage, current, and engine RPM are recorded during testing. Comparing the peak current drawn from the battery will inherently compare the difference in internal resistances based on SOC and temperature. This is assuming that the load is constant for each temperature. To ensure this assumption, as explained before, the same engine is used for each test at the same temperature. The peak current results can be seen in Table 12.

Table 12: Peak Current Results of Crank Testing

Temperature	Peak Current (A) Battery N1			Peak Current (A) Battery N2		
72 F	1284	1259	1159	1283	1275	1182
0 F	1153	1113	1028	1148	1115	1053
-22 F	1054	985	916	1016	974	903

(Color represents SOC = 90%, 75%, 65%)

These results show that as the battery temperature decreases, its internal resistance increases. This is consistent with the literature and previous experiments. Batteries operate with less efficiency at lower temperatures, and these losses in efficiency can be related to its resistance. An increase in internal resistance at a lower temperature describes how the battery becomes less efficient at lower temperatures. A physical explanation can be found in the Arrhenius rate law. This law describes how chemical reactions can occur at faster rates at higher temperatures. Since battery operation is a

chemical reaction, this rate law would explain why the battery is less efficient at lower temperatures. The reaction inside the battery is not reacting at as high of a rate as it would in higher temperatures.

Additionally, the results verify the findings from the EIS measurements at different SOC's. For the cranking tests, as the SOC decreased, the peak current also decreased. Once again, a decrease in peak current implies an increase in internal resistance. Thus the crank tests also show an increase in internal resistance with a decrease in SOC.

Figure 94 and 95 provide an example of the data collected for one of the crank tests. During the test, the voltage of the battery dropped below 9 volts for every crank, which corresponded directly with the high current supplied to the engine. Additionally, the engine RPM estimation shows that the engine cranks at approximately 200-400 RPM and then jumps to around 900 RPM after starting.

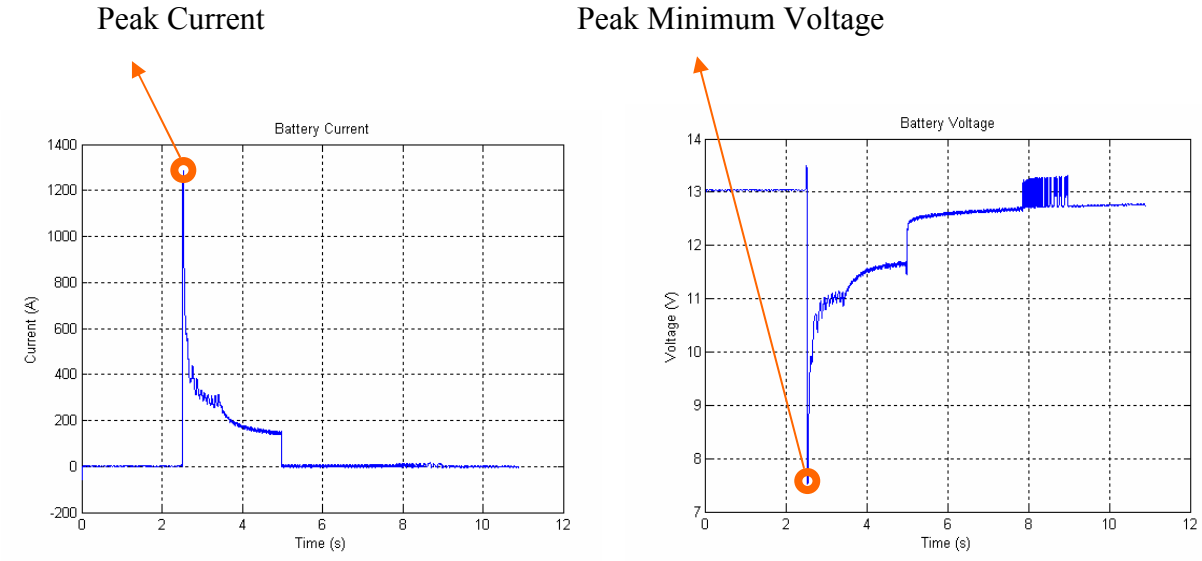

Figure 94: Battery Current and Voltage During Cranking

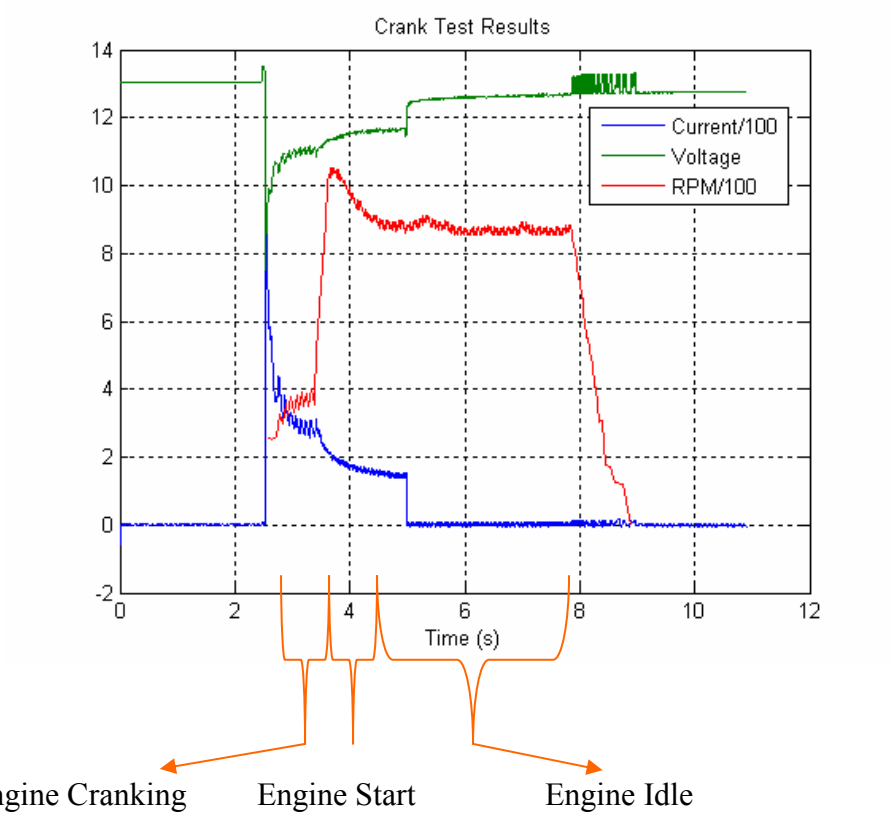

Figure 95: Engine Cranking Results and Description

Figure 95 shows the transitions the engine and battery make during starting. The initial peak in current and voltage drop shown overcome the inductance load of the motor. Then the engine begins to crank at around 200-400 RPM while both the current and voltage begin to recover from their peaks. Then when the engine starts the battery is only needed for a few more seconds before the current drops down to zero, the alternator takes over, and the engine idles.

7.5 Open Circuit Voltage Mapping

As an additional feature to characterizing the battery, an open circuit voltage (V_{oc}) map is created for the battery. This helps determine the SOC of the battery based on its V_{oc}.

Investigating the relationship between SOC and V_{oc} helps with the parameter estimation procedure discussed above. Creating a general V_{oc} map provides a useful estimation the SOC of the battery which is needed as a condition for the modeling tests. Additionally, this map is utilized in the determination for the three SOC's needed for the cranking tests.

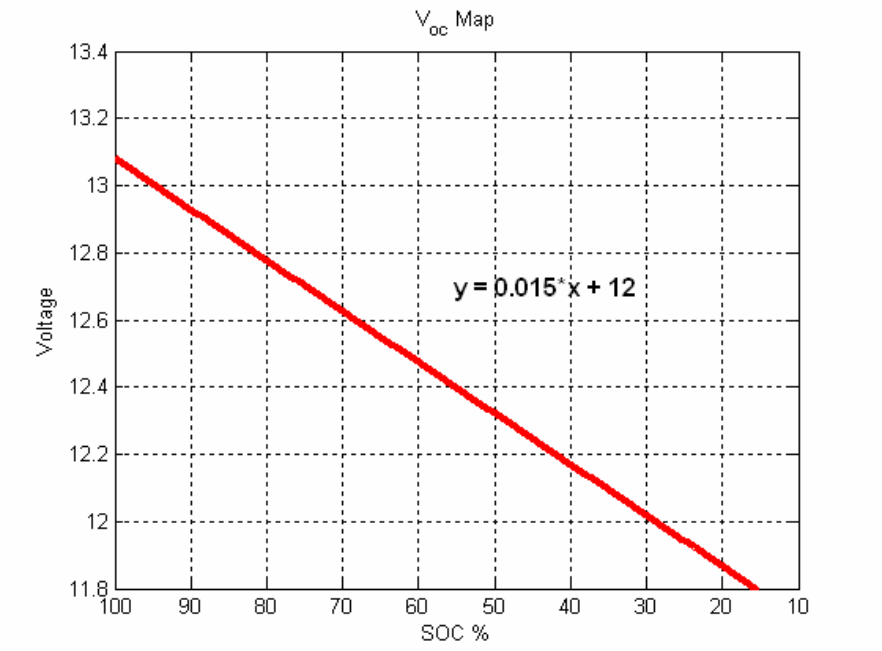

Figure 96: V_{oc} Map

This map is a combination of a discharge and charge map. There is an apparent hysteresis after the battery has discharged and charged. However, if allowed to rest long enough, the map can be approximated by a linear relationship. To create this map, the battery is discharged in segments of 6.25% SOC and allowed to rest from 1.5-2 hours before an open circuit voltage is taken. Additionally, a longer rest period is implemented every few readings to determine how accurate the assumption is for the settled voltage. For instance, a 12 hour rest period is implemented every few readings. Figure 97 provides a visual difference between the two rest periods, and it was determined that a 1.5 hour rest period is sufficient enough for a V_{oc} reading after a discharge.

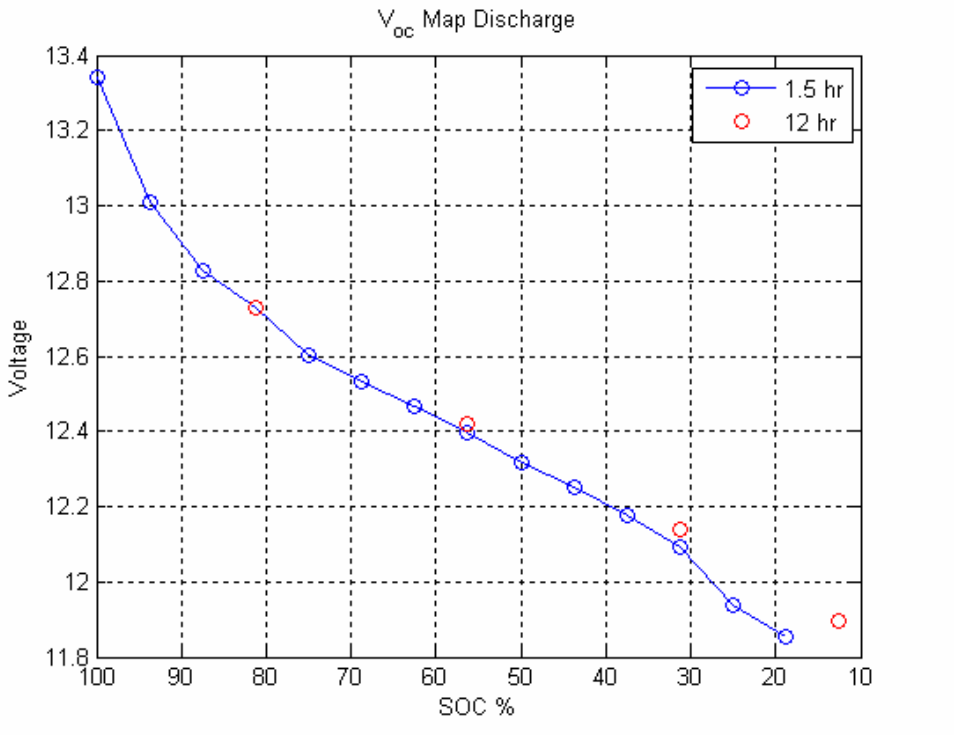

Figure 97: Voltage Mapping Rest Periods for Discharge

The same procedure is applied for a charging regime. These results show that the settling voltage for charging took much longer than for discharging. At least a 12 hour rest period is needed for an accurate V_{oc} reading. The drop in voltage for the charge regime is represented by the 'overnight' points which represent a rest period of at least 12 hours.

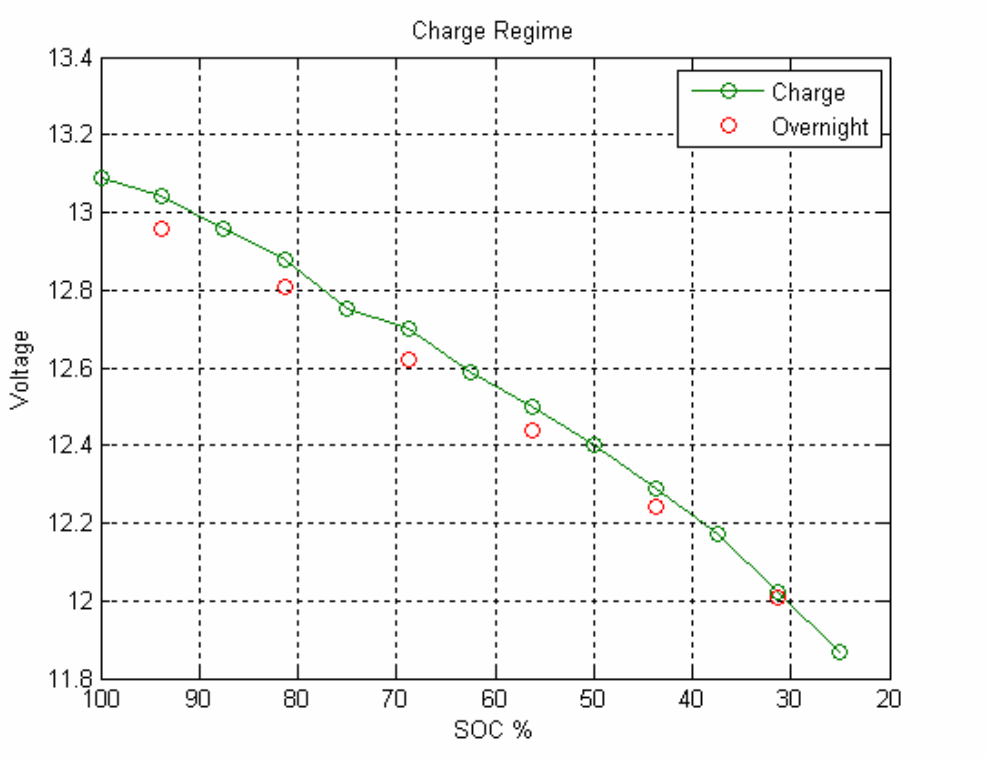

Figure 98: Charge Regime V_{oc} Mapping

The charging and discharging regimes can then be combined and a linear relationship can be estimated. For this research, this estimation will be sufficient since it is not expected that the battery aging and parameters will very dramatically with small differences in SOC. Therefore, testing the batteries at approximately the same open circuit voltage, will allow for a reasonable assumption that they are indeed at the same SOC.

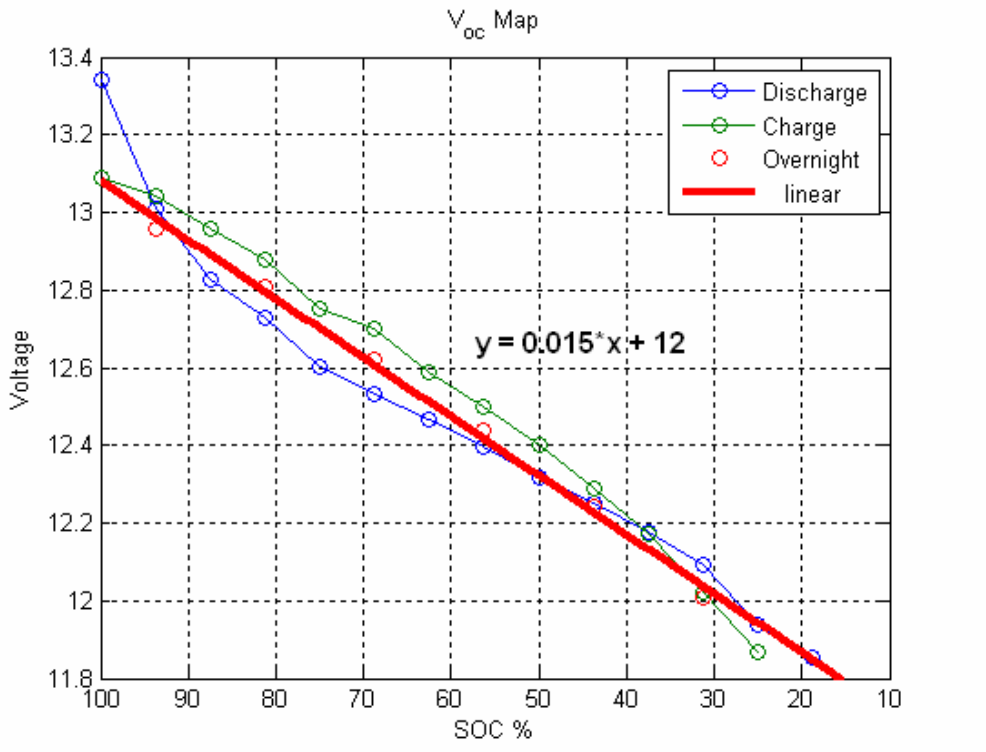

Figure 99: Voltage Mapping Charging and Discharging

7.6 CONCLUSIONS

When using the EIS modeling technique, the best fit linear model is a third order Randle Model. Results also show a relationship with internal resistance and SOC; as the SOC decreases, the internal resistance increases. This can be seen through both the EIS measurements and the engine cranking. It is most notably due to the sulfation build up on the electrodes which increases the battery resistance. As a battery discharges, sulfation will collect at the electrode. A decrease in SOC is a result of a discharge which causes sulfation, and therefore results in an increase in resistance. When using the large signal response modeling technique, a second order Randle Model is needed to fit the responses with some limitations. More experimentation and validation is needed for further refinement and to provide results for comparison with the EIS third order model.

Both applications show a large dependence on current level for the battery model parameters. This means that the battery is a nonlinear system and will prove to be difficult in finalizing a complete equivalent circuit model.

8. SUMMARY AND CONCLUSION

All batteries undergo small but permanent degradations which lead to their aging and ultimate failure. The 'aging' of the battery can be characterized through the system of aging diagnosis tests conducted in this research. EIS shows great potential in becoming an on-board method for judging a battery's age and state of health, but cannot be directly related to the battery's capacity.

In order to characterize the battery as it ages, certain qualities have to be tested. First, an estimation of SOC is needed through a mapping of open circuit voltage and SOC. This map showed a nearly linear relationship for Lead-Acid battery SOC and V_{oc}. Second, the effects of a battery's SOC needed to be investigated to understand its use in characterization. Results from EIS and engine cranking measurements show that the battery's internal resistance increases with a decrease in its SOC. In other terms, a battery is unable to provide the same amount of power at lower states of charge. Third, the EIS characterization of a Lead-Acid battery showed that a third order model is needed to fit the entire spectrum, but only a second order model is needed when fitting to a Large Signal Response. More research is needed to investigate these differences.

The Lead-Acid battery has two common failure modes that will be studied for a deeper understanding of its aging. Two profiles were created that are expected to generate the different failure modes, and these effects will be helpful in creating an aging model for Lead-Acid batteries.

A comprehensive aging model for batteries can be created by decomposing real battery data in a basis cycle set and analyzing the aging effects for each cycle. These effects can then be used in estimating the remaining battery life by assuming an additive property for battery aging similar to that in mechanical failure through fatigue and crack propagation. The basis cycle set for NiMH batteries show that only the first 4 basis cycles are needed to regenerate at least 90% of the real world cycles. Further testing and research is needed to complete and validate these theories.

9. REFERENCES

[1] Z. Chehab, 'Aging Characterization of NiMH Batteries for Hybrid Electric Vehicles'. Masters Thesis. The Ohio State University. 2006.

[2] I. Buchmann, 'Batteries in a Portable World.' Isidor Buchmann. Cadex Electronix Inc. 2001.

[3] Automotive Alternators. Wikimedia Foundation Inc. 2007. www.wikipedia.org

[4] A. Fasih, 'Modeling and Fault Diagnosis of Automotive Lead-Acid Batteries'. Undergraduate Honors Thesis. The Ohio State University. 2006.

[5] Energizer. *NiMH Application Manual*. 2001.

[6] M. Keyser, A. Pesaran, M. Mihalic, 'Charging Algorithms for Increasing Lead Acid Battery Cycle Life for Electric Vehicles'. National Renewable Energy Laboratory. 2001.

[7] Nickel Metal Hydride Prismatic Cell Design. Cobasys LLC. 2007. www.cobasys.com

[8] R. Hansen, 'Valve-Regulated Lead-Acid Batteries for Stationary Applications'. Department of the Air Force. Air Force Pamphlet 32-1186. 1999.

[9] J. Kopera, 'Considerations for the Utilization of NiMH Battery Technology in Stationary Applications'. Cobasys. Orion, MI. 1999.

[10] Panasonic Ni-MH Overview, Panasonic OEM battery division, http://www.panasonic.com/industrial/battery/ February 2002

[11] USABC. *Electric Vehicle Battery Test Procedures Manual*. 1996.

[12] L. Guenne, P. Bernard, 'Life Duration of NiMH Cells for High Power Applications'. Journal of Power Sources. 2002.

[13] Moltech Corporation. *NiMH Application Manual*. http://www.moltech.com/techdata/appmanuals/NiMH_Application_Manual.asp

[14] Panasonic EV Energy Co. *Ni-MH battery for EV*. http://www.peve.panasonic.co.jp/catalog/e_kaku.html

[15] R. Somogye, 'An Aging Model Of Ni-MH Batteries For Use In Hybrid-Electric Vehicles'. Master Thesis. The Ohio State University. 2004.

[16] G.R. Delpierre, B.T. Sewell, The Lead-Acid Accumulator. 1992-2006. www.physchem.co.za/Redox/cells.htm

[17] P. Pascoe, A. Anbuky, 'VRLA Battery Discharge Reserve Time Estimation'. IEEE Transactions on Power Electronics. Vol. 19, no. 6, 2004.

[18] D. Linden, T. Reddy, *Handbook of batteries*. New York: McGraw-Hill. 2002.

[19] Panasonic Corporation. 'HHR650D nickel metal hydride batteries: individual data Sheet'. Online.

[20] Panasonic Technical Handbook. 2006. www.batterywholesale.com

[21] D. Loveday, P. Peterson, B. Rodgers, "Evaluation of Organic Coatings with Electrochemical Impedance Spectroscopy". JCT CoatingsTech. August 2004

[22] M.A. Miner, J. Appl. Mech. 12 (1945) 159-164.

[23] M.T. Todinov, "Necessary and sufficient condition for additivity in the sense of the Palmgren-Miner rule". *Computational Materials Science*. 21, pp. 101-110, (2001).

[24] D. Chelidze, J. P. Cusumano, 'A Dynamical Systems Approach to Failure Prognosis'. *ASME Transactions, Journal of Vibration an Acoustics*. 126(1), pp. 2 – 8, (January 2004).

[25] B. Liaw, A. Urbina, T. Paez, *Life Prediction Modeling of Lead-Acid Batteries in Stationary Backup Power Applications*. Sandia National Laboratories. 2003.

[26] R. Smith, A. Bray, 'Impedance Spectroscopy as a Technique for Monitoring Aging Effects in Nickel Hydride and Nickel Metal Hydride Batteries'. Texas Research Institute Austin, Inc. IEEE. 1992.

[27] SAE. *End-of-Life Battery Test Methods*. 2006. SAE Test Method J1634.

[28] A. Yamada, O. Hirahara, T. Tsuchida, N. Sugano, M. Date, 'A Practical Method for the Remote Control of the Scanning Electron Microscope'. Japanese Society of Microscopy. 2003.

[29] E. Baring-Gould, H. Wenzl, R. Kaiser, N. Wilmont, F. Mattera, S. Tselepis, F. Nieuwenhout, C. Rodrigues, A. Perujo, A. Ruddell, P. Lundsager, H. Bindner, T. Cronin, V. Svoboda, J. Manwell, 'Detailed Evaluation of Renewable Energy Power System Operation: A Summary of the European Union Hybrid Power System Component Benchmarking Project'. National Renewable Energy Laboratory. 2005.

[30] P. Cheng, I. Chen, 'High Efficiency and Nondissipative Fast Charging Strategy'. IEEE Proceedings. Online # 20030255, vol. 150, no. 5. September 2003.

[31] Z. Salameh, M. Cassaca, 'Determination of Lead Acid Battery Capacity Via Mathematical Analysis'. IEEE Transactions. ID # 0885-8969(92)026-5, vol. 7, no. 3. September 1992.

[32] J. Disosway, 'Comparison of Service Test Results with Analytical Predictions for a Lead Acid Battery'. IEEE Transactions. ID # 0885-8969(92)027-3, vol. 7 no. 3. September 1992.

[33] M. Ceraolo, ‘New Dynamical Models of Lead-Acid Batteries’. IEEE Transactions. ID # 0885-8950(00)10436-3, vol. 15, no. 4. November 2000.